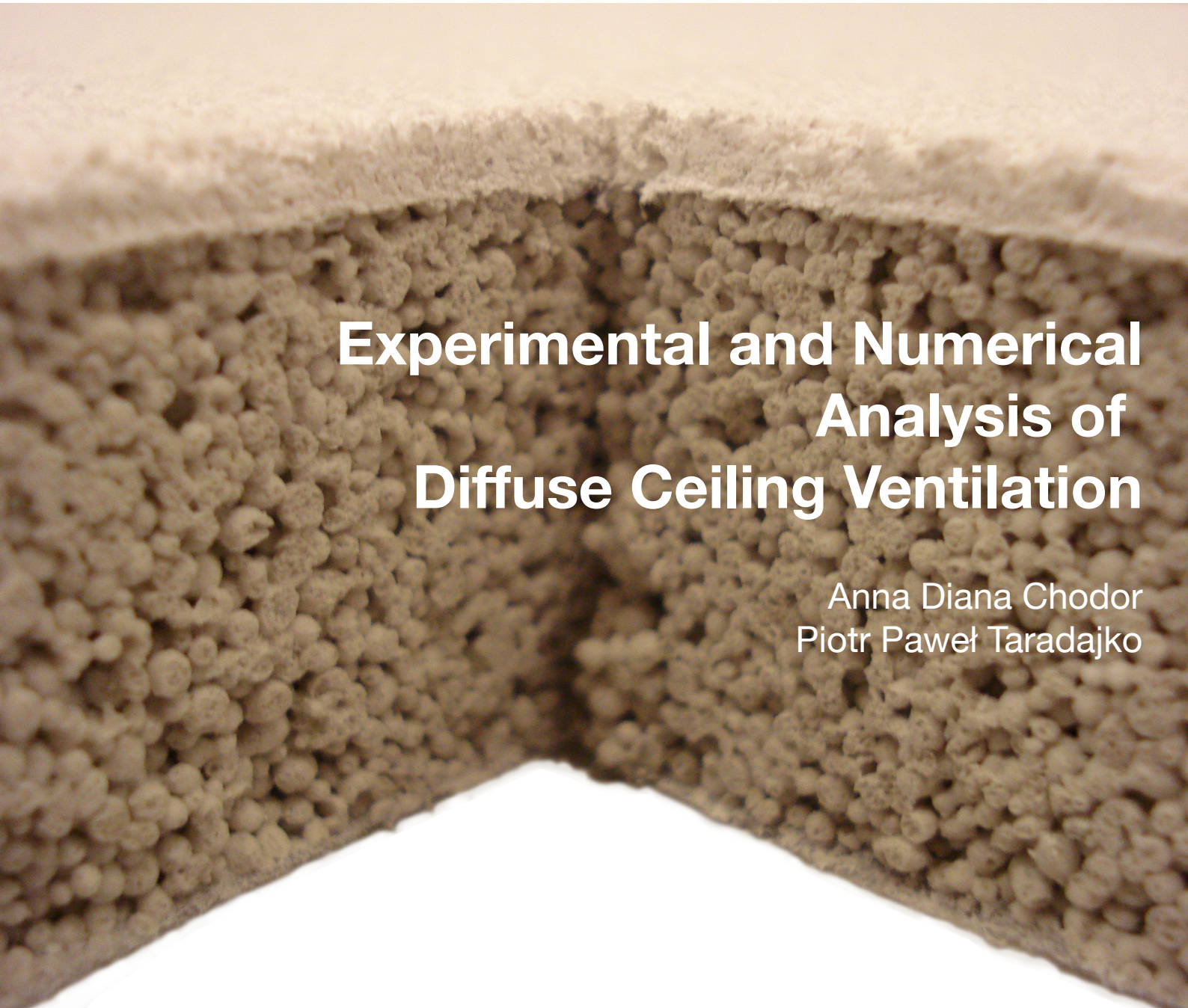




AALBORG UNIVERSITY
STUDENT REPORT



Experimental and Numerical Analysis of Diffuse Ceiling Ventilation

Anna Diana Chodor
Piotr Paweł Taradajko

Title:

Experimental and Numerical Analysis of Diffuse Ceiling Ventilation

Project period:

November 2012 - March 2013

Project group:

B-216e

Participants:

Anna Diana Chodor

Piotr Paweł Taradajko

Synopsis:

This report is an analysis of performance of diffuse ceiling ventilation system and both experimental and numerical analysis are included. All of the experiment results are recalculated to a design chart, which enables to find maximum acceptable q and ΔT values, which ensure that draught risk in the room is in the acceptable range.

Supervisors:

Peter Vilhelm Nielsen

Li Liu

Rasmus Lund Jensen

Editions: 4

Number of pages: 90

Number of appendixes: 2

Completed: 14th of March 2013

The content of this report is freely available, but publication with the source references should only be done in agreement with the authors.

Abstract

Presented report is an analysis of performance of diffuse ceiling ventilation system and both experimental and numerical analysis are included.

Experimental part involves full-scale measurements on the DCV. Number of experiments are carried out under different thermal and air flow conditions. One of the main issues, which is investigated, is influence of the heat loads location in the room on the airflow pattern. It is checked how much conditions in the room will change depending on the heat loads distribution- equally distributed heat sources, point heat sources in different locations or heat sources only on one side of the room. Influence of vertical heat loads location is tested as well. With equally distributed heat loads a problem with unstable airflow pattern may occur and it is tried to investigate its nature. Another broad field of interest is the importance of the supply area of the ceiling. All of the results are recalculated to a design chart, which enables to find maximum acceptable q and ΔT values, which ensure that draught risk in the room is in the acceptable range. What is more a pressure loss across the real ceiling is measured and it is investigated what is the influence of ceiling's construction on the pressure drop.

Second main part of this report is CFD modeling and a Star CCM+ software is used to create a model of the test room. One of the cases, which is tested in the real experiment is a base for the model's geometry and boundary conditions. Next it is tried to validate the model by comparing results of the simulation with measurements results. Finally the test room's model geometry is changed by decreasing the height of the room to be able to see, what is the influence of the room's height on the bouancy forces in the room, as these are the main forces generating airflow for DCV system.

Abstract in polish

Poniższy projekt analizuje działanie sufitowej wentylacji dyfuzyjnej. Obejmuje on zarówno analizę pomiarową, jak i poprzez metody numeryczne.

Część pomiarowa obejmuje eksperymenty sufitowej wentylacji dyfuzyjnej w pełnej skali. Liczba pomiarów przeprowadzona jest w różnorodnych warunkach cieplnych i przepływowych. Jednym z głównych problemów, który jest zbadany, jest wpływ lokalizacji zysków ciepła w pomieszczeniu na rozptył powietrza. Pomiary mają na celu sprawdzenie, jak bardzo warunki w pomieszczeniu zależą od dystrybucji zysków ciepła - zysków ciepła rozłożonych równomiernie, punktowych zysków ciepła w różnych lokalizacjach oraz zysków ciepła w jednej części pomieszczenia. Zbadany jest również wpływ zysków ciepła w zależności od ich wertykalnej pozycji. W przypadku zysków ciepła rozłożonych równomiernie, jest ryzyko wystąpienia problemu niestabilności przepływu powietrza w pomieszczeniu i jego natura jest analizowana. Kolejne szerokie pole badań, to istotność pola powierzchni, przez które powietrze nawiewane jest do pomieszczenia. Wszystkie rezultaty zaprezentowane są na wykresie projektowym, $q\text{-}\Delta T$, który umożliwia znalezienie maksymalnych wartości q i ΔT , dla których ryzyko przeciągu w pomieszczeniu jest w akceptowalnym zakresie. Ponadto, przeprowadzone są pomiary spadku ciśnienia na suficie dyfuzyjnym i zbadane jest jaki wpływ na spadek ciśnienia ma konstrukcja sufitu.

Drugą, istotną częścią raportu jest modelowanie CFD, do którego użyty jest program Star-CCM+ i wygenerowany jest model pomieszczenia testowego. Warunki jednego z pomiarów w prawdziwym pomieszczeniu są bazą dla geometrii i warunków brzegowych użytych w modelu. Walidacja modelu przeprowadzona jest poprzez porównanie wyniku eksperymentu z wynikami symulacji. Następnie geometria modelu jest zmieniona poprzez zmniejszenie wysokości pomieszczenia, w celu sprawdzenia, jak duży jest wpływ wysokości pomieszczenia na siły wyporu w pomieszczeniu, które są głównymi siłami generującymi przepływ powietrza w tego typu systemie wentylacji.

Preface

This Master Thesis is a documentation of the project called Experimental and Numerical Analysis of Diffuse Ceiling Ventilation. Project was written in the Master of Science programme at the faculty of Indoor Environment Engineering at the Department of Civil Engineering at Aalborg University during the period from November 2012 to March 2013.

The main report is an analysis of performance of diffuse ceiling ventilation system and both experimental and numerical analysis are included. All of the experiment results are recalculated to a design chart, which enables to find maximum acceptable q and ΔT values, which ensure that draught risk in the room is in the acceptable range. It consists of chapters including problem description, literature study, design criteria, experimental set-up, experimental results and CFD investigations. Main report is followed by the appendix, which contains information about experiments, additional results and CFD results.

The authors of this project are sincerely thankful to their supervisors - Professor Peter Vilhelm Nielsen, Li Liu and Rasmus Lund Jensen for time spend during the project and helpful guidelines.

The authors would also like to thank Bente Jul Kjaelgaard for help with preparing necessary documents and informing about formalities and deadlines.

The authors would also like to express their gratitude to laboratory staff for valuable assistance.

Read guidance

The project is divided into two reports - a main report and an appendix report. In the main report theory, methods, assumptions, set-up, measurements and results are presented and references will continuously be performed to the appendix report, which should be read as a reference to the main report. The appendix report contains additional descriptions, calculations, tables and figures. As a supplement to both the main and appendix report, an appendix CD is also attached to the back of the main report. This contains calculations and other additional information regarding this project. References to the CD-appendix will have the name appendix B.

Chapters are individually numbered chronologically. All figures and tables are numbered according to the chapter. Thus, the first figure in Chapter 3, number 3.1, the second has number 3.2, etc. Explanatory text for figures and tables can be found below the given figures and tables, and the source is indicated if the object does not have own production. Relevant assumptions and limitations are described continuously.

The report will contain references, all of which are collected in a bibliography at the very end of the report. Source citation is given by *Harvard method*, so a source in the text refers to Surname [Year] and when the whole part of text is referred to the source it can be seen as [Surname Year]. However, given norms and regulations with abbreviated names, for example [CR 1752 1998], will be referred to by the given number of the standard. If the source has more than one author, these are indicated by "*et al.*" Performs the same author several times, the surname will also be numbered alphabetically. The bibliography details books by author, title, edition and publisher, while websites

are indicated by author, title, and download date. If a source is placed within a sentence before the dot, it refers to the sentence, whereas it refers to the entire section if it is placed after the dot.

Symbols and units

Symbols

A	Area	$[\text{m}^2]$
C	Pollution concentration	$[\text{ppm}]$
c_p	Specific heat capacity	$[\text{J}/\text{kg K}]$
E	Emissivity	$[-]$
F	View factor	$[-]$
g	Gravitational acceleration	$[\text{m}/\text{s}^2]$
J	Radiosity	$[\text{W}/\text{m}^2]$
l	Reference length	$[\text{m}]$
n	Air change rate	$[\text{h}^{-1}]$
p	Pressure	$[\text{Pa}]$
q	Volumetric flow	$[\text{m}^3/\text{s}]$
t	Temperature	$[\text{°C}]$
T	Temperature	$[\text{K}]$
u	Velocity	$[\text{m}/\text{s}]$
Ar	Archimedes number	$[-]$
Re	Reynolds number	$[-]$
Tu	Turbulence intensity	$[\%]$
α	Convective heat transfer coefficient	$[\text{W}/\text{m}^2 \text{ K}]$
β	Expansion coefficient	$[\text{1}/\text{K}]$
ε	Effectiveness	$[-]$
λ	Thermal conductivity	$[\text{W}/\text{m K}]$
σ	Stefan-Boltzmann constant	$[\text{W}/\text{m}^2 \text{ K}^4]$
ρ	Density	$[\text{kg}/\text{m}^3]$

Subscripts

*	Dimensionless
a	Asymmetry
bz	Breathing zone
cl	Clothing
e	Extract
l	Local
oz	Occupied zone
t	Temperature
s	Supply
RA	Radiant asymmetry
VTG	Vertical temperature gradient
v	Ventilation

Acronyms

ACR	Air Change Rate
CFD	Computational Fluid Dynamics
DCV	Diffuse Ceiling Ventilation
DR	Draught rate
HVAC	Heating, Ventilation and Air-Conditioning
OZ	Occupied zone
PD	Percentage Dissatisfied
SFP	Specific Fan Power

Table of contents

1	Problem description	1
1.1	Introduction	1
1.2	Problem Formulation	1
1.3	Scope of investigations	3
2	Literature Study	5
2.1	Design chart	5
2.2	Diffuse ceiling ventilation	9
2.3	DCV in offices	10
2.4	DCV in schools	14
3	Design Criteria	17
3.1	Occupied zone	17
3.2	Thermal comfort	18
3.3	Indoor air quality	20
4	Experiment set-up	23
4.1	Test room	23
4.2	Measurement points and methods	26
4.3	Test cases	32
5	Experiment results	39
5.1	Experiment data	39
5.2	Design chart for DCV	42
5.3	Airflow distribution	49
5.4	Dimensionless analysis	59
5.5	Indoor environment	61
5.6	Radiation in DCV	66
5.7	Pressure test	68
6	CFD investigations	73
6.1	Test room model	74
7	Conlusions and perspectives	79
I	Appendix	83
A	Appendix report	85

B	CD appendix	87
B.1	Experiment results	87
B.2	CFD results	87
	Bibliography	89

Problem description

In this chapter the problems and possible span of work considered for diffuse ceiling ventilation will be introduced and described. Furthermore the scope of the project will be delimited by formulating main focus points.

1.1 Introduction

Nowadays buildings are better insulated and more tight and thanks to it using less energy for heating. At the same time role of ventilation in the tight buildings is getting more important and buildings have to be ventilated during larger period of the year. What is more increasing thickness of building's insulation is limited by its efficiency and economical reasons and that is why people consider more other ways of improving the buildings design, often by focusing on the systems inside the building. Choosing correct ventilation system is crucial not only to provide fresh air, but also to keep good indoor environment in the building and remove unnecessary heat, which nowadays can be very difficult due to increasing heat loads in the spaces connected with high occupancy and equipment use. What is more, the expectations regarding thermal comfort and indoor air quality in building are rising and at the same time there is still a desire to lower the energy use. One of the ways to reach a compromise between energy savings and better indoor environment in the building is to use all the benefits from the most efficient ventilation system.

1.2 Problem Formulation

In this master thesis a new type of ventilation system, diffuse ceiling ventilation, will be described. Although DCV is used on a large scale in livestock buildings in Denmark for more than a decade, it has much wider potential and can be successfully implemented in office buildings, schools or museums. This change however is connected with new requirements regarding thermal comfort and indoor air quality in the spaces designed for people. Even though some investigations on the DCV were done in recent years, there is still lack of information about the system's performance and what is more there is no design guideline for the diffuse ceiling inlet. It is hoped that this report will extend the knowledge about DCV and will be useful both for future research and for practical design of HVAC systems.

Comparing to the other air distribution systems like mixing, displacement or vertical ventilations knowledge of DCV is still insufficient to commonly design ventilation system in buildings. Separate cases that were investigated show the possibilities and effectiveness of this air distribution system,

but are not enough to extrapolate the results for all the room designs. It is important to investigate how the buoyancy force generated by heat loads affect the thermal comfort and indoor air quality in the room and to check how big is the influence of the room's geometry on the buoyancy forces. As one of the main advantages of DCV that is considered is the fact it can handle high heat loads without causing draught. Therefore it should be checked to which extent the system works as a draught free and if other comfort parameters are also fulfilled. What is more the effect of various heat sources distributions within the space on the airflow pattern should be investigated.

Diffuse ceiling inlet is assumed to be used for the whole ceiling but in some cases it can be difficult because part of the ceiling should be used by other systems. What is more there are different types of ceiling construction that can be used in the room. It is worth to give the possibility to designers to know what effect on the ventilation will have change of the inlet area, geometry and construction. This information make possible to consider different solutions and weight their usefulness. Using the whole ceiling as an inlet has another advantage, which is radiant cooling of the room. When cool air is supplied to the room it decreases the surface temperature and cools down the room without a draught risk.

Moreover the investigations made so far focus mainly on diffuse ceiling ventilation used for cooling the room. It is necessary to research further how the DCV can be applied efficiently during heating season or how to use DCV to distribute air to heat the room. When air distributed by diffuse ceiling is warmer than room temperature it can create temperature stratification and decrease significantly thermal comfort in the room.

On the other hand, when cool air is supplied by diffuse ceiling there are concerns that the cool air can accumulate below the ceiling and, due to higher density, at one point it can suddenly flip with the warm air in the room. This can induce high draught in the occupied zone and create strong discomfort. It should be studied if and when it can occur, what can be the reasons for it to happen and how it can be counteracted. The same phenomenon can create or induce instability in the flow pattern in the room, for example by causing unstable direction of the flow.

There are many possibilities to study this problems. Starting from theoretical analysis and similarity principle the buoyancy force can be studied for instance for different room geometry. Another possibility is to make full-scale or small-scale measurements. Because the full-scale measurements are more realistic and straight-forward, they are probably better choice than the small-scale measurements. Next approach to receive results of air distribution from diffuse ceiling can be Computational Fluid Dynamics, CFD.

Because costs of measurements for the new ventilation system and the number of necessary experiments can be very high, Computational Fluid Dynamics may appear very useful and helpful for creating design procedure for diffuse ceiling ventilation. When the CFD model of DCV is ready it gives a way to study many solutions of this air distribution system. Additionally establishing correct model for the specific ventilation system makes implementation of it in design process of new buildings easier. The simple models can be used in preliminary design stage to find the most fitting systems for the building and more detailed models can be used in the detailed design stage.

1.3 Scope of investigations

Two main parts of the investigations can be distinguished. First part includes full-scale measurements on the DCV. Firstly a pressure loss across the real ceiling is measured and it is investigated what is the influence of ceiling's construction on the pressure drop. Next, number of experiments in a test room are carried out under different thermal and air flow conditions. A lot of attention is paid to the influence of the heat loads sources location in the room on the air distribution. It is checked how much conditions in the room will change depending on the heat sources localization—equally distributed heat sources, point heat sources in different locations or heat sources only on one side of the room. Also the influence of height of the heat loads location is tested. With equally distributed heat loads a problem with room air pattern stability may occur and it is tried to investigate it. Another broad field of interest is the importance of the supply area of the ceiling. All of the measurements are conducted in a cooling situation and involve temperature and velocity measurements in various locations in the room. Crucial problem in many rooms, especially with high heat loads is draught, that is why in all of the cases maximum velocity parameter is fundamental. Besides draught rate other thermal comfort indices are analyzed. What is more a size of radiation heat exchange in the room is checked. Finally test with the tracer gas is conducted in the room with purpose of determining the ventilation efficiency.

Second main part of this report is CFD modeling and a Star CCM+ software is used to create a model of the test room. One of the cases, which is tested in the real experiment is a base for the model's geometry and boundary conditions. Next it is tried to validate the model by comparing results of the simulation with measurements results. Finally the test room's model geometry is changed by decreasing the height of the room to be able to see, what is the influence of the room's height on the bouancy forces in the room, as these are the main forces generating airflow for DCV system.

Literature Study

In this chapter available knowledge and literature regarding diffuse ceiling ventilation will be presented. At first a method used for comparing different distribution systems, called a design chart will be described. Next, chosen research results regarding DCV in offices and classrooms will be introduced.

2.1 Design chart

To create good indoor environment and decrease energy consumption in the building it is important to choose and design proper ventilation system. There are known different fresh air supply systems, for instance mixing ventilation, displacement ventilation or piston flow based ventilation. What is more each of the systems can variate depending on different solutions. For instance in case of mixing ventilation it can be different inlet diffusers, such as radial, radial with swirl, nozzle, grille or linear. Different systems have different advantages and disadvantages and when choosing the right system both indoor environment parameters and energy consumption should be taken into consideration. Explanation of main parameters describing thermal comfort and indoor air quality can be found in chapter 3. As discussed in Skistad et al. [2002] many indoor environment factors need to be considered, because different systems can create different problems in the building. For example, when temperature gradient is considered in the room for mixing ventilation it has rather modest effect on the comfort, but for displacement ventilation it can often create problems.

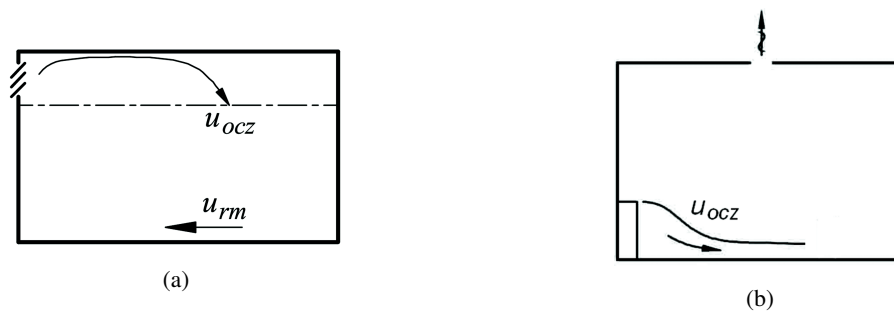


Figure 2.1: Possible locations of maximum velocities in the room considered for design of a) mixing and b) displacement ventilations. u_{ocz} stands for velocity entering occupied zone and u_{rm} stands for reversed motion velocity. [Nielsen 2007]

Another example can be the draught rate, which highest value is often connected with maximum velocity occurring in the occupied zone. That is why for mixing ventilation draught risk is considered mostly on borders of occupied zone, as momentum decreases in a distance, however for displacement ventilation the main problem is at the level of ankles. Possible locations of maximum velocities in the room for mixing and displacement ventilation systems are presented on figure 2.1.

When using ventilation system to counteract temperature increase in the room due to heat gains it is important to know which system can be the most effective and can keep the wanted temperature in the room with the possibly best indoor environment. To choose a system that can keep good indoor environment it is necessary to compare different solutions. One of the ways to do that was to present different solutions on design chart, which was suggested by Nielsen [2011]. The chart was developed based on similarity principle.

The air distribution in the room depends mainly on two forces, which are momentum and buoyancy forces. From similarity approach for air distribution there are two similarity numbers, on which the flow pattern is dependent. The former is Reynolds number, Re , describing the ratio of momentum force to viscous force. The latter is Archimedes number, Ar , describing the ratio of buoyancy force to momentum force and presented in equation 2.1. Expansion coefficient, gravitational acceleration and reference length can be considered as constants for the ventilation in the room. What is more supply velocity can be presented as flow supplied to the room divided by diffuser reference area, see equation 2.2. The area of diffuser is constant for specified system therefore there are only two variables, which are temperature difference and supply air flow. As a result Ar number is presented in equation 2.3.

$$Ar = \frac{\beta g l \Delta T}{u^2} \quad (2.1)$$

$$u = \frac{q_s}{A_s} \quad (2.2)$$

$$Ar = func\left(\frac{\Delta T}{q_s^2}\right) \quad (2.3)$$

Ar	Archimedes number [-]
β	Expansion coefficient [$1/K$]
g	Gravitational acceleration [m/s^2]
l	Reference length [m]
ΔT	Temperature difference between return and supply flow [K]
u	Supply velocity [m/s]
q_s	Supply air flow [m^3/s]
A_s	Diffuser reference area [m^2]

When flow in the room is turbulent and fully developed, which means that Reynolds number is above the critical value, dimensionless variables, like velocity or temperature, should not be dependent on

Reynolds number, however they are still dependent on Archimedes number. It should be noted that flow in the room can be also dependent on different system, inlet area, room geometry and boundary conditions. When the flow in the room is fully developed conditions in the room for instance dimensionless velocity can be express as a function of Archimedes number. When Archimedes number is low the flow in the room is driven by momentum force and when Archimedes number is high the flow is driven by buoyancy forces.

Change of the flow and comfort parameters in the room can be presented on a $q - \Delta T$ graph, which is called a design graph. When designing a ventilation system it is important to know when the system with wanted q and ΔT can be used and will create good indoor environment. The limitation for the system can be for instance minimum air flow to ensure indoor air quality, low noise or minimum supply temperature. The design graph with exemplary limitations can be seen on figure 2.2. Nielsen [2011]

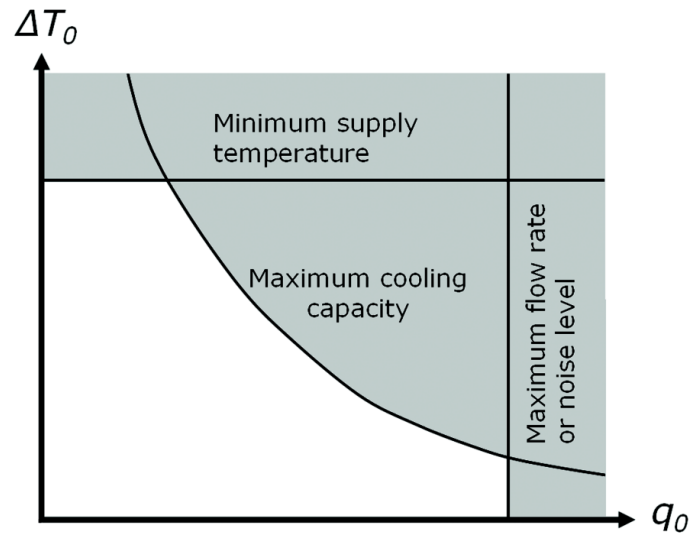


Figure 2.2: Design graph with limitations for distribution systems. [Nielsen 2007]

One of the most important parameters that affect comfort in the room is velocity in the occupied zone. Detailed criteria for allowable air velocities are specified in [DS/EN ISO 7730 2006], but to explain the design procedure in this section it will be assumed, that the maximum acceptable velocity is 0.15 m/s . It is wanted to know the maximum values of ΔT and q for which the velocities in the room will be in comfortable range. One of the possibilities may be conducting an experiment, in which the maximum velocity occurring in the room will be equal to the maximum allowable velocity, however exactly these conditions are very difficult to obtain. It is possible however to recalculate any known conditions in the room (ΔT , q and maximum velocity in the room must be known) to the maximum conditions that are allowed in the room. The process is presented on a design chart on figure 2.3. Grey point represents the measured point with known conditions, this point is next recalculated to the point lying on a limiting curve which corresponds to the velocity equal to 0.15 m/s . This recalculation is possible due to the fact, that airflow parameters are only dependent on Archimedes number, which is kept constant, and independent of Re number. In graphical form this process can be shown as moving on the curve for constant Ar up or down to reach the line

corresponding to 0.15 m/s . What is another advantage of the design chart is that when more points are known for different systems and conditions in the room and they are all plotted on the design chart it is possible to compare these different systems with each other. [Nielsen 2007]

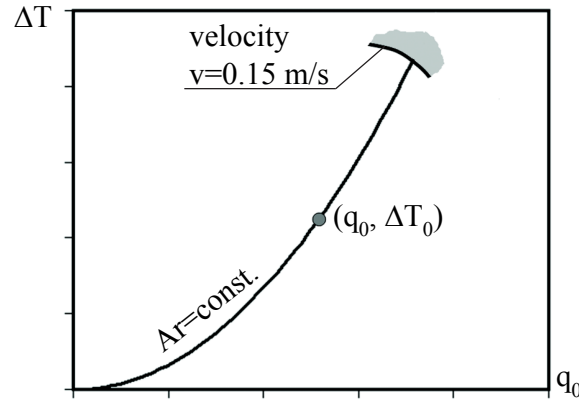


Figure 2.3: Exemplary measured point and the limiting curve representing velocity of 0.15 m/s in the occupied zone presented on a design chart. Nielsen [2007].

In Nielsen [2007] tests with five different air distribution systems for one room are described. The results are presented on a design chart with requirements for maximum velocity equal to 0.15 m/s and maximum vertical temperature gradient in the room between head and ankles level equal to 3 K . Test for the diffuse ceiling are described in [Jakubowska 2009]. The graph connecting all these measurements can be seen on figure 2.4.

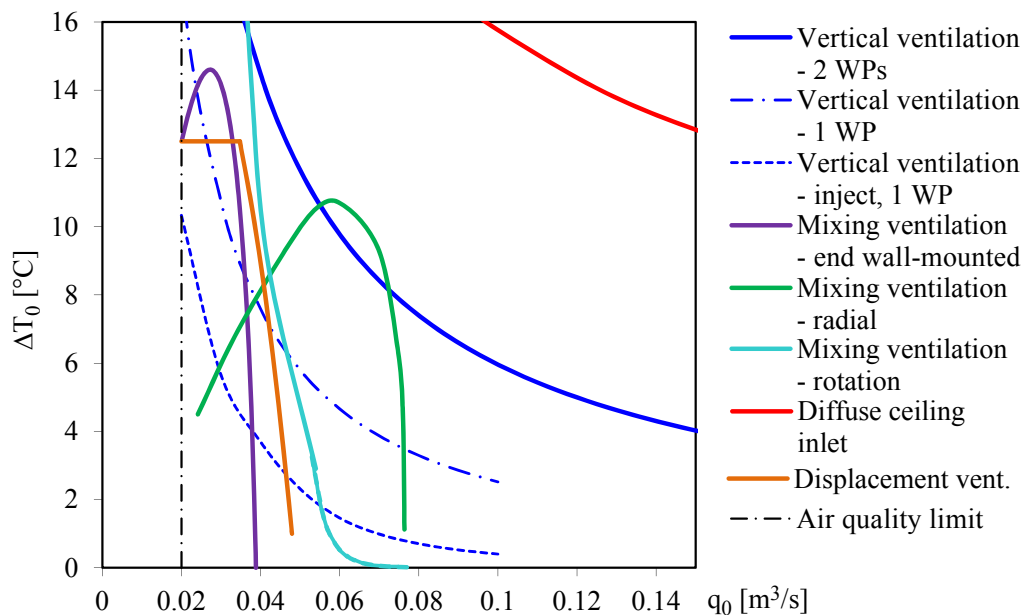


Figure 2.4: Design chart presenting different air distribution systems. WP stands for work place. [Jakubowska 2009]

It is possible to compare different systems with each other and find the most suitable solution. It can be seen that diffuse ceiling ventilation can handle higher heat loads in the room comparing with the rest of the measurements. As a result design chart can support the decision of choosing the air distribution system, however it should be noted the comparison can be done only for the same room size and heat loads distribution.

2.2 Diffuse ceiling ventilation

Diffuse ceiling ventilation is a system in which air is supplied to the room through whole area of the ceiling. According to Nielsen [2011] there can be two types of DCV, one which is controlled by buoyancy flows from heat sources and second one, which is controlled by momentum flow from the supply opening.

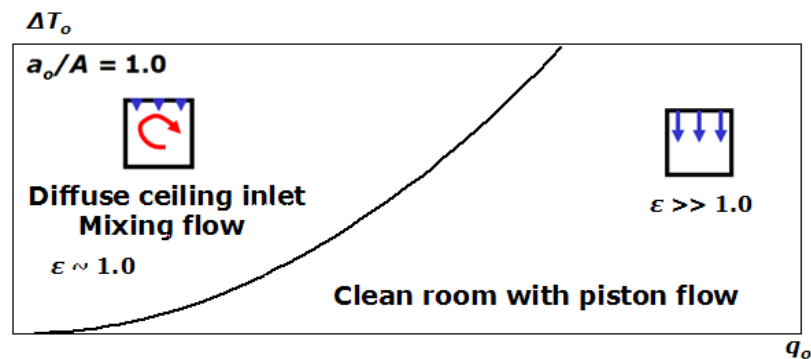


Figure 2.5: Two types of diffuse ceiling systems presented on a q - ΔT graph. [Nielsen 2011]

Figure 2.5 presents these two types of ventilation on a q - ΔT graph. It can be seen that clean rooms with piston flow can be characterised by very high air flow supplied to the room, therefore the air distribution in the room is controlled by the momentum flow. It can be also noticed that piston flow principle is very efficient, which is required in the clean rooms. In this report however the type of DCV with mixing flow will be investigated, in which air distribution in the room is controlled by the heat sources and from now on whenever in the report DCV will be used, it will be related to this type of ventilation. Mixing flow solution can also be seen on figure 2.5 and because it is characterised by high Archimedes number it is placed in different part of the graph, than high momentum flow system. According to Nielsen [2011], when the air change rate in the room is in range from 1 to 5 h^{-1} , the ventilation effectiveness is equal to around 1.0 and therefore this kind of ventilation can be considered as a kind of mixing ventilation. What is one of the biggest advantages of this system however is that it can handle high loads without causing draught, as the air flow is determined by the heat sources and not by the momentum flow from the supply opening.

Originally diffuse ceiling was used in a livestock buildings and this application of DCV is well known in Danish agriculture for more than a decade. According to a PhD thesis from 2006 year, see Jacobsen [2008], diffuse ventilation with fresh air supplied through the entire ceiling was utilized in more than 60% of the finishing pig housing in Denmark. It is known however that there is a

wider potential of using DCV in other types of buildings, like schools, offices, museums and mainly these type of rooms will be the field of investigations in this thesis. In literature it is possible to find papers about investigations of DCV performance in offices and schools and chosen results are presented below.

2.3 DCV in offices

DCV performance in offices was investigated by Peter V. Nielsen and described in a number of articles. In the master thesis, Jakubowska [2009], which was supervised by Peter V. Nielsen and in an article partly based on the aforementioned thesis, Nielsen and Jakubowska [2009], measurements in a full-scale office layout room are described with diffuse ceiling inlet and then compared to 5 other air distribution systems. The set-up of the test room can be seen on figure 2.6(a). The office layout room is simulated using two mannequins and two tables with computers and lamps. Construction of the diffuse ceiling can be seen on figure 2.6(b) and it consists of stone wool insulating panels. The connection between them is very important for the performance of the whole ceiling, because measurements show that almost all air is supplied through the connection slots.

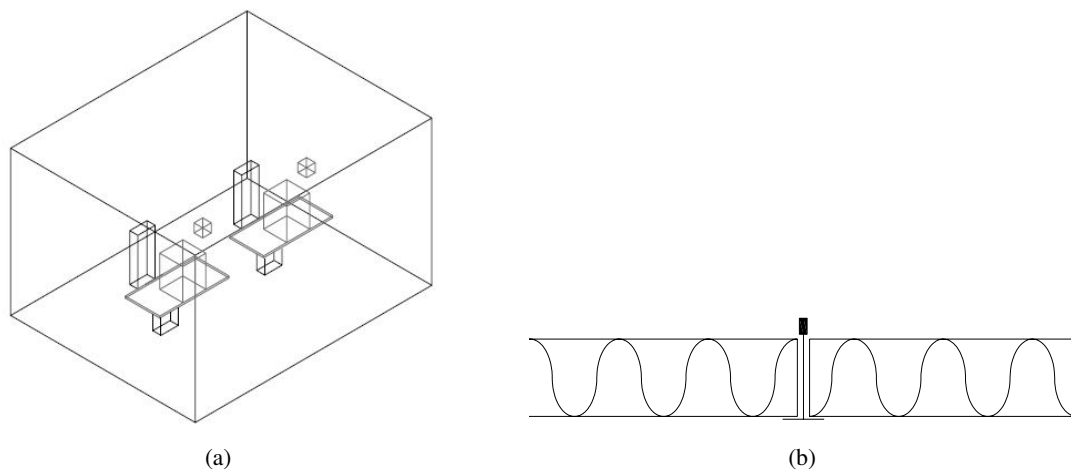


Figure 2.6: Pictures showing a) scheme of the test room set-up used in the full-scale measurements, b) connection of two stone wool insulating panels used in the ceiling's construction. [Jakubowska 2009]

Based on smoke experiment the air distribution in the room is investigated and the results are presented on figure 2.7. It can be seen that the air is supplied through the slots in the ceiling and is falling down in the corners of the room and along the walls, where the highest velocities are observed. Next, the thermal plum of the heat sources in the room is attracting the supplied air and because of the density difference the air is moving up and mixing again with the air supplied from the slots in the upper part of the room.

Some of the results based on temperature and velocity measurements in the test room under different heat load conditions are presented further. In the case with DCV it is showed that there is a dependence between the velocities in the occupied zone and the heat loads in the room, see figure 2.8.

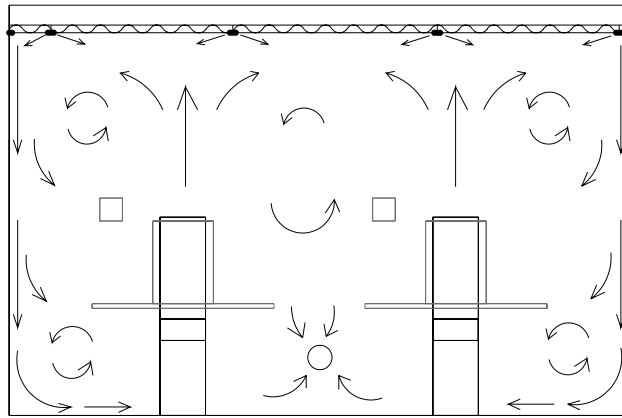


Figure 2.7: Scheme of the air distribution in the test room.[Jakubowska 2009]

It is stated as well that the air flow into the room is not influencing the draught in the occupied zone. Finally it is proved that diffuse ceiling system can handle the highest heat loads in the room without causing a draught, compared to other tested ventilation systems, e.g. mixing ventilation, displacement ventilation or vertical ventilation.

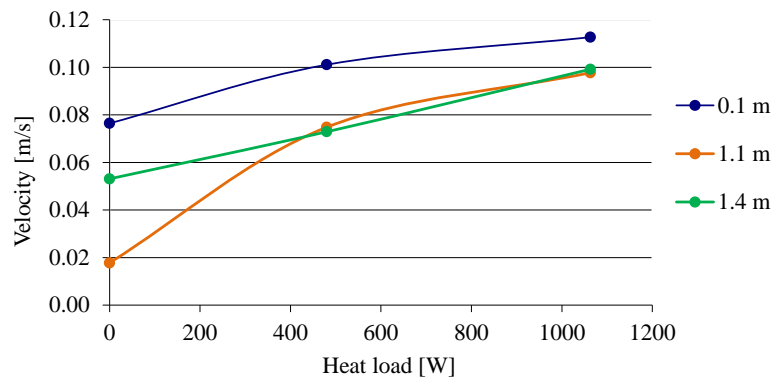


Figure 2.8: Averaged velocities at different heights depending on the heat load in the room.
Flow rate to the room is equal to $0.1 \text{ m}^3/\text{s}$. [Jakubowska 2009]

In above-mentioned papers only cases with cooling in the room are taken under consideration. In further investigations heating situation in the room with DCV was additionally tested. Results of the measurements, as well as CFD predictions for the heating case can be found in Nielsen et al. [2010]. The layout of the office room with one mannequin and a table with computer and a lamp can be seen on figure 2.9. Firstly smoke experiments were made, both for cooling and heating case. They confirmed that the air flow in the room is caused by the heat sources and that the level of draught in the room is low. Smoke experiment also showed that high velocities and entrainment may occur up to 0.5 m from the ceiling, so the ceiling should be mounted at least with this distance from the occupied zone. It was showed as well that there is a minor influence of the exhaust openings locations for the air flow distribution.

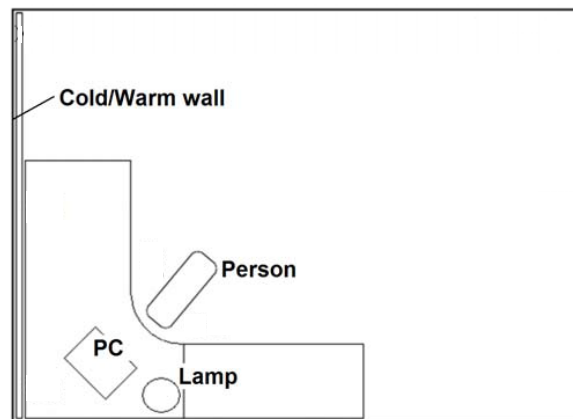


Figure 2.9: Set-up of the test room with locations of the heat sources. [Nielsen et al. 2010]

Experiment with the cooling case and high heat load in the room, as well as high air change rate, equal to 8 h^{-1} , showed that the level of comfort in the office is sufficient. What is more the vertical gradients in the room in different locations are small, see figure 2.10(a). Experiment with the heating case was supposed to simulate a night case without any heat loads, when it is wanted to keep comfort conditions in the rooms until people start working in the morning. As it was expected a vertical gradient is created in the room in this situation and because of no heat sources in the room mixing in the room is minimized, see 2.10(b). That is why in the case of heating it is always recommended to support the system by using additionally a radiator or a floor heating. What is more CFD predictions were made for the heating case and the results of the velocity distribution can be found on figure 2.11. CFD predictions showed that the vertical gradient may be even higher than in the full-scale experiment and what is more there may appear low temperatures in critical locations, e.g. close to a cold wall in winter. This problem can be most likely solved by applying some heat sources in the room.

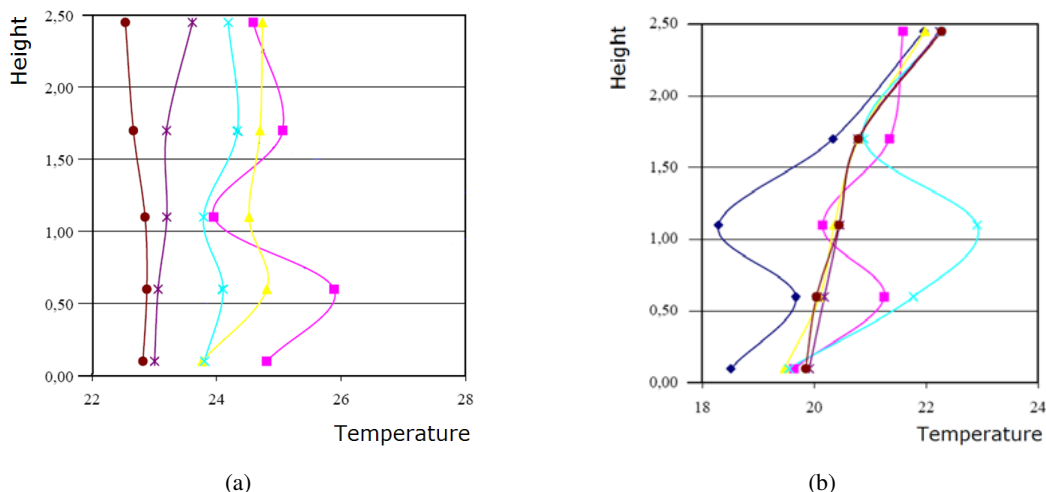


Figure 2.10: Vertical gradients in the room a) case with cooling, 8 h^{-1} air change rates, b) case with heating, 3.5 h^{-1} air change rates. Different colours represent various measurement locations in the room.[Nielsen et al. 2010]

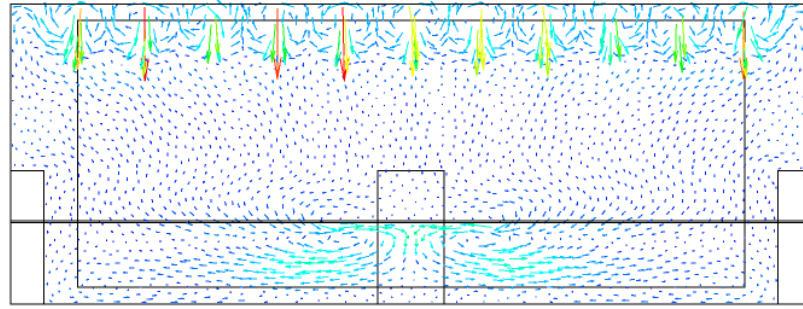
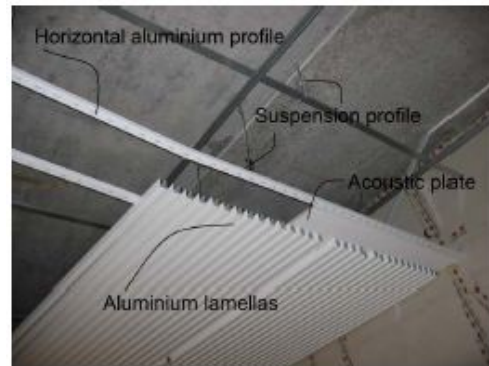


Figure 2.11: CFD predictions of the velocity distribution in the office room with heating case. [Nielsen et al. 2010]

Finally, one more master thesis should be mentioned in the literature study written at the Technical University of Denmark, see Yang [2011]. Full-scale measurements of the DCV were done with purpose of determining the ventilation effectiveness and thermal comfort in the room equipped with an acoustic ceiling. The set-up of the test room can be seen on figure 2.12(a), the office layout of the room is obtained using two symmetrically located desks with computers and two occupants replaced by heated dummies. Furthermore four lights were mounted on the ceiling and electric heating foil is attached to one of the internal walls to simulate solar radiation. Diffuse ceiling construction is presented on figure 2.12(b), it consists of horizontal aluminium profiles, acoustic plates and aluminium lamellae. Supply air is going down through 7 mm holes drilled in the aluminium profiles and further through the spaces between aluminium lamellae.



(a)



(b)

Figure 2.12: Pictures showing a) experiment set-up b) construction of the diffuse ceiling. [Yang 2011]

Results of the experiment showed that the mean ventilation effectiveness is close to 1.0 and exemplary results of continuous 50-minutes measurements for ACH equal to 3.5 h^{-1} are presented on figure 2.13. Ventilation effectiveness close to 1.0 proves very good mixing in the room with DCV ventilation. It should be also noted that measurements with higher ACH equal to 5.1 h^{-1} were also performed and the results did not show significant improvement of the ventilation effectiveness. Results of velocity and temperature are presented on figure 2.14. Vertical air temperature profile in the whole room shows uniform temperature distribution with vertical gradient less than 1 K. Especially

above 1.0 m in the room there is almost no temperature gradient, which confirms very good mixing in the upper part of the room. Results of velocity show that the highest velocities occur on the ankle level in the room, which according to the author might be caused by the reverse flow from the walls towards occupants. What is more, draught rate was calculated in the master thesis, which proved that DCV ensures draught free indoor climate.

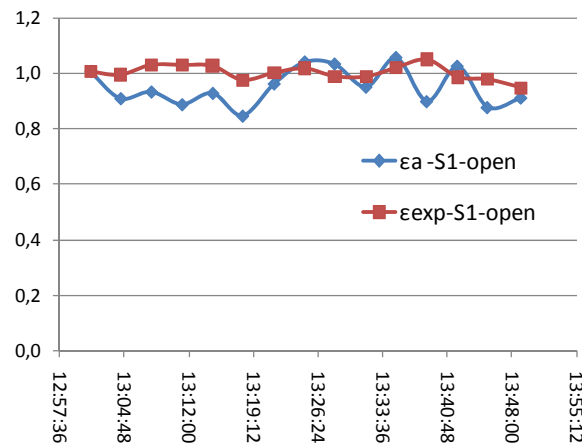


Figure 2.13: Graph presenting ventilation effectiveness in the room. ϵ_a stands for air change efficiency and ϵ_{exp} for personal exposure index. [Yang 2011]

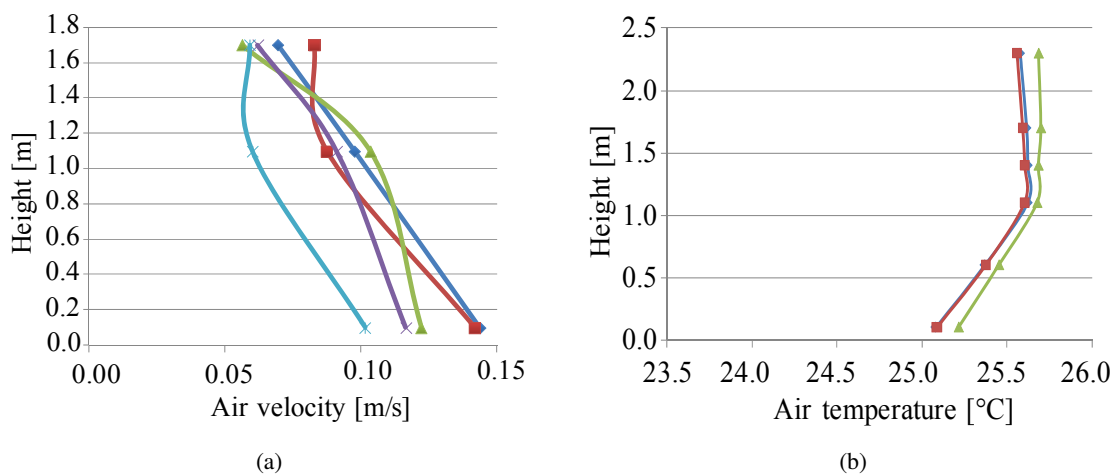


Figure 2.14: Gradients of a) velocity b) temperature in different locations in the room. The ACH in the room is equal to 5.1 1/h. [Yang 2011]

2.4 DCV in schools

Dense occupancy in classrooms is connected with high heat loads and contaminants production and results in high ventilation demands. That is why to avoid risk of draught not sufficient ventilation rate is often used, which results in poor indoor air quality in heating season, while in cooling season common problem is overheating. Keeping thermal comfort and indoor air quality in classrooms is therefore very difficult, that is why a concept of using DCV in classrooms appeared and so far it is

known most widely in Netherlands.

In Jacobs et al. [2008] authors tested implementing DCV in classrooms with regard to thermal comfort, indoor air quality and energy consumption. Three different types of ceiling construction, see figure 2.15, were tested in the laboratory test room of dimensions 4.9 by 3.6 by 3.0 m ceiling height. At first performance of the system was tested in critical laboratory conditions and with two types of heating in the room: radiators below the windows and with floor heating. On figure 2.11 exemplary results of air velocity are presented for two types of heating in the room and for two different air flows. It can be noticed that the supplied air flow is not influencing significantly velocities in the room. At the same time it can be seen that the case with floor heating is showing higher velocities compared to the case with radiators below windows, which indicates how important is the location of heat sources in the room.

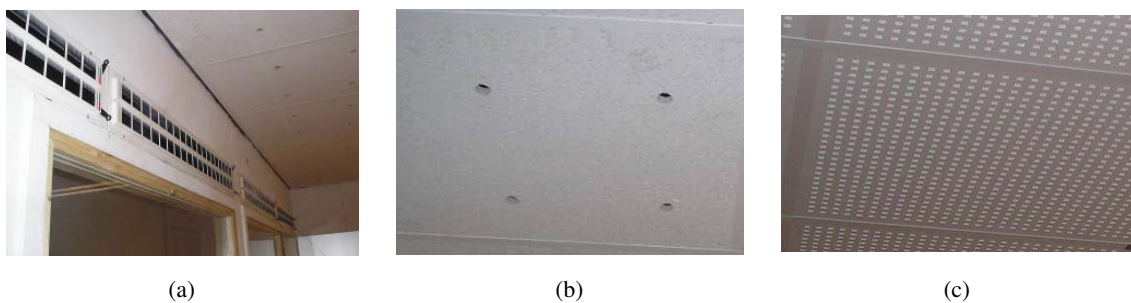


Figure 2.15: Pictures of different construction types: a) facade supply, b) DCV large perforations, c) DCV small perforations. [Jacobs et al. 2008]

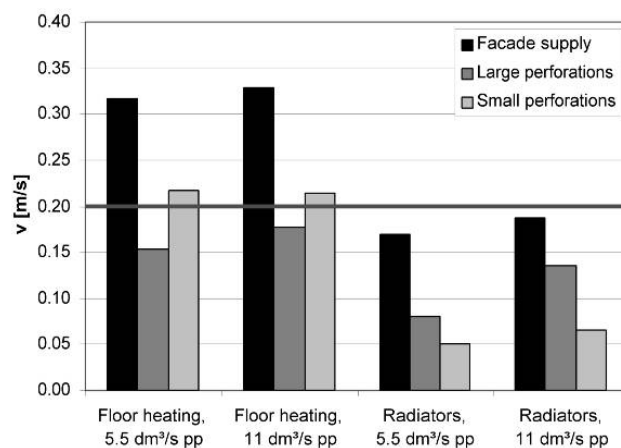


Figure 2.16: Velocities measured at a height of 0.1 m. [Jacobs et al. 2008]

Second part of the experiment was a full-scale study in real classrooms, which lasted 6 weeks during a heating period. In the pilot classroom a simple DCV system was installed, see figure 2.17, and conditions in this classroom were monitored as well as conditions in a reference, not modified classroom.

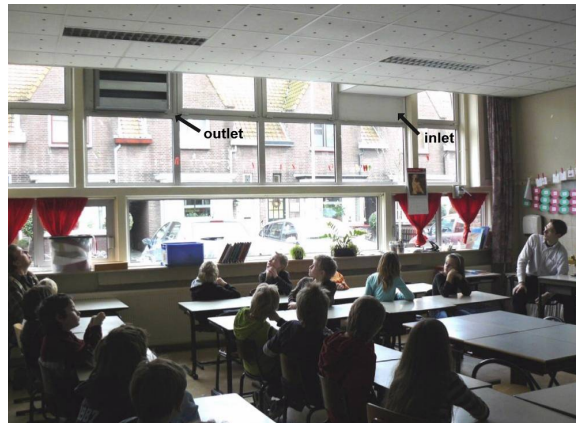


Figure 2.17: DCV system mounted in the pilot classroom. [Jacobs et al. 2008]

As a result of the experiment it was proved that the diffuse ceiling concept can be successfully implemented in the classroom. The ventilation rate in the pilot classroom was controlled by CO₂ with the set point equal to 1200 ppm. In this way it was possible to keep the CO₂ concentration below this level, while in the reference classroom the CO₂ concentration reached up to 2700 ppm. At the same time questionnaires were given to children during the experiment period, with questions about the quality of air in the classrooms and results proved that the IAQ in the classroom was improved significantly. In the paper Jacobs et al. [2008] it is not clearly stated, what was the ventilation principle in the reference classroom and it is possible that indoor air quality can be improved also by using other system than DCV with support of CO₂ control. It is shown however that DCV in classroom can work successfully and can ensure good indoor environment without a draft risk in a wide range of flow rates and temperatures. What is more authors stated that the key factor for obtaining a ventilation system without draught is the proper air distribution and the optimal one for DCV is to use the whole ceiling as an air supply area.

Design Criteria

In this chapter design criteria, which will be used further in the report are going to be defined. These includes criteria for thermal comfort and indoor air quality, generally named as indoor environment criteria. It should be noted that acoustic environment criteria will not be included in this report.

At the beginning it is important to define the aimed category of environment quality. According to CR 1752 [1998] there are three categories of indoor environment quality, namely category A, B and C. In current report it is decided to use category B, with average level of expectations, as a reference one. Category B ensures comfortable indoor environment and at the same time does not require as high amount of energy use as category A. That is why category B will be used further to specify the design criteria for thermal comfort and indoor air quality. It should be stated however, that no matter which building category is chosen, when designing in Denmark the requirements in the Danish Building Regulations has to be always fulfilled, see BR10 [2010].

All the defined criteria are required to be met in the part of space, which is called an occupancy zone and that is why at first this zone will be described. Further in this chapter design criteria for thermal comfort and indoor air quality criteria will be introduced.

3.1 Occupied zone

The concept of occupied zone, OZ, is created to distinguish the volume of the room that is used the most from the part that people do not need to spend time or the conditions in the room can be worse. In standard buildings it is hard to keep correct conditions for instance next to windows or radiator. Moreover in some spaces it is irrelevant for people what are conditions for example at 3 m height from floor or at the corner of the room, where people are not present.

Therefore the occupied zone can be defined as a volume in which requirements of the thermal comfort and indoor air quality for people are needed to be satisfied. As a result only part of the room should be taken into consideration when designing conditions in the room. Also European standards define what is occupied zone and what volume ought to be considered in the room. The detailed information about default distances used for non-residential buildings can be found in table 3.1. The exemplary occupied zone is presented on figure 3.1. [EN 12792 2003] [EN 13779 2007]

Element	Default value [m]
External windows, doors, radiators	1.0
External and internal walls	0.5
Floor (lower boundary)	0.05
Floor, standing position (upper boundary)	1.8
Floor, sitting position (upper boundary)	1.3
Doors, transit zones	Special

Table 3.1: Default distances defining occupied zone in the room for a non-residential building. [EN 13779 2007]

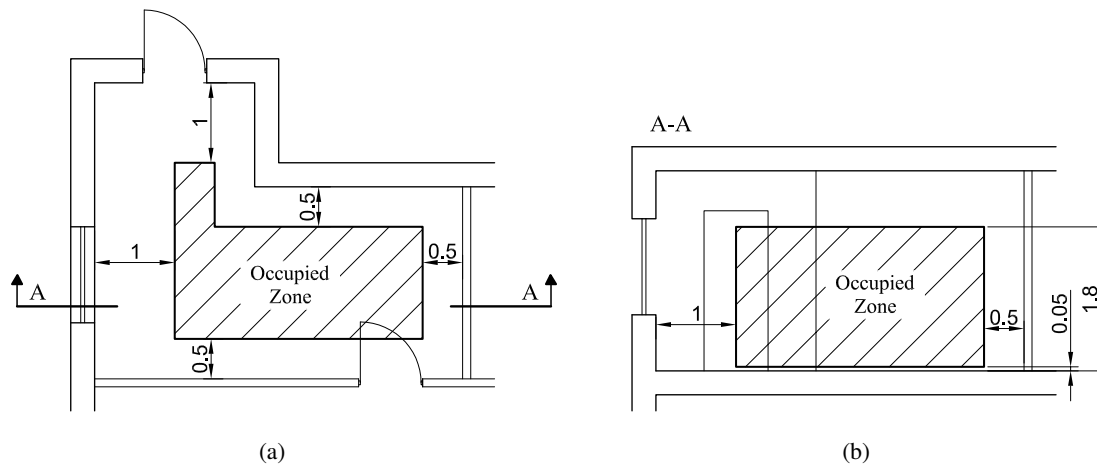


Figure 3.1: Default distances defining occupied zone in an exemplary room for a non-residential building presented on a) plane and b) cross-section. On the basis of EN 13779 [2007].

3.2 Thermal comfort

According to the BR10 [2010] comfortable and healthy temperatures should be maintained in the building depending on the operational conditions of the building and the activity level of people inside. Danish Building Regulations refer then to the international standard DS/EN ISO 7730 [2006], where design criteria for different types of spaces are specified. Thermal environment criteria are presented for category B buildings for types of rooms like single and landscaped offices, classrooms and conference rooms. Operative temperature in cooling season should be equal to $24.5 \pm 1.5^\circ\text{C}$. Criteria for the operative temperature are based on the activity level, here 70 W/m^2 , which corresponds to a sedentary activity, and is defined for clothing which is 0.5 clo during the cooling season. Mean air velocity should be lower than 0.19 m/s . The criteria for maximum mean air velocity corresponds to a turbulence intensity of approximately 40%.

An issue connected with thermal comfort is temperature effectiveness of the ventilation system, which according to Skistad et al. [2002] can be calculated using equation 3.1.

$$\varepsilon_t = \frac{t_e - t_s}{t_{oz} - t_s} \quad (3.1)$$

ε_t	Temperature effectiveness [-]
t_e	Extract air temperature [°C]
t_s	Supply air temperature [°C]
t_{oz}	Mean air temperature in occupied zone [°C]

Further in this section particular indices regarding local thermal discomfort will be described, however here is presented a collective table 3.2 with the requirements for these indices in category B of buildings.

DR	PD_{VTG}	PD_{RA}
[%]	[%]	[%]
<20	<5	<5

Table 3.2: Requirements regarding local thermal discomfort indices, namely Draught Rate (DR), Percentage Dissatisfied due to vertical temperature gradient (PD_{VTG}) and Percentage Dissatisfied due to radiant asymmetry (PD_{RA}) for category B of buildings. [CR 1752 1998]

3.2.1 Draught rate

One of the most common problems in the ventilated spaces is draught. That is why in this report it is decided to focus a lot on a draught in the room as one of the main local discomfort parameters. In accordance with DS/EN ISO 7730 [2006] draught rate, DR, is used to describe risk of draught, which represents the percentage of people predicted to be bothered by draught. DR can be calculated using equation (3.2), the draught model applies mainly to a sedentary activity, with a thermal sensation for the whole body close to neutral. It should be noted that the model predicts draught at the neck level and can overestimate the values for feet and arms level. It should be also highlighted that the maximum velocity that is allowable in the occupancy zone is connected with draught risk and it can vary due to the same parameters, namely local air temperature and local turbulence intensity. This means that for either higher air temperature and lower turbulence intensity mean air velocity could be higher.

$$DR = (34 - t_1) (\bar{u}_1 - 0.05)^{0.62} (0.37 \cdot \bar{u}_1 \cdot Tu + 3.14) \quad (3.2)$$

DR	Draught rate [%]
t_1	Local air temperature, from 20°C to 26°C, [°C]
\bar{u}_1	Local mean air velocity, < 0.5 m/s, [m/s]
Tu	Local turbulence intensity, 10% to 60%, [%]

3.2.2 Other local discomfort indices

Another important factor, which may cause local discomfort is vertical air temperature difference between person's head and ankle level, 1.1 and 0.1 m. The index, which describes it is Percentage Dissatisfied, PD_{VTG} , which is a function of the temperature gradient between head and ankles. Equation, which is used to calculate PD_{VTG} can be found in appendix A1.1. PD_{VTG} equal to 5%, which is a limiting value for B category of buildings, corresponds to a temperature difference between head and ankles equal to 3 K.

The last local discomfort parameter, which will be taken into consideration in this report is connected with the radiant asymmetry in the room. Although people are the most sensitive to an asymmetry caused by warm ceiling or cool walls and in the case of diffuse ceiling ventilation it is expected to have a situation with cool ceiling, it is good to check if the asymmetry caused by cool ceiling will be in the comfortable range. In this case Percentage Dissatisfied index, PD_{RA} , is used, which here is a function of the radiant asymmetry, equation used to calculate the index can be found in appendix A1.1. PD_{RA} equal to 5%, which is a limiting value for B category of buildings, for the case with cool ceiling corresponds to a radiant temperature asymmetry equal to 14 K difference between floor and ceiling temperature.

3.3 Indoor air quality

According to CR 1752 [1998] there are two main requirements regarding the indoor air quality in the room. First is that breathing in the room should not cause health risk and second requirement is that occupants should perceive air in the room as fresh and pleasant. In this report health aspects are not going to be taken into consideration and only some of the comfort aspects related to the perceived air quality are going to be checked. Following previous assumptions about the aimed category of building, also here the requirements for perceived air quality are going to be given for the B category of buildings. In CR 1752 [1998] can be found ventilation rates for different category of buildings and various types of the rooms. Requirements for types of rooms similar to the ones considered in further parts of the report are presented in 3.3, where specified ventilation rates apply to the enclosed occupancy in the room. Later in the report, where it is referred to IAQ, two values for minimum ventilation airflow are used. For single and landscaped office the values are rounded to $0.04 \text{ m}^3/\text{s}$ and for classrooms to $0.12 \text{ m}^3/\text{s}$.

Room type	Occupancy [person/m^2]	Ventilation rate [l/sm^2]	Minimum airflow [m^3/s]
Single office	0.1	1.4	0.039
Landscaped office	0.07	1.2	0.033
Classroom	0.5	4.2	0.117
Conference room	0.5	4.2	0.117

Table 3.3: Required ventilation rate for standard occupancy for different types of rooms in category B buildings with exemplary minimum airflow results for the test room. [CR 1752 1998]

It should be noted that the requirements for the ventilation rate in the above table apply for the ventilation effectiveness equal to one. According to CR 1752 [1998] ventilation effectiveness in the room can be calculated using equation (3.3). This equation can be used to present how effective is the ventilation system to supply fresh air. With higher efficiency of the system good indoor environment can be maintained using lower energy consumption for ventilation.

$$\epsilon_v = \frac{C_e - C_s}{C_{bz} - C_s} \quad (3.3)$$

ϵ_v	Ventilation effectiveness [-]
C_e	Pollution concentration in the extract air [ppm]
C_s	Pollution concentration in the supply air [ppm]
C_{bz}	Pollution concentration in the breathing zone [ppm]

Experiment set-up

In this chapter experiment set-up is described. At first test room and the construction of diffuse ceiling inlet is presented, next measurement points are introduced and finally particular cases set-up is specified. It should be noted that all the dimensions on drawings in the report are given in meter units.

4.1 Test room

The full-scale measurements are carried out in the laboratory of Civil Engineering Department of Aalborg University. The test room is located inside one of the laboratory rooms and it has inner dimensions of 6.00 by 4.65 by 4.40 m height. Given height is the height of acoustic ceiling mounted in the room, see figure 4.1(a).

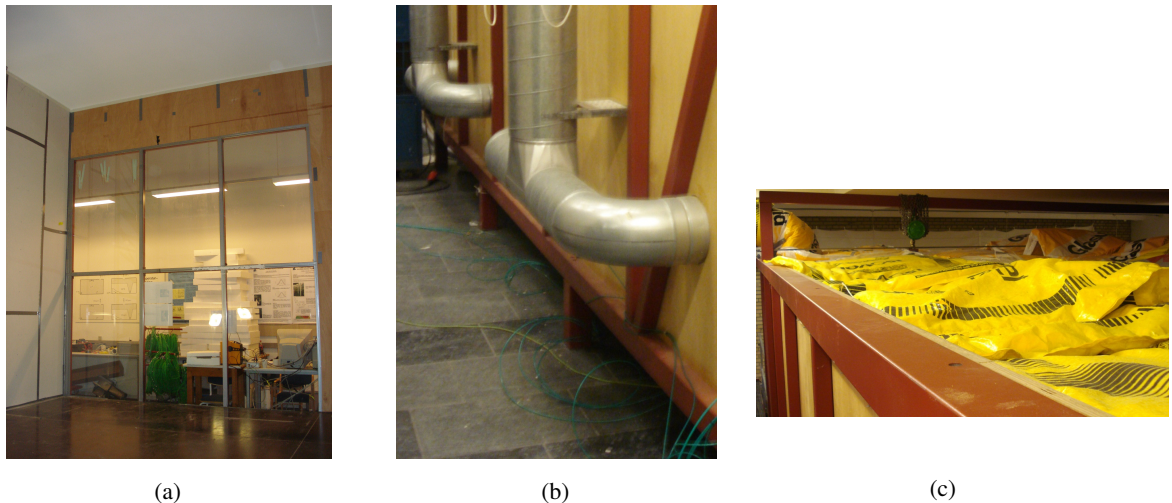


Figure 4.1: Pictures showing a) test room from inside, b) test room from outside, c) insulation above the room.

Schemes of the room with basic dimensions can be seen on figure 4.2. More detailed drawings of the room can be found in appendix I. The room has two wooden walls, on the scheme signed as Wall 1 and Wall 4, one wall is a drywall, Wall 2, and one wall is almost all made of glass, Wall 3. Wooden floor is partly insulated with foamed polystyrene, the walls are not insulated and above the room there is mineral wool insulation, see figure 4.1(c). Because the test room is located in the

laboratory room, see figure 4.1(b), it is surrounded by indoor air with controlled temperature, so lack of insulation on some of the surfaces should not influence significantly the conditions of experiment.

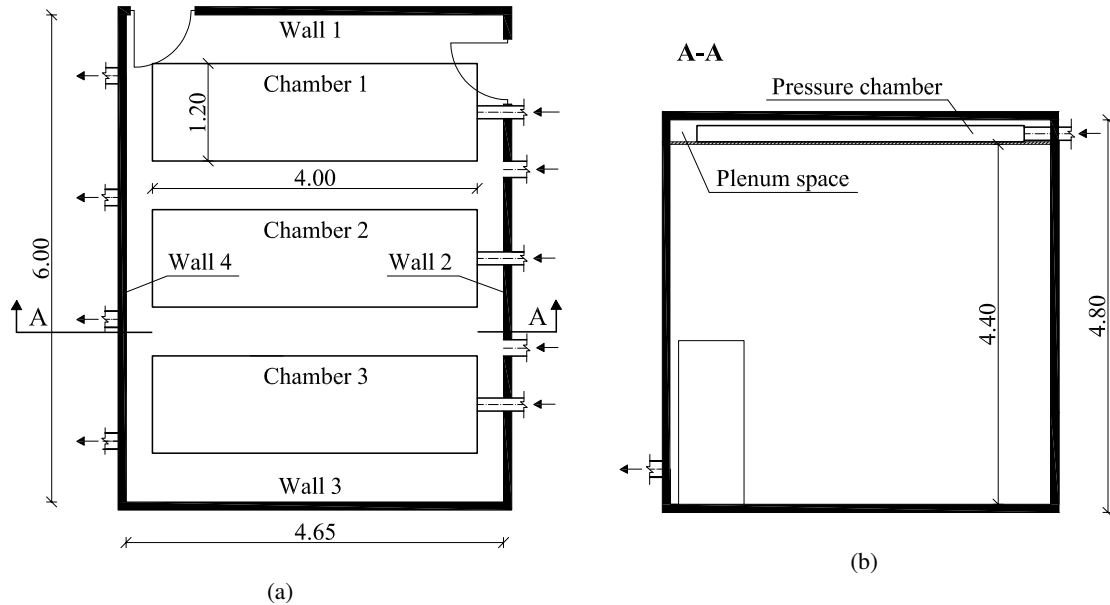


Figure 4.2: Schemes of the test room a) plan view, b) cross-section.

4.1.1 Construction of the ceiling

The ceiling in the test room is used as supply air inlet diffuser. As mentioned above, acoustic ceiling is mounted on 4.40 m height. Construction of the ceiling is design and made by STO company. Volume above the ceiling is divided into four spaces. Three of them are pressure chambers and the last one is a plenum space that fills the rest of the space around and above the chambers. Precise size and location of the chambers and plenum space can be seen on figure 4.2. Inlet air is supplied to the chambers and the plenum space directly from inlet ducts. A picture of Chamber 2 during construction before the ceiling was added can be seen on figure 4.3. The connection between the ceiling and the chambers is tighten.



Figure 4.3: Picture showing Chamber 2 during construction process of system above the ceiling.

One of the requirements for the ceiling's construction is to make it as clean, white and plane as possible, because some of the test are made for investigation of possible application of the ceiling for Oslo National Museum. Therefore additional advantage of the diffuse ceiling ventilation is the aesthetic aspect of the ceiling without any visible diffusers. Surface of the ceiling can be seen on figure 4.4(a), where the contrast between the ceiling and walls can be observed. The final layer of the ceiling is made of white paint that is applied on the diffusive part a few times. On figure 4.4(b) close-up of the ceiling surface is shown, where it can be seen that the paint has a sand structure and the particles are much smaller than 0.5 mm. That is why the ceiling looks like a plane surface, even when seen from a small distance, however disadvantage of this solution might be that because the small particles are close to each other and the space between them is strongly limited, they can affect airflow through the ceiling.



Figure 4.4: Picture of a) ceiling surface, b) close-up of ceiling surface construction.

The main part of the ceiling diffuser is made of larger particles with diameter varying between 1 and 2 mm. The shape of particles is mostly round and the surface is smooth, but the material is porous to make the ceiling lighter. The particles are connected with each other, which form a 25 mm layer. The sample of the ceiling diffuser with presented three layers of different materials can be seen on figure 4.5.

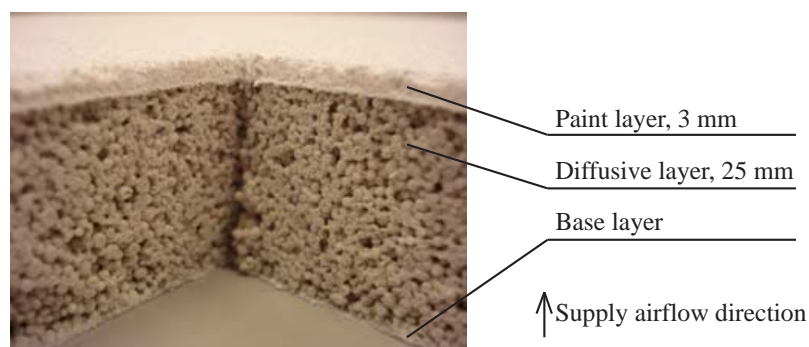


Figure 4.5: Picture showing a cross-section of a diffuse ceiling sample with description for three construction layers. The sample is turned upside down comparing to normal location in the ceiling.

It can be observed that the spaces between the particles in the diffusive layer are much bigger than in paint layer. It should be noted that the purpose of the diffuse ceiling is not only to distribute air equally, but also to attenuate the noise level, so it can also be called an acoustic ceiling.

The third layer is a material that is a base used to start construction process of the ceiling. Summing up the construction of the ceiling is not uniform and the paint layer is very condense comparing to diffusive part. Diffusive layer not only distribute supply air but also can work as acoustic ceiling to decrease noise level.

4.2 Measurement points and methods

In this section points, where various parameters, namely velocity, temperature and tracer gas concentration, are measured in the experiment, will be described. What is more information about some of the measurement methods are given. Measurements will be described separately for velocity, temperature and tracer gas concentration measurements. When describing various measurement points reference is made to adequate equipment, which is described in section A2.1 in appendix. Figures in this chapter presenting location of the equipment and sensors are based on symbols, which can be seen in table 4.1.

Symbol	Description
●	Thermocouple
○	Anemometer
⊠	Tracer gas concentration
✕	Movable measuring column
✕	Fixed measuring column

Table 4.1: Symbols used to present sensors and equipment.

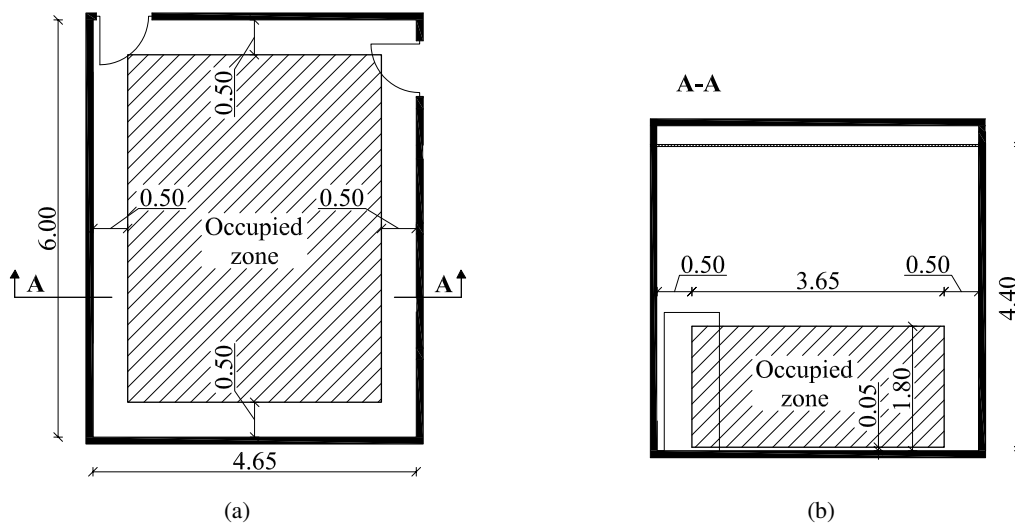


Figure 4.6: Occupied zone in the room on a) plan, b) cross-section.

The main purpose of the measurements is to check the thermal comfort in the occupied zone and therefore the majority of measurements are conducted in this volume. It can be assumed that the room is located inside the building, so referring to dimensions from section 3.1 the occupied zone for the room can be seen on figure 4.6.

4.2.1 Velocity

Firstly to analyse conditions in the occupied zone 25 locations for three different heights are set in the room. For all the measurements it is wanted to find the maximum velocity in the occupied zone and the velocity distribution within it. It is also important to measure conditions at border of occupied zone and that the measuring points are equally distributed in the area of the floor to represent the area correctly. To measure velocity hot-sphere anemometers are used, which are described in section A2.1. Precise location of measuring points can be seen on figure 4.7. For each location of movable column there are three heights, where velocity is measured, namely 0.1 m, 1.1 m and 1.7 m. The heights for head, abdomen and ankle levels are chosen based on DS/EN ISO 7726 [2001] for standing person, comfort heterogeneous conditions and can be seen on a movable column on figure 4.7(b). Moreover height 1.1 m can be used as a height of sedentary person head.

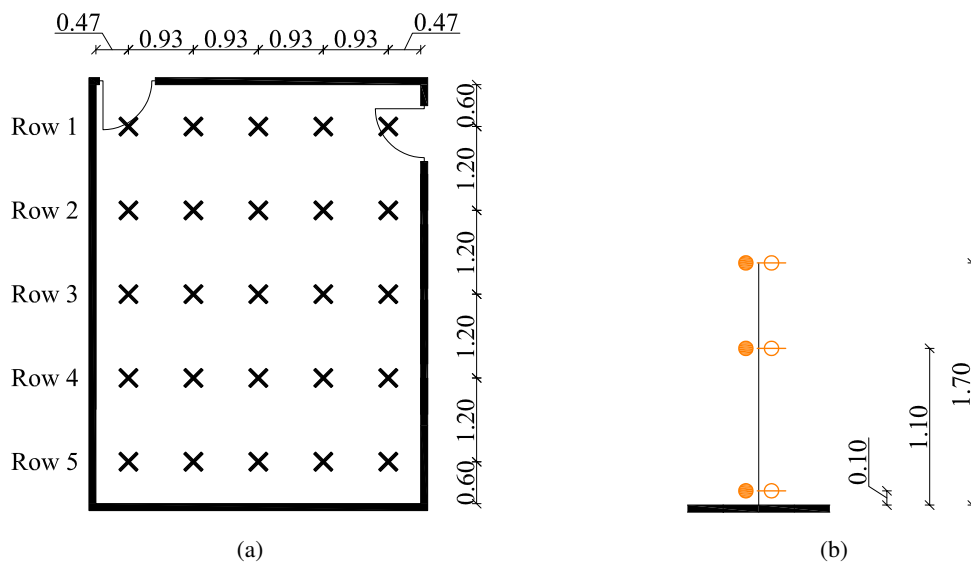


Figure 4.7: Scheme of a) location of movable columns on a plane view, b) measuring points on three different heights on a movable column.

For the measurements five movable columns are used and the measurements are conducted five times, in five rows. Picture of movable column with sensors on 0.1 m, 1.1 m and 1.7 m heights can be seen on figure 4.8(a). On each height there is mounted a hot sphere anemometer and next to it a thick thermocouple. More information about temperature measurements can be found in section 4.2.2. The close-up on the sensors can be seen on figure 4.8(b). Summing up there are 15 anemometers used for measuring velocities for one row and there are 75 velocity measuring points in total.

All the velocities in described points are measured during 3.5 minutes with a 0.1 s interval and the measurements are performed 5 times with a one second break, which gives total time of mea-

measurements equal to around 17.5 min. Next mean velocity values are calculated for all of the points from total, 17.5 min, measuring period. As described above it is the most important to find maximum velocities in the occupied zone and these velocities should not be directly affected by the heat sources plume's influence and therefore during data treatment not representative velocities are excluded from the investigations.

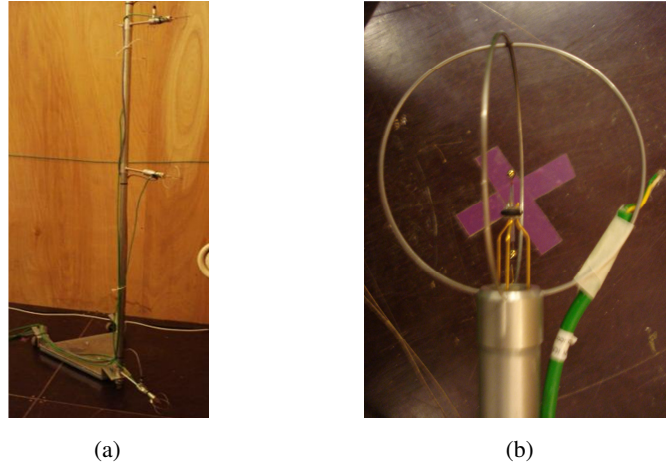


Figure 4.8: Pictures of a) movable column with three sensor locations, b) temperature and velocity sensors with violet cross on background representing movable column sensors location.

4.2.2 Temperature

Firstly to analyse conditions in the occupied zone thermocouples are placed at the same locations as anemometers, which are 25 locations on a plane for movable columns and in each location there are three different heights, see figure 4.7. On each height there is mounted a thick thermocouple next to an anemometer. Thermocouples are mounted on side of anemometers with a minimum distance to the heated sphere equal to 6 cm, see figure 4.8(b). It is advised to place thermocouples on a side with a distance to anemometers due to the effect that the heated sphere of anemometer has on the temperature measurement. According to measurements conducted by cited authors and discussed in personal correspondence the effect of heated sphere on thermocouple can be neglected for distance larger than 6 cm [L.M. Jensen and A.S. Palle, personal communication, March 05, 2013]. Detailed description of thick thermocouples used in measurements can be found in appendix in section A2.1.

Secondly to observe conditions in the rest of the room and to see a vertical temperature gradient there are established two fixed columns. The former column is located in the middle of the room and the latter column is in the corner of the room between Wall 1 and Wall 2. Detailed location of the fixed columns on a plane of the room can be found on figure 4.9(a). On each fixed column there are eight thermocouples, which can be seen on figure 4.9(b). The first three points starting from the floor are on the same height as for the movable columns. The highest point is located 10 cm below the diffuse ceiling. The last four sensors are distributed with a distance of 0.6 m from each other starting from the thermocouple at 1.7 m height and going up. Picture of the fixed column located in the middle of the room can be seen on 4.9(c).

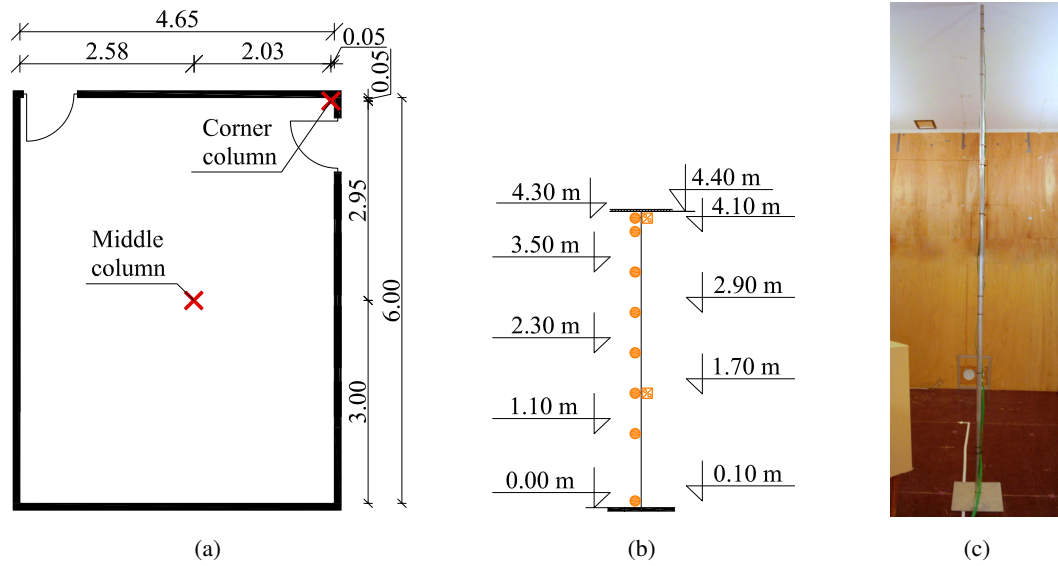


Figure 4.9: Fixed columns measuring points a) location on a plane, b) location on a middle column, c) picture for middle column.

Another thermocouples are placed in the middle of the room, below the ceiling. These thermocouples are thin and are added above the middle column to be able to focus on vertical temperature gradient below the ceiling to see effect of radiation heat exchange between the room and the ceiling. Detailed description of thin thermocouples can be found in appendix in section A2.1. The scheme of the thermocouples location can be seen on figure 4.10(a) and a real picture on figure 4.10(b).

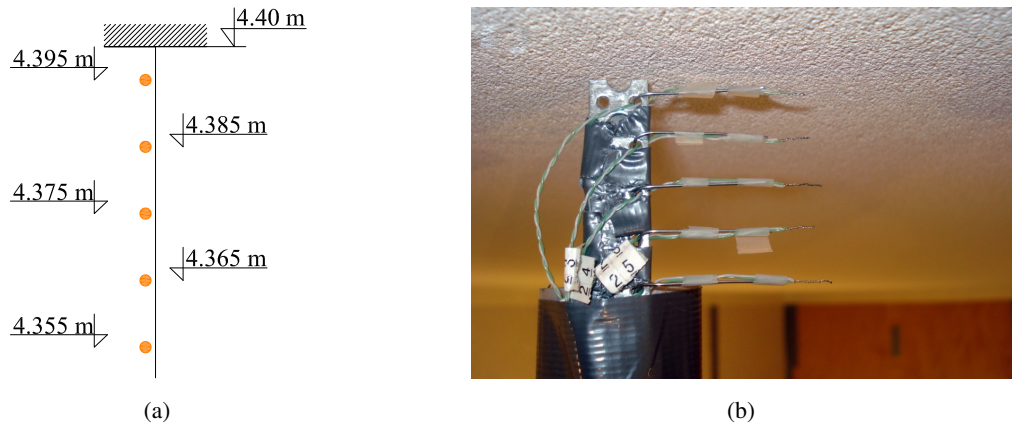


Figure 4.10: Thin thermocouples located below the ceiling on a) scheme, b) picture.

Next thermocouples are used to measure temperature of the room surfaces. For each wall and floor there are two thin thermocouples connected to the surface by silicon paste, which increase heat transferred between surface and sensor. Because Wall 1 and Wall 3 and also Wall 2 and Wall 4 have the same size the placement of thermocouples is similar. Location of thin thermocouples on the Walls 1 and 3, Walls 2 and 4 and on the floor can be seen on figure 4.11(c), 4.11(a) and 4.11(b), respectively.

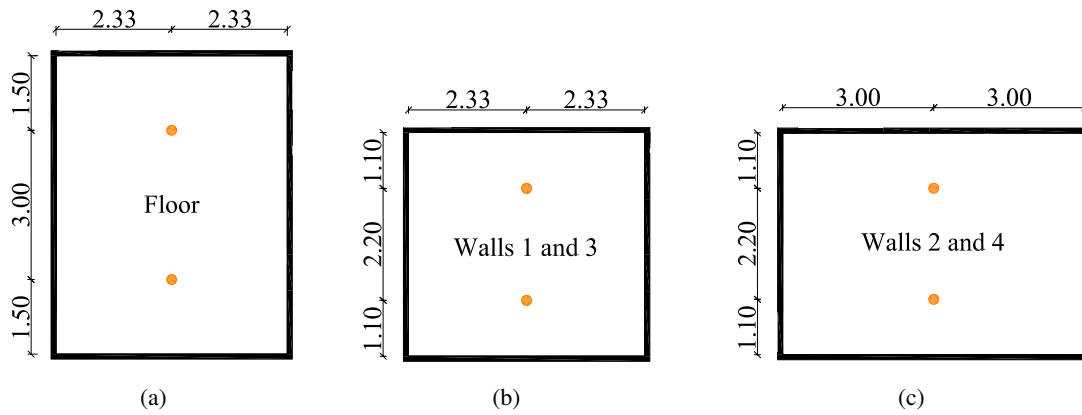


Figure 4.11: Thin thermocouples located on a) floor, b) Wall 1 and Wall 3, c) Wall 2 and Wall 4.

Another thin thermocouples are placed on the ceiling. Because they are used to measure surface temperature again thermocouples are connected with the surface using a silicon paste, see figure 4.12(a). Below each chamber there is placed one thermocouple, however below Chamber 1 there are placed three thermocouples in total to observe if the temperature of supply air is uniform on the ceiling surface. The location is chosen so it can represent equal area of the chamber. Because the rest of the ceiling can have different temperature it is decided to place three thermocouples on each side of Chamber 1, with a distance to its edge equal to 0.3 m. The thermocouples placed on the diffuse ceiling can be seen on figure 4.12(b). For some of the measurements the thermocouple below Chamber 2 is not measuring correctly and a mean value from other chambers is used in gray colour in these results.

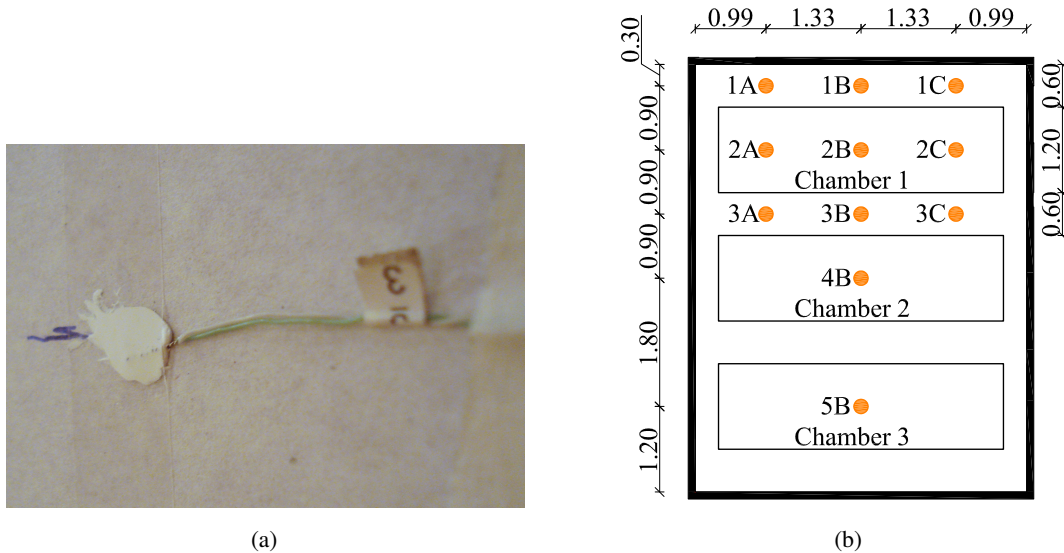


Figure 4.12: Thin thermocouples: a) placement on the surface with use of silicone pasta, b) located on the ceiling.

The last thermocouples, which are thick, are placed in the exhaust and inlet ducts to measure air temperature and in the areas surrounding the room to measure temperature around the room. Two

thermocouples placed in exhaust can be seen on figure 4.13(a). Next five thermocouples are placed in the inlet ducts. It is wanted to measure inlet temperature, which should be constant and uniform in all the inlet ducts. Because of it the ducts are insulated, see figure 4.13(b). Three thermocouples are placed in three inlet ducts for three chambers and two thermocouples in duct supplying air to the rest of diffuse ceiling, but one of these two is broken, so it is not presented in results and drawings. Precise location of these thermocouples can be seen in appendix I.

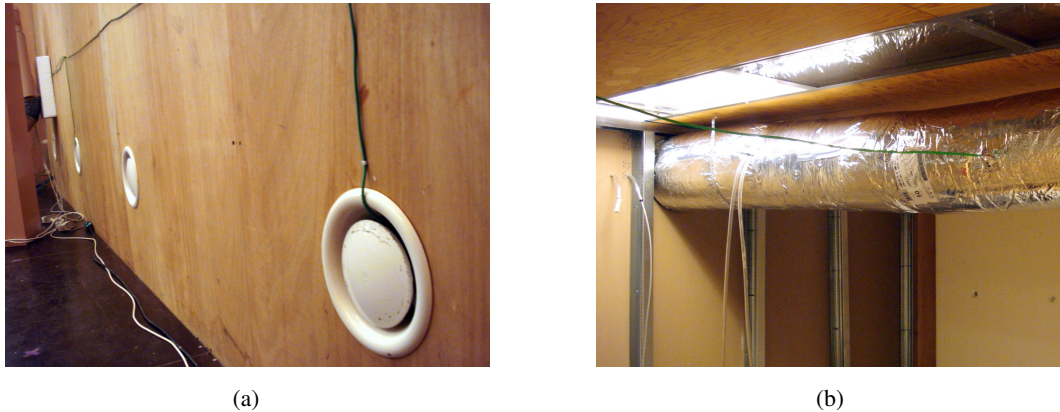


Figure 4.13: Thermocouples measuring air temperature placed in a) exhaust ducts, b) insulated inlet duct.

It should be noted that all tests in the experiment are performed in the steady state conditions, so it is expected that temperatures are constant during whole measuring time. Before each test is started it is ensured, that conditions in the room are stabilised and to minimize possible errors the temperatures in particular points during data treatment are recalculated to mean values of temperatures logged for the stabilized measuring time.

4.2.3 Tracer gas concentration

Equipment used for tracer gas concentration monitoring is described in appendix in section A2.1. Tracer gas concentration can be measured in six points at one time. In measurements performed for the ventilation efficiency calculations first point is located next to the bottle with tracer gas to assure low concentration of N_2O in the laboratory. In the next two points concentration is measured in Chamber 3 and Chamber 1. Location of measuring points in chambers and exhaust duct can be seen in details in appendix I. It should be noted that dosing to and sampling from chambers is conducted by porous pipes so the tracer gas and its samples are distributed in or from whole chamber. Sampling tubes are located in Chambers 1 and 3 to be able to observe reverse flow that can be generated from heat gains located below them. Because it is important to have white ceiling for long time the reverse flow should be negligible, otherwise the pollution from the room can be fouled the ceiling surface. Fourth point is located in common exhaust duct. Fifth and sixth tubes are placed in the room on the middle column on height equal to 1.7 m and 4.3 m, see 4.9(b). It should be noted that additional measurements of tracer gas concentration are performed to check the performance and tightness of the ceiling's construction and the set-up for these measurements is not included in the main report and can be found in appendix A3.3.

4.3 Test cases

In this section set-up of various test cases carried out in the experiment is introduced. Firstly heat sources used in the experiment to create different test cases are introduced and next particular test cases conditions are specified. It should be noted that set-up of Case 5, Case 14 and Case 13 with heat gains in the room equal to 25 W/m^2 are used as well for measurements for Rambøll company performed at the Aalborg University and carried out exclusively by authors of this master thesis.

4.3.1 Heat sources

There are four types of heat sources which are used, mannequins, radiators, light bulbs and heating wires. What is more within the mannequins three different types can be distinguished, mannequins in standing position, sedentary mannequins and standing mannequin with angular shape, see figure 4.14. It is assumed that the heat released by all of the mannequins is equal. It should be also noted that in further sections of the report and in CFD models different types of mannequins are not distinguished and their shape is chosen as for averaged one of standing mannequin, the height is equal to 1.7 m and area at the bottom is equal to 0.1 m^2 .

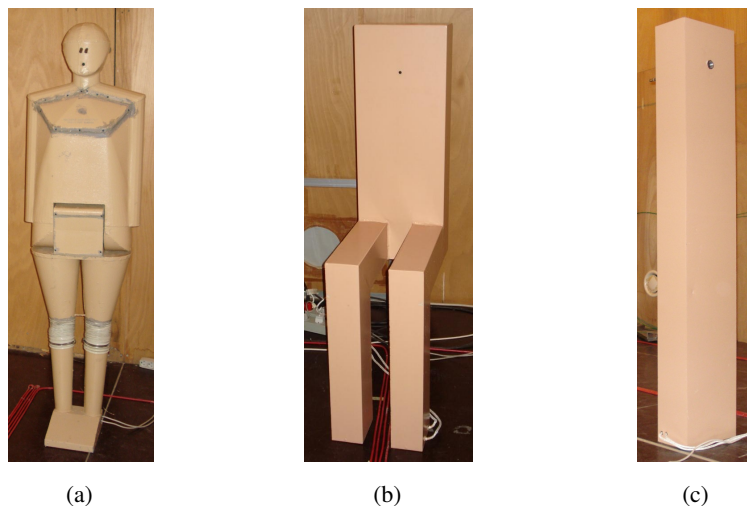


Figure 4.14: Pictures showing three different types of mannequins used in the experiment
a) standing one, b) sedentary one, c) standing one with angular shape.

Another heat sources used in the experiment are radiators, see figure 4.15(a), of averaged height equal to 0.45 m. In the room there are also mounted ten light bulbs, see figure 4.15(b) at the height of 3.50 m. Finally heating wires, placed on the floor, are used in some test cases, see figure 4.15(c).

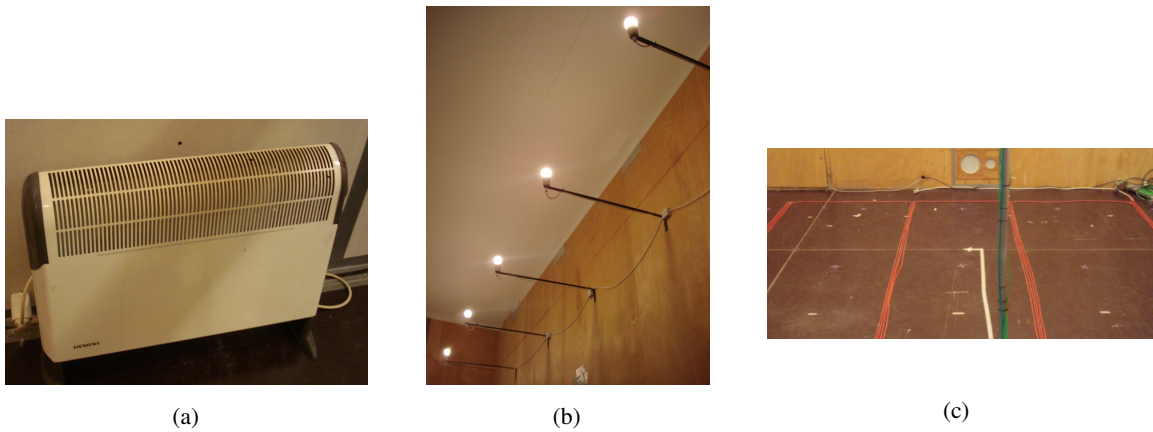


Figure 4.15: Pictures showing heat sources used in the experiment a) radiator, b) light bulbs, c) heating wires.

Legend with symbols of the heat sources used on drawings in further sections is presented in table 4.2.

Symbol	Description
●	Light bulb
□	Mannequin
—	Radiator
≡	Heating wires

Table 4.2: Legend of symbols of the heat sources.

4.3.2 Test cases conditions

Cases with the same types of heat sources are grouped together. Within the group however there can more than one test with different location of the heat sources, various heat released by the heat sources or with different inlet area. Inlet area for entire experiment is changed from whole ceiling, through three chambers supplying air for most of the cases, and decreased to only two or one chamber working as an inlet. All these conditions will be described in the particular cases description and are specified in collective table, see table 4.3.

Additionally for some of the cases more than one set of measurements is carried out for different temperatures of supplied air and various supplied air flows. For whole experiment the inlet temperatures vary from 4.8 up to 15.7 °C and the air flows supplied to the room are between around 0.07 and 0.20 m³/s. Detailed parameters of supplied air, q , ΔT , for different cases will not be presented in this section and can be found in collective table describing all of the measurements conditions, see table 5.1 in section 5.1. It should be noted that for cases with different heat loads in the room, product of q and ΔT is changed as well, to be sure that temperature conditions in the test room are similar to temperatures in the laboratory and heat exchange between these two rooms can be neglected.

For all of the cases measurements of temperature and velocity in different locations in the room are carried out. Additionally there is one case for which measurements of tracer gas concentration

are performed, Case 13 with mannequins densely located in one part of the room, which will be described in the end of this section. Details regarding measuring points can be found in section 4.2.

It should be noted that for all of the cases only schemes showing heat sources location will be presented under particular cases description. Detailed drawings with the dimensions of heat sources locations can be found in section A2.2 in appendix.

Case	Heat loads [W/m ²]	Bulbs [%]	Mannequins [%]	Radiators [%]	Heating wire [%]	Inlet area
1	72	35	65	-	-	Chambers 1, 2, 3
2	72	35	65	-	-	Whole ceiling
3	72	35	65	-	-	Chambers 1, 2
4	72	35	50	15	-	Chambers 1, 2, 3
5	57	44	37	19	-	Chambers 1, 2, 3
6	72	35	-	65	-	Chambers 1, 2, 3
7	72	35	-	65	-	Chambers 1, 2, 3
8	72	35	-	-	65	Chambers 1, 2, 3
9	54	47	-	-	53	Chambers 1, 2, 3
10	36	70	-	-	30	Chambers 1, 2, 3
11	36	-	-	-	100	Chambers 1, 2, 3
12	36/25	100	-	-	-	Chambers 1, 2, 3
13	25	-	86	14	-	Chamber 1

Table 4.3: Table with heat loads, percentage part of particular heat sources in the total heat loads and inlet area for the test cases.

Mannequins equally distributed in the room

Cases: 1, 2, 3

In these cases heat loads compose of 6 mannequins equally distributed in the room and light bulbs. The base inlet area consist of three chambers and is changed up to whole ceiling and down to two chambers for different cases. Picture showing room set-up with equally distributed mannequins can be seen on figure 4.16. Schemes presenting set-up of these cases can be seen on figure 4.17. For each case drawing on the left describes the heat sources located in the room and drawing on the right the inlet area.

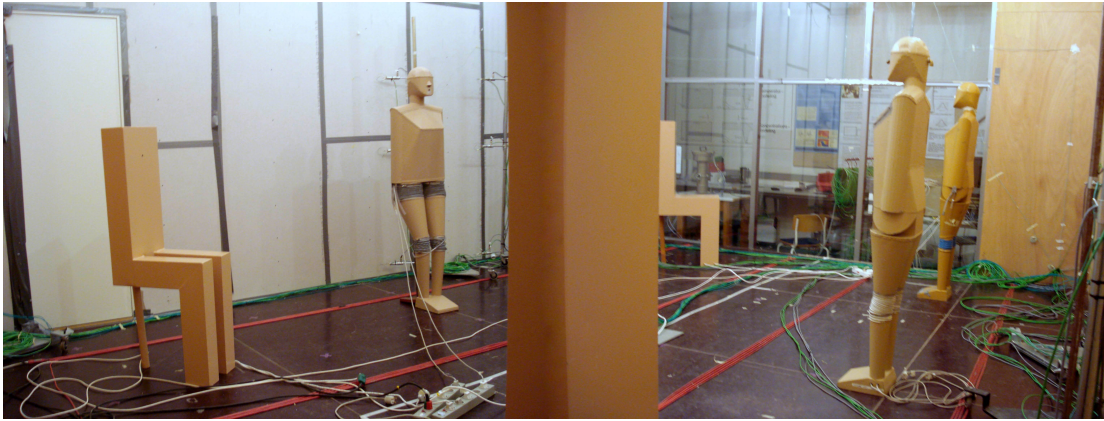


Figure 4.16: Picture showing set-up of the room with equally distributed mannequins.

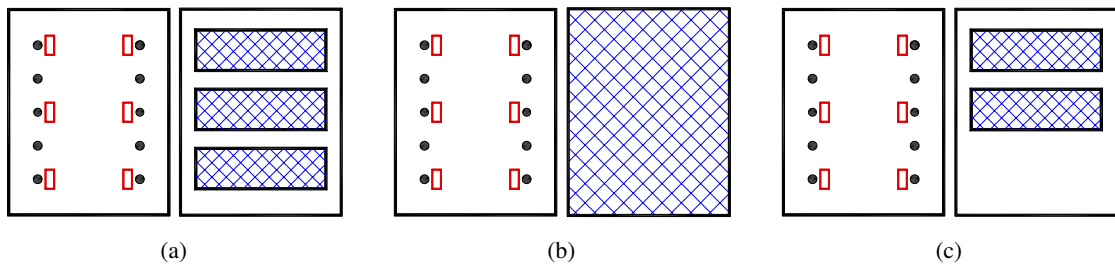


Figure 4.17: Schemes describing set-up of cases with mannequins equally distributed in the room a) Case 1, b) Case 2, c) Case 3.

Mannequins and radiators on one side of the room

Case: 4

In this case heat loads compose of 5 mannequins and 2 radiators located on one side of the room and light bulbs. The inlet area consists of three chambers. Picture showing mannequins and radiators location on one side of the room can be seen on figure 4.18(a). Schemes presenting set-up of the case can be seen on figure 4.18(b).

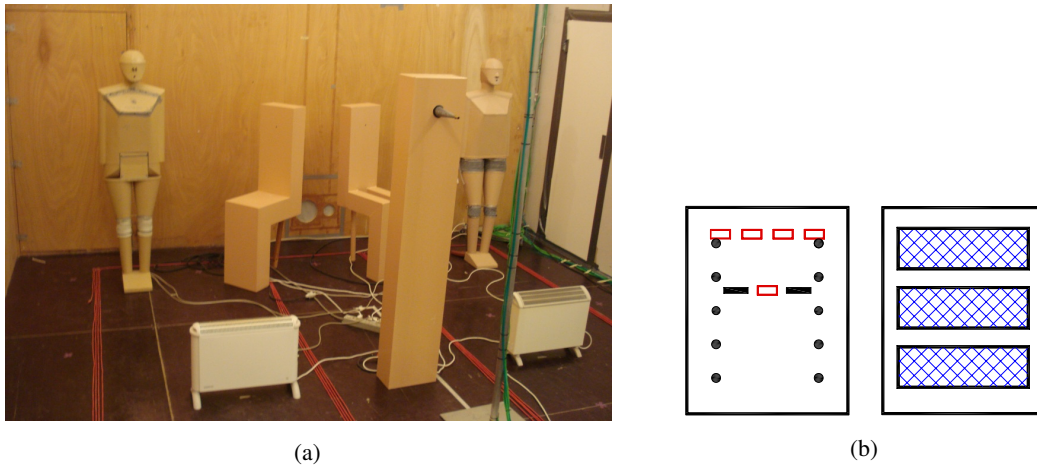


Figure 4.18: Figure showing a) picture of room set-up for the case with mannequins and radiators located on one side the room, b) schemes describing set-up of case 4.

Mannequins densely located in one part of the room and light bulbs

Case: 5

In this case heat loads compose of 5 mannequins densely located in other part of the room, light bulbs and radiator in a corner of the room. The inlet area consists of three chambers. Picture showing mannequins location in the room can be seen on figure 4.19(a). Schemes presenting set-up of the case can be seen on figure 4.19(b).

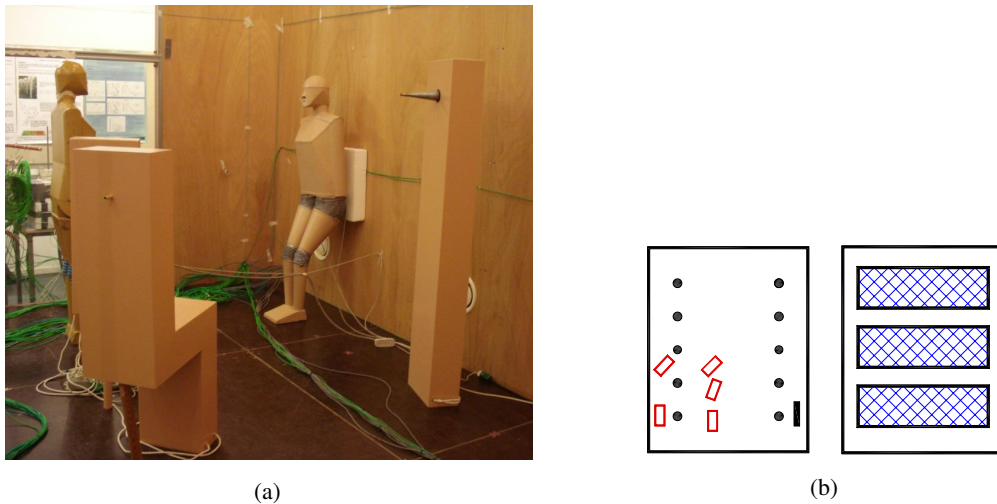


Figure 4.19: Figure showing a) picture of mannequins densely located in one part of the room, b) schemes describing set-up of case 5.

Radiator and light bulbs

Cases: 6, 7

In these cases heat loads compose of one radiator and light bulbs. The only difference between these two cases is that in one of them radiator is located in the corner of the room and in second it is placed

in the middle of the room. The inlet area consists of three chambers. Schemes presenting set-up of the cases can be seen on figure 4.20.

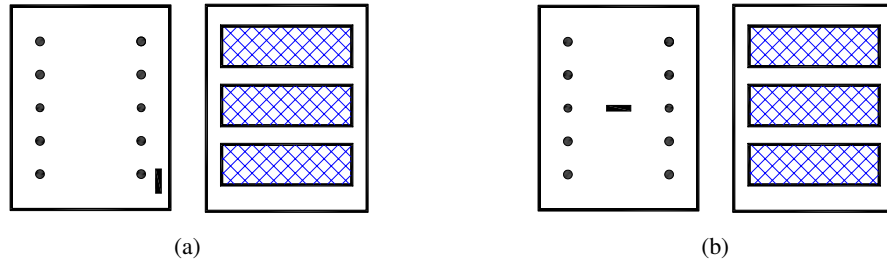


Figure 4.20: Schemes describing set-up of cases with radiator and light bulbs a) Case 6, b) Case 7.

Heating wires and light bulbs

Cases: 8, 9, 10

In these cases heat loads compose of heating wire placed on the floor and light bulbs. Heat released by the heating wire is changed from 300 W up to 1300 W and the heat released by the light bulbs is kept at a constant level, 700 W, to be able to check performance of the system with different ratio of heat released by these two sources. Schemes presenting set-up of Cases 8, 9, 10 can be seen on figure 4.21.

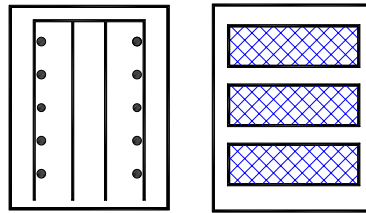


Figure 4.21: Schemes describing set-up of cases with heating wires and light bulbs.

Heating wires

Case: 11

In this case heating wire are the only heat source in the room. The inlet area consists of three chambers. Schemes presenting set-up of the case can be seen on figure 4.22. Location of the heating wire is like in Cases 8, 9, 10 and can be found on figure A2.9 in section A2.2 in appendix.

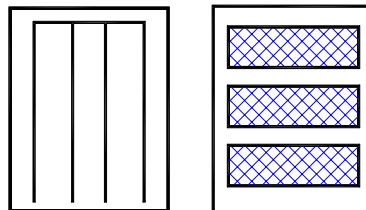


Figure 4.22: Schemes describing set-up of case with heating wire.

Light bulbs**Case: 12**

In this case light bulbs are the only heat source in the room. There are two test with different heat released by the light bulbs and different conditions of supplied air. The inlet area consists of three chambers. Schemes presenting set-up of Case 12 can be seen on figure 4.23. Locations of the light bulbs are the same for all of the cases and can be found on figure A2.4 in section A2.2 in appendix.

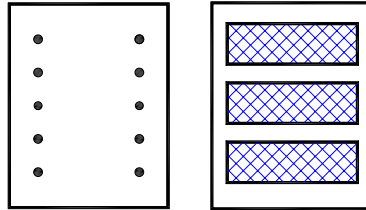


Figure 4.23: Schemes describing set-up of case with light bulbs.

Case with tracer gas concentration measurements. Mannequins densely located in one part of the room

Case: 13

This is the case for which tracer gas concentration measurements are performed in order to calculate the ventilation efficiency. Heat loads compose of 5 mannequins densely located in one part of the room and radiator in a corner of the room. The inlet area consists of only one chamber, Chamber 2. Schemes presenting set-up of the case can be seen on figure 4.24. Location of the heat sources is like in Case 5, except that the light bulbs are switched off. Therefore detailed dimensions of location of mannequins and radiator can be found on figure A2.6 in section A2.2 in appendix.

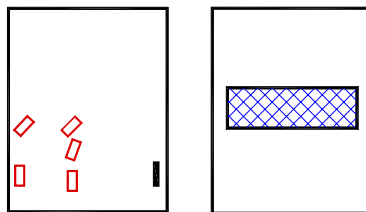


Figure 4.24: Schemes describing set-up of case with mannequins densely located in one part of the room.

Experiment results

In this chapter experiment results are introduced and analysed. Design chart based on the measurement data is presented and results are discussed regarding to various parameters, namely horizontal and vertical distribution of heat loads and inlet area and location. Furthermore, airflow distribution in the room for different cases is analysed and a problem connected with instability of airflow in the room is discussed. It is also tried to compare results of design chart for the test room with other measurements, conducted in a room of smaller size, by means of simple dimensionless analysis. Next additional parameters regarding indoor environment, not included on the basic design chart, are presented based on measurements in the test room. Finally pressure test results for tested ceiling are presented and compared with other ceiling's constructions.

5.1 Experiment data

In this section the most important measurement results are introduced, which are next analysed in further parts of this chapter. All the cases conducted in the experiment are described in section 4.3 and within some of the cases more than one test is carried out with different airflow parameters. On figure 5.1 can be seen a graph with q and ΔT conditions for all tests conducted in the experiment. It should be noted that each case is represented by different point and additionally graphical symbols are given, which show location of heat gains or inlet area for particular case. Legend for used symbols can be found on the graph. What is more a collective table with airflow rates, various temperatures and maximum velocities for all of the tests is presented, see table 5.1.

It should be noted that the main purpose of measurements is to obtain data, which is next used for the design chart investigations. Because design chart is based on the assumption that airflow in the room is independent of the Reynolds number, it is required that the flow is turbulent and fully developed. That is why, it is tried to obtain high velocity values in all of the tests, however for Case 12, with only light bulbs working this requirement may not be fulfilled. It should be also noted that for the design chart calculations three presented parameters are used, namely q , ΔT between supply air temperature and temperature in the occupied zone, and maximum velocity in the occupied zone. Maximum velocities are chosen from mean velocities measured within the occupied zone, details about velocity measurements and points can be found in section 4.2.1.

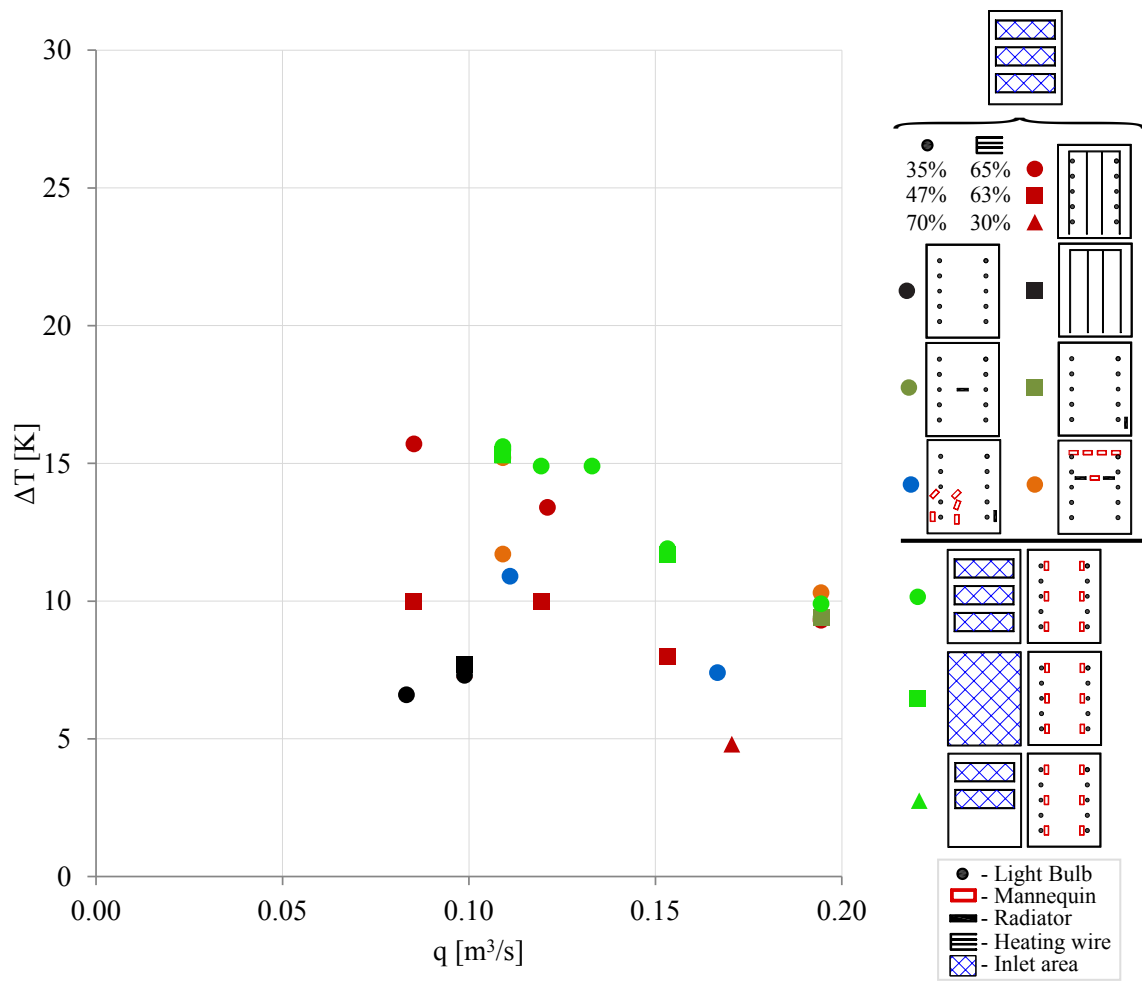


Figure 5.1: Conditions of the measurements conducted for diffuse ceiling ventilation.

Case	Test	q [m ³ /s]	t _s [°C]	t _e [°C]	t _{oz} [°C]	ΔT [K]	u _{max} [m/s]
1	1a	0.194	13.1	22.8	23.1	9.9	0.199
1	1b	0.153	11.6	23.1	23.5	11.9	0.197
1	1c	0.133	7.3	21.9	22.2	14.9	0.203
1	1d	0.119	7.9	22.4	22.8	14.9	0.166
1	1e	0.109	7.6	22.9	23.3	15.6	0.167
1	1f	0.109	8.5	23.6	24.0	15.5	0.161
2	2a	0.153	12.4	23.8	24.1	11.7	0.139
2	2b	0.109	8.1	23.2	23.5	15.3	0.131
3	3	0.109	8.0	22.9	23.3	15.3	0.260
4	4a	0.194	13.1	23.2	23.4	10.3	0.276
4	4b	0.153	11.1	22.6	22.8	11.8	0.268
4	4c	0.109	8.0	23.0	23.2	15.2	0.265
5	5a	0.167	16.1	23.3	23.5	7.4	0.192
5	5b	0.111	12.3	23.0	23.2	10.9	0.214
6	6	0.194	13.1	22.4	22.5	9.4	0.167
7	7	0.194	13.1	22.4	22.5	9.4	0.237
8	8a	0.194	12.9	21.8	22.2	9.3	0.311
8	8b	0.121	9.8	22.0	23.2	13.4	0.276
8	8c	0.085	8.5	22.8	24.2	15.7	0.264
9	9a	0.205	17.4	23.0	23.2	5.9	0.233
9	9b	0.153	15.6	23.3	23.6	8.0	0.246
9	9c	0.119	13.5	23.3	23.6	10.0	0.239
9	9d	0.085	10.5	23.4	23.7	13.2	0.204
10	10a	0.171	18.4	23.0	23.2	4.8	0.169
10	10b	0.099	15.9	23.2	23.4	7.5	0.136
11	11	0.099	15.8	23.4	23.5	7.7	0.240
12	12a	0.099	15.9	22.9	23.2	7.3	0.077
12	12b	0.083	15.8	22.0	22.4	6.6	0.071
13	13	0.069	16.6	22.9	23.1	6.5	-

Table 5.1: Table with airflow rates, various temperatures and maximum velocities for all of the tests. ΔT stands for temperature difference between supply air temperature and mean temperature in the occupied zone.

5.2 Design chart for DCV

In this section design chart for the diffuse ceiling ventilation is introduced, based on measurements presented in section 5.1 and recalculated to a limiting velocity equal to 0.15 m/s . Detailed method of developing a design chart is described in section 2.1 and calculations can be found in appendix B.1 - *DCV_design_chart.xls*. It should be noted that chosen limiting velocity value is connected with the decision to use category B of indoor environment quality for tested room, however this value can be easily recalculated according to requirements for other categories of building, see section 5.5.4.

It should be also stated that presented design chart is limited only by the velocity value, what ensures draught free design. However there is a possibility of introducing on the graph additional criteria regarding indoor environment, like minimum airflow rate due to indoor air quality, what is presented in section 5.5. What is more, the graph is made only for the test room and there may appear some differences when other geometry of the room is used. To be able to observe how change in geometry is affecting airflow and comfort in the room it is necessary to conduct dimensionless calculation or find the correlation between the results and the geometry. Simple dimensionless analysis of the problem can be found in section 5.4.

Resulting graph can be seen on figure 5.2. When few measurements are conducted for the same case, they can be connected by a curve. The curve is based on assumption that the product of q and ΔT is constant, which is considered in Nielsen et al. [2010] as typical for systems with low momentum and driven by buoyancy forces from heat gains. What is more, curves seen on the graph are representing mean product of q and ΔT for all of the tests within the case. It should be noted that tests for Case 10, marked with red triangles, are not connected due to high distance from theoretical mean curve for these points. Also for Case 1, represented by green round points, some discrepancies can be found between tests, probably caused by unstable airflow pattern in the room. That is why the points can be collected into two groups, which are connected by separate curves. More information about this issue can be found in section 5.3.

On the graph it can be seen that for recalculated conditions temperature difference variate from 2 to 30 K and airflow from 0.05 to $0.20 \text{ m}^3/\text{s}$, so the cooling capacity for the system can variate from 8 W/m^2 for case with only heating wires up to 230 W/m^2 for case with only light bulbs in the room. What is more, it can be seen that variations between the recalculated points are larger than on figure 5.1 for measurement points, so parameters like horizontal and vertical distribution of heat loads and inlet area and location can significantly influence conditions in the room. Each parameter will be discussed in following sections and presented on separate graphs in adequate sections to be able to focus on the specific problems.

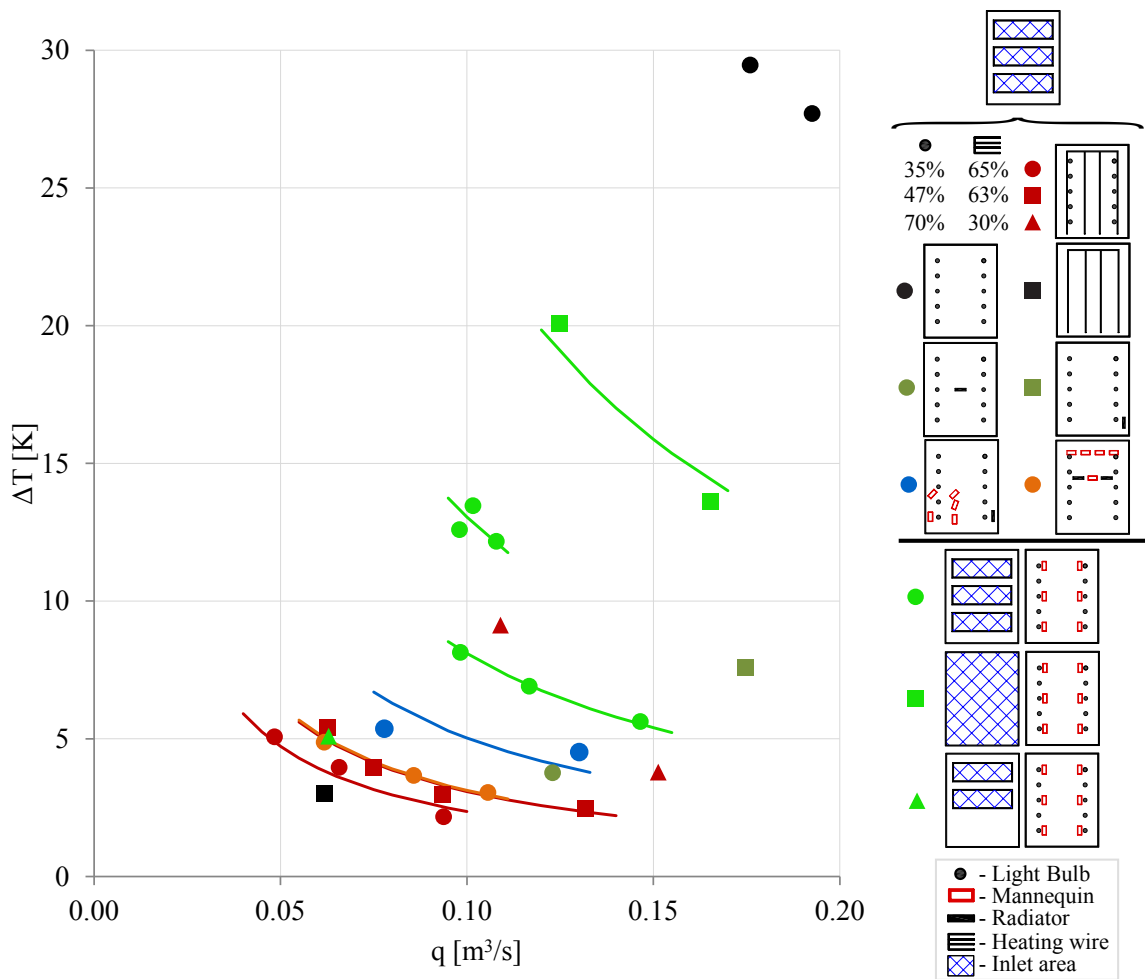


Figure 5.2: Design chart for the measurements conducted for diffuse ceiling ventilation.

5.2.1 Horizontal location of heat sources

In spaces with diffuse ceiling inlet system airflow is driven by buoyancy forces, which makes location of heat sources in the room very important. That is why when designing such a system knowledge about total heat loads in the room might be insufficient and it can be useful to know what is possible location of heat sources based on a desired function of the space. In some type of spaces heat sources location is easy to predict, for example in classrooms location of heat sources can be considered as kind of one side distribution, as all of the students are normally sitting in front of the teacher. In such a case a designer should be aware of the system's performance with given heat sources distribution. What is more, if the most preferable location of heat sources is known, when designing interior of the space this knowledge might be taken into account and if it is possible some heat sources might be located in the favourable area. That is why in the experiment cases with different heat sources distribution are performed and their location on the design chart is discussed here.

Graph presenting design chart with results for cases considered in this part can be seen on figure 5.3. It should be noted that only horizontal variations of heat sources distribution within the space are taken under consideration and vertical location is discussed in section 5.2.2.

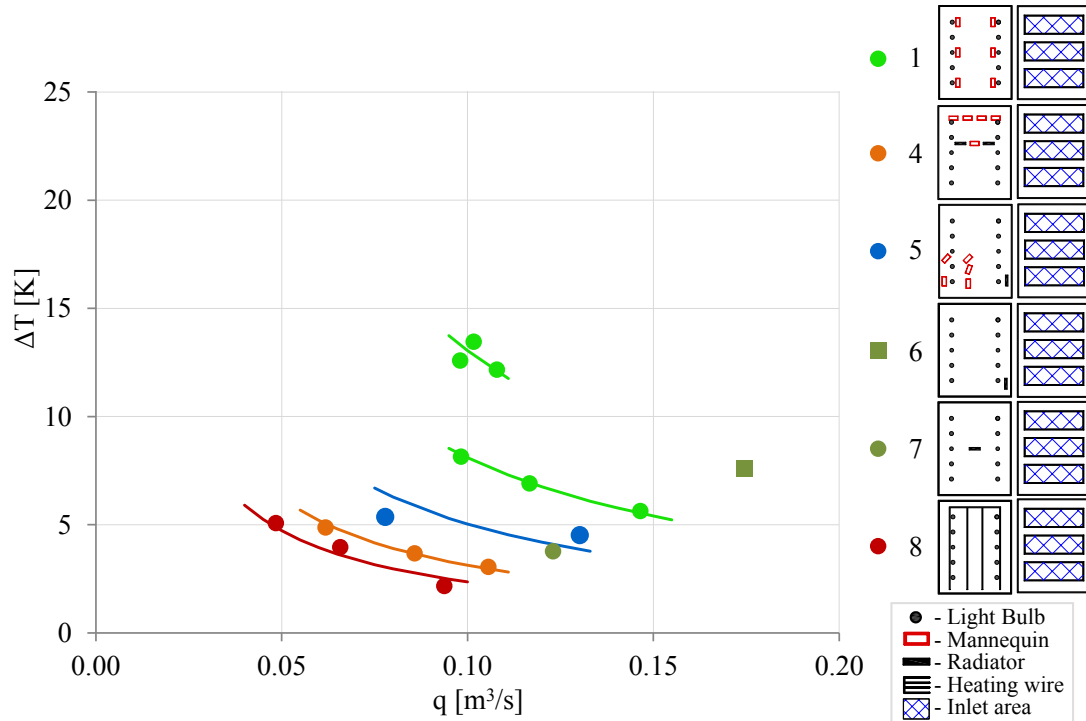


Figure 5.3: Design chart for the measurements concerning horizontal location of the heat sources. It should be noted that numbers on the right side of the cases symbols stand for the cases numbers.

It can be seen that the highest cooling capacity of supply air without causing draught can be obtained for Case 6, with radiator located in the corner of the room, which can be considered as a strong point heat source. What is interesting, curve for other case with strong point heat source, but located in the middle of the room, Case 7, is limited by significantly lower product of q and ΔT . To explain so well performance of Case 6 it is necessary to refer to results of velocity distribution in the room, see section 5.3.1. It can be noticed that airflow distribution for these two cases is different, for Case 6 air seems to rise up above the radiator and cross the room below the ceiling to fall down on the opposite wall. For Case 7 air below the ceiling is expected to divide into two air currents and fall down in two different corners of the room. However based on this information it is still difficult to explain lower velocities obtained for Case 6. It is possible that the main difference between these two cases is not location of radiator in the middle of the room or in the corner, but the fact that radiator in the corner is located below light bulbs, which disturb radiator's plume and results in lower velocities of air, that fall down on opposite site and enter the occupied zone. That is why, if strong point sources has to be located in the room it might be advantageous to place them under another heat source located in the upper part of the room, which is common location of lighting in spaces.

Next case with unequally distributed heat sources is Case 4, with mannequins and radiators on one side of the room. Location of a curve for this case is one of the most critical ones on the design

chart. Looking at the velocity distribution for this case in section 5.3.1 similarities can be noticed with Case 6, with radiator in the corner, as the main air current in the room also seems to circulate between the heat sources and the opposite wall. For Case 4, however, high velocities are measured in larger area in the room, which means that air fall down in whole space close to the opposite wall. Even though it might be expected that this larger area would result in lower velocities, it is not observed in the results. Possible explanation of this situation is connected with location of the heat sources for Case 4, as they are placed in kind of a line, they force air to move close to the floor all along this imaginary line and then air is entrained by the heat sources. All this gives very strong current in the room, which is enough forceful to limit disturbances caused by the light bulbs, which might be possible for Case 6. That is why if large heat load needs to be located in one part of the room if possible it might be good idea to try to balance it with some heat sources in other part of the room. To check these conclusions it is interesting to compare results of Case 4 with the last case with unequally distributed heat loads, Case 5. The room's set-up consist of mannequins densely located in part of the room and radiator in other corner and is quite similar to Case 4, but heat sources are not forming a line and it is possible that radiator's plume can balance the airflow pattern. Results for Case 5 on the design chart seems to confirm correctness of this investigation, as the curve can be characterised by higher possible cooling capacity, compared to Case 5.

Case 1, with mannequins equally distributed in the room gives one of the highest possible cooling capacities of supply air without causing draught. As described in section 5.3.2 due to the fact that heat sources are scattered within the room air currents are weaker and airflow pattern is more mixed compared to Case 4, which results in such a good performance of this case. However, an exceptional location of points for different tests can be observed, which might be caused by a problem with unstability of airflow in the room, which is described further in section 5.3. Due to the fact that the system's performance might oscillate between higher and lower curve, it can be advised to consider the lower curve as limiting for the cooling capacity. What is more, because a problem with unstability of airflow pattern can cause a discomfort for the occupants, a conclusion might be that a sparse distribution of heat sources within the room is a favourable solution, but their location if it is possible, should not be very uniform.

Finally, the last case presented on the design chart graph for the horizontal location of heat sources is Case 8, with heating wire placed on the floor. As discussed in section 5.3.1 very strong air currents are formed between lines of the heating wire, because the air is bounded by its plume, and this explains why the curve for this case represents the lowest product of q and ΔT among all the cases. Nevertheless heat sources location in this case is rather unusual and probably this problem would seldom happen in a practical design.

5.2.2 Vertical location of heat sources

In many cases not only a horizontal location of heat sources can affect flow in the room, but also a height on which the heat loads are placed. In schools, offices and similar buildings main heat loads are generated by people and equipment that are located in occupied zone, however, for instance lighting can be placed on different heights. Application of general or individual lighting can have additional effect on airflow distribution in the room. It is decided to compare three kinds of heat sources, which are heating wire, mannequins and light bulbs. It is tried to equally distribute all of the heat loads to be able to easier compare the results, however as described in section 5.2.1, shape

of the heating wire may have significant influence on the airflow distribution. Six cases chosen for the comparison are shown on figure 5.4.

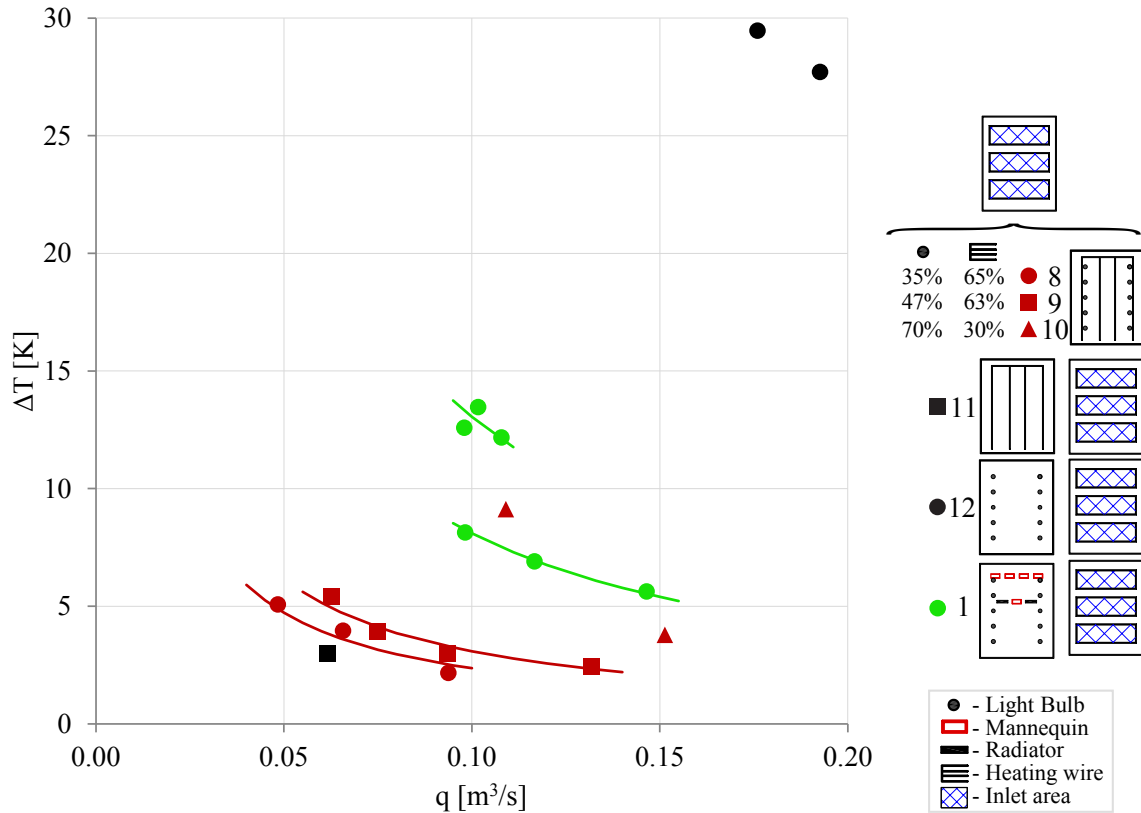


Figure 5.4: Design chart for the measurements concerning different vertical heat loads location. It should be noted that numbers on the right side of the cases symbols stand for the cases numbers.

Firstly to demonstrate the importance of vertical location of the heat loads extreme results of Cases 11 and 12 are introduced. On figure 5.4 it can be seen that these are the most outstanding results that are obtained for the design chart, which can implicate that vertical location of heat sources can be very important. When only light bulbs are used as heat loads it shown that risk of draught in the room is very low. Possible cooling capacity of the system in this situation is equal to around 230 W/m^2 , which indicates that even strong heat loads located above occupied zone do not cause draught in the room. On the other hand, when the case with only heating wire is considered, the lowest cooling capacity of the system is observed, compared with other cases. Even though the effect can be overestimated due to specific airflow, when heating wire is used, difference between the results is significant.

The importance of vertical distribution of heat loads can be investigated further by changing ratio of loads released by heating wire and light bulbs, what is done for Cases 8, 9 and 10. Observing the location of curves for these cases it can be seen, that cooling capacity is increasing with higher ratio of heat generated by light bulbs. This means that localization of heat gains in top of the room not only does not generate high draught risk, but also can decrease it. What is more, the increase in ratio

of power released by the light bulbs between Cases 8 and 9 is equal to 12% and between Cases 9 and 10 the increase is 23%, and the same trend in growth of cooling capacity for curves of these three cases is observed on the graph. Because protective effect of using heat loads generated by highly located lighting in the room can be very beneficial, it should be investigated further according to their horizontal distribution in respect to floor, inlet area and heat gains.

Finally, because in spaces with diffuse ceiling ventilation most of the maximum velocities are measured on the floor level, 0.1 m height, it might be crucial not to use heat loads concentrated on the floor, like heating wire. Comparing results for Case 1 and Case 8 significant difference between using mannequins and heating wire can be noticed, which confirm aforementioned thesis. Even though, as mentioned before, results for heating wire are probably overestimated, there is still large difference between their performance compared to mannequins in the room.

5.2.3 Inlet area and location

For diffuse ceiling ventilation it is assumed that the whole ceiling or at least large part of the ceiling should work as supply inlet. However, in design of some spaces it may be necessary to use part of the ceiling for other systems, that is why it is important to analyse the effect of changing the inlet area and its location on airflow pattern in the room. Three cases with different supply area and location are investigated and the results can be seen on figure 5.5. For all the cases mannequins equally distributed in the room generate the heat loads.

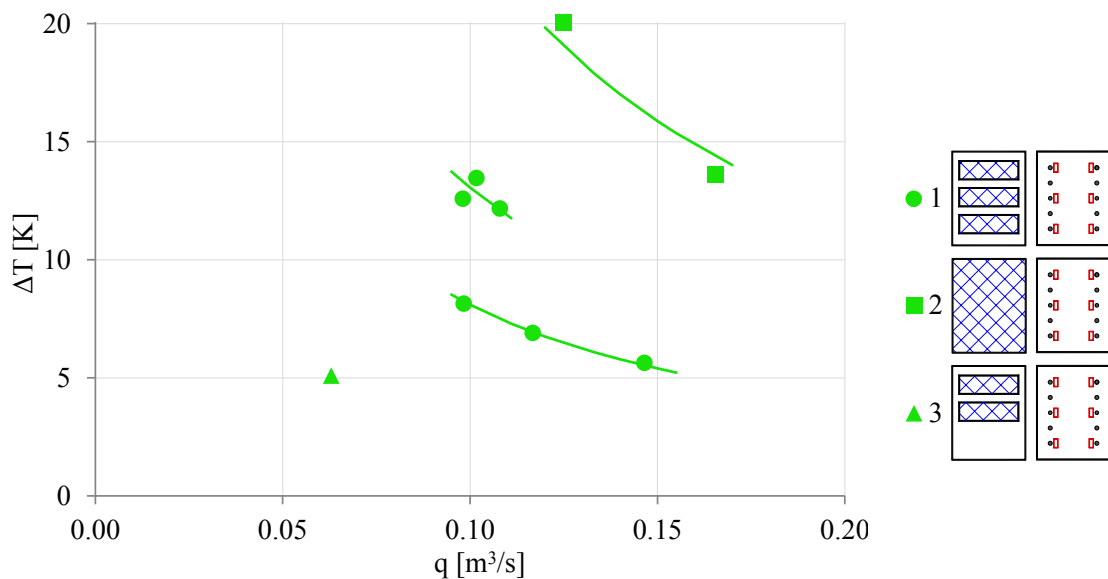


Figure 5.5: Design chart for the measurements concerning different inlet area and location. It should be noted that numbers on the right side of the cases symbols stand for the cases numbers.

Firstly, when Case 2, with whole ceiling area working as an inlet, is compared with Case 1, with three pressure chambers used as an inlet, results indicate that the inlet area can have strong influence on maximum velocities in the occupied zone. It is shown in section 5.3.1 that measured velocity field in the room is different for the two cases. For three chambers the cold air is often dropping

from the ceiling on one of the walls and enter the occupied zone, while for the whole ceiling the air enter the occupied zone from both sides of the room. This split of the flow could explain decrease in velocities in the room.

However, another issue can influence the results, as it is observed that the whole ceiling inlet does not work as it is expected. When the flow per area is set to be equal for three chambers and the plenum space it can be seen that the surface of the ceiling does not have equal temperatures, see table 5.2(a). Temperatures of the ceiling surface can be seen as well for test with three chambers working as an inlet, test 1f, see table 5.2(b). It should be mentioned that the conditions for compared tests are similar, only small changes in the room temperatures can be observed. Even though for test 2b temperatures of the plenum space decrease, see rows 1 and 3 in the table, and increase for pressure chambers, see rows 2, 4 and 5 in the table, they are still not uniform. The differences in temperatures can indicate heat or airflow losses in plenum space. Because both q and ΔT used in calculations for the design chart are based on measurements of supply air in ducts before the plenum chamber, it is possible that the results are overestimated compared to real situation and the curve for Test 2b would be moved down. Nevertheless, even taking into account possible error, the cooling capacity of system with whole ceiling working as an inlet is significantly higher, compared to system with three chambers working.

	Temp. [°C]		
	A	B	C
1	20.8	19.7	19.1
2	19.1	18.4	18.1
3	20.4	20.0	20.2
4		18.5	
5		18.5	

(a)

	Temp. [°C]		
	A	B	C
1	22.3	21.9	21.9
2	18.6	18.2	17.9
3	22.2	22.0	22.7
4		18.2	
5		18.2	

(b)

Table 5.2: Table with surface temperature of the ceiling for a) Test 2b, b) Test 1f.

Finally an assymetric situation of Case 3, where only Chamber 1 and Chamber 2 are used to supply fresh air, is considered. On figure 5.5 it can be seen that possible cooling capacity of Case 3 is significantly lower than for Case 1 and 2. This can be explained, when velocity pattern in the room is investigated, see section 5.3.1, where it is shown that general pattern of the flow for Case 3 is very similar to Case 4. When only two chambers on one side of the room are working it creates an imbalance in airflow in the room similar to the Case 4 for heat gains located on one side of the room. The cold air that is supplied only on one side of the room generates high buoyancy forces, because they are not balanced on the other side of the room and cold stream is dropping on one side of the room and entering occupied zone with high velocities. Additional influence on the results can have distance that air needs to overcome to enter occupied zone. When three chambers are working, comparing to the case with two chambers, the air that is coming from the additional third chamber has always a longer way before it enters occupied zone. This can lower the final measured velocities.

It can be concluded that larger area of the diffuse ceiling inlet and symmetric location of the inlet have positive influence on the cooling capacity of the system, however, only few cases are investigated. More variations of the inlet area are needed to obtain more knowledge about the influ-

ence of the inlet geometry. Additionally it should be noted that only cases with equally distributed mannequins are used in this comparison and the effect for other solutions is unsure.

5.3 Airflow distribution

In this section airflow distribution in the room is described. At first results of velocity measurements in the room are described for various cases. What is more, for two cases with different location of heat sources air movement is visualized in the smoke test and the output is presented. Finally, an issue connected with the airflow distribution, the stability of airflow for diffuse ceiling system, is described. In published literature there is lack of information about the stability problems. However, in informal opinions about this system, there are some doubts about the stability of airflow in the rooms with DCV and possible unsteady direction of the flow. That is why, in this section it is wanted to investigate steadiness of the flow in different test cases. This is done by means of velocity measurements and for two cases by means of smoke experiments, for which airflow can be visually observed and described.

5.3.1 Velocity distribution

Velocity measurements are performed for all the cases, but in main report results are presented only for few representative cases. The rest of tests can be found in section A3.1.1 in appendix. Details about the measurement points and methods are described in section 4.2.1. Velocity results are presented in tables with values for all the measurement points. For some of the measurement points, however, there are no values, which means that velocities are not measured due to problems with equipment or lack of anemometers. It should be also noted, that some of the sensors may measure velocities affected directly by the plume of heat sources and these velocities are not considered as important to describe draught in the room.

Cases with unequally distributed heat sources

Firstly, cases with heat sources distributed unequally in the room are described, Cases 4, 6 and 7. On figure 5.6 tables with velocity results are presented. In Test 4b mannequins and radiators are located on one side of the room and, due to plumes from heat sources, there should be strong upward airflow on this side of the room. According to the results for velocity, see figure 5.6(a), high velocities are measured in the part of the room opposite to the one, where heat sources are located. This indicates that the air is going up with the plume next to the mannequins and radiators, then it is crossing the room and falling down on the opposite site. However, it can be noticed that these high velocities occur not only close to the wall, but also in the distance of around 1.8 m from the wall at 0.1 m height and this is the area where the highest velocities are measured. This may be explained by the fact that air is moving down also in some distance from the wall and the place where all of the air reaches floor level is the one with the highest velocity.

Results of Case 6 with radiator in the corner of the room can be seen on figure 5.6(b). General pattern in the room appears to be very similar to Test 4b, with high velocities next to wall opposite to the radiator and with highest velocities in 1.8 m distance from the wall. In this case, however, it can be noticed that this downward airflow is not spread equally in whole width of the room, but it is

stronger on right side of the room, which is the site where the radiator is placed. What is more, on the left side of the radiator an area with low velocities can be observed, which may cause risk of air stagnation in this part of the room.

		Velocity [m/s]				
		A	B	C	D	E
1	1.7 m	0.13	x	x	0.13	0.21
	1.1 m	0.10	0.16	0.16	0.10	0.15
	0.1 m	0.07	0.09	0.09	0.08	0.07
2	1.7 m	0.10	x	x	0.11	0.19
	1.1 m	0.08	0.22	0.10	0.09	0.20
	0.1 m	0.07	0.13	0.14	0.07	0.11
3	1.7 m	0.08	x	x	0.09	0.07
	1.1 m	0.08	0.08	0.06	0.11	0.07
	0.1 m	0.13	0.16	0.11	0.09	0.11
4	1.7 m	0.08	x	x	0.08	0.08
	1.1 m	0.12	0.11	0.13	0.11	0.11
	0.1 m	0.21	0.27	0.25	0.20	0.22
5	1.7 m	0.09	x	x	0.10	0.20
	1.1 m	0.12	0.18	0.21	0.09	0.18
	0.1 m	0.18	0.21	0.17	0.16	0.16

(a)

		Velocity [m/s]				
		A	B	C	D	E
1	1.7 m	0.07	x	x	0.08	0.13
	1.1 m	0.07	0.10	0.14	0.08	0.11
	0.1 m	0.11	0.13	0.13	0.14	0.13
2	1.7 m	0.05	x	x	0.08	0.05
	1.1 m	0.08	0.05	0.05	0.09	0.06
	0.1 m	0.10	0.15	0.16	0.17	0.15
3	1.7 m	0.06	x	x	0.08	0.03
	1.1 m	0.08	0.08	0.04	0.10	0.04
	0.1 m	0.05	0.05	0.08	0.15	0.13
4	1.7 m	0.03	x	x	0.07	0.05
	1.1 m	0.05	0.04	0.07	0.07	0.06
	0.1 m	0.02	0.02	0.04	0.05	0.03
5	1.7 m	0.02	x	x	0.25	0.07
	1.1 m	0.02	0.03	0.06	0.10	0.07
	0.1 m	0.03	0.05	0.03	0.05	0.02

(b)

		Velocity [m/s]				
		A	B	C	D	E
1	1.7 m	0.22	x	x	0.02	0.04
	1.1 m	0.20	0.07	0.06	0.03	0.03
	0.1 m	0.15	0.21	0.18	0.03	0.09
2	1.7 m	0.06	x	x	0.03	0.05
	1.1 m	0.05	0.07	0.06	0.05	0.05
	0.1 m	0.16	0.17	0.15	0.04	0.09
3	1.7 m	0.05	x	x	0.03	0.07
	1.1 m	0.07	0.09	0.09	0.04	0.06
	0.1 m	0.05	0.10	0.07	0.02	0.03
4	1.7 m	0.06	x	x	0.02	0.03
	1.1 m	0.07	0.06	0.05	0.05	0.04
	0.1 m	0.11	0.12	0.04	0.02	0.03
5	1.7 m	0.22	x	x	0.02	0.04
	1.1 m	0.24	0.04	0.05	0.04	0.06
	0.1 m	0.14	0.24	0.15	0.04	0.06

(c)

Figure 5.6: Velocity distribution in the room for a) Test 4b, b) Case 6, b) Case 7.

The last unequally distributed case presented here is Case 7 with radiator in the middle of the room. The velocity results presented on figure 5.6(c) show a pattern a lot different from two cases presented before. What can be expected is that the radiator's plume generates strong upward flow in the middle of the room. Results show that the highest velocities occur in two corners on the left side of the room, which probably means that the air after being raised by the radiator's plume is splitting into

two strong air currents, which are next falling down in these two corners. In right part of the room, especially next to the right wall very low velocities are observed, which indicates low mixing of air with the rest of the room's air and can cause a risk of air stagnation in this area. Results of rest of the tests with unequally distributed heat sources, Test 4a, 4c and whole Case 5 are not presented here, as they are showing pattern very similar to Case 4b and all these results can be found in appendix on figures A3.1 and A3.2.

Cases with heating wires and light bulbs

Next Case 11 with heating wires on the floor and Case 12 with light bulbs as only heat sources are described. On figure 5.7(a) can be seen results for the case with heating wires. The highest velocities in the room can be found at the level of 0.1 m. Strong air currents are formed in between the lines of heating wires, as the air is apparently trapped between the floor and the plume of the heat sources. It is difficult to make conclusions about the main current in the rest of the room, however, it may look like there is an upward flow close to row 5 of measurements and downward flow close to row 1. Except that, it can be seen that velocities at points above the floor level are quite uniform, which may be connected with the entrainment of air by the plume of heat sources.

		Velocity [m/s]				
		A	B	C	D	E
1	1.7 m	0.13	x	x	0.12	0.16
	1.1 m	0.13	0.15	0.14	0.12	0.15
	0.1 m	0.14	0.16	0.17	0.13	0.13
2	1.7 m	0.10	x	x	0.11	0.10
	1.1 m	0.12	0.14	0.13	0.11	0.12
	0.1 m	0.17	0.23	0.23	0.15	0.19
3	1.7 m	0.12	x	x	0.11	0.10
	1.1 m	0.13	0.13	0.14	0.12	0.12
	0.1 m	0.17	0.23	0.24	0.16	0.20
4	1.7 m	0.13	x	x	0.13	0.10
	1.1 m	0.13	0.13	0.12	0.13	0.12
	0.1 m	0.15	0.20	0.23	0.15	0.19
5	1.7 m	0.14	x	x	0.15	0.16
	1.1 m	0.13	0.14	0.15	0.14	0.14
	0.1 m	0.09	0.09	0.12	0.10	0.08

(a)

		Velocity [m/s]				
		A	B	C	D	E
1	1.7 m	0.08	x	x	0.07	0.05
	1.1 m	0.07	0.06	0.04	0.06	0.04
	0.1 m	0.04	0.05	0.05	0.06	0.04
2	1.7 m	0.05	x	x	0.03	0.06
	1.1 m	0.05	0.05	0.05	0.03	0.05
	0.1 m	0.04	0.05	0.07	0.06	0.05
3	1.7 m	0.05	x	x	0.05	0.04
	1.1 m	0.06	0.05	0.05	0.05	0.06
	0.1 m	0.05	0.05	0.06	0.06	0.06
4	1.7 m	0.03	x	x	0.06	0.04
	1.1 m	0.05	0.04	0.04	0.05	0.06
	0.1 m	0.07	0.07	0.05	0.04	0.03
5	1.7 m	0.06	x	x	0.07	0.07
	1.1 m	0.05	0.06	0.06	0.07	0.06
	0.1 m	0.03	0.03	0.04	0.03	0.02

(b)

Figure 5.7: Velocity distribution in the room for a) Case 11, b) Case 12.

On figure 5.7(b) results for a case with only light bulbs working are presented. This case is quite opposite to the one with the heating wires, as the light bulbs are located at the height of 3.5 m. All the measured results are in low velocity range and are quite uniform, which indicates slow mixing in the whole occupied zone. Possible reason of this situation may be that in the area between the light bulbs and the ceiling a kind of protective layer of formed, in which the plume of light bulbs is mixing with the supplied air before it enters the occupied zone with rather low velocities. Results of Cases 8, 9 and 10 are not presented here, as the velocity distribution in the occupied zone is very similar to Case 11 with only heating wires, and can be found in appendix on figures A3.3, A3.4,

A3.5 and A3.6. The discussion about the effect of these cases on maximum velocities in the room is presented in section 5.2.2.

Case with equally distributed heat sources

Next Case 1 with mannequins equally distributed in the room is going to be described. Three different tests are going to be presented, Tests 1b, 1c and 1d.

		Velocity [m/s]				
		A	B	C	D	E
1	1.7 m	0.13	x	x	0.09	0.11
	1.1 m	0.12	0.11	0.09	0.08	0.10
	0.1 m	0.08	0.13	0.11	0.08	0.07
2	1.7 m	0.12	x	x	0.10	0.11
	1.1 m	0.12	0.12	0.09	0.10	0.10
	0.1 m	0.10	0.16	0.15	0.08	0.13
3	1.7 m	0.10	x	x	0.11	0.10
	1.1 m	0.10	0.14	0.10	0.11	0.10
	0.1 m	0.10	0.16	0.15	0.07	0.09
4	1.7 m	0.13	x	x	0.09	0.10
	1.1 m	0.13	0.11	0.08	0.10	0.08
	0.1 m	0.13	0.20	0.18	0.07	0.11
5	1.7 m	0.16	x	x	0.08	0.12
	1.1 m	0.15	0.11	0.08	0.07	0.09
	0.1 m	0.08	0.15	0.13	0.07	0.10

(a)

		Velocity [m/s]				
		A	B	C	D	E
1	1.7 m	0.14	x	x	0.10	0.09
	1.1 m	0.13	0.14	0.11	0.11	0.09
	0.1 m	0.08	0.14	0.15	0.13	0.10
2	1.7 m	0.09	x	x	0.10	0.08
	1.1 m	0.09	0.11	0.09	0.09	0.08
	0.1 m	0.11	0.14	0.14	0.12	0.08
3	1.7 m	0.11	x	x	0.10	0.09
	1.1 m	0.11	0.14	0.10	0.10	0.09
	0.1 m	0.10	0.15	0.13	0.11	0.07
4	1.7 m	0.14	x	x	0.09	0.09
	1.1 m	0.13	0.10	0.07	0.09	0.08
	0.1 m	0.11	0.17	0.16	0.09	0.05
5	1.7 m	0.14	x	x	0.11	0.08
	1.1 m	0.14	0.10	0.08	0.10	0.07
	0.1 m	0.09	0.14	0.11	0.08	0.05

(b)

		Velocity [m/s]				
		A	B	C	D	E
1	1.7 m	0.11	x	x	0.11	0.12
	1.1 m	0.11	0.13	0.10	0.12	0.11
	0.1 m	0.11	0.14	0.13	0.11	0.13
2	1.7 m	0.11	x	x	0.10	0.11
	1.1 m	0.10	0.12	0.10	0.10	0.11
	0.1 m	0.10	0.14	0.14	0.11	0.15
3	1.7 m	0.12	x	x	0.10	0.11
	1.1 m	0.10	0.12	0.10	0.11	0.12
	0.1 m	0.13	0.20	0.18	0.15	0.17
4	1.7 m	0.12	x	x	0.10	0.11
	1.1 m	0.12	0.09	0.07	0.09	0.09
	0.1 m	0.09	0.12	0.11	0.06	0.08
5	1.7 m	0.13	x	x	0.09	0.15
	1.1 m	0.12	0.10	0.09	0.09	0.12
	0.1 m	0.07	0.10	0.09	0.06	0.08

(c)

Figure 5.8: Velocity distribution in the room for a) Test 1b b), Test 1d, c) Test 1c.

On figure 5.8(a) results for Test 1b can be seen and it can be noticed that the highest velocities are observed close to the floor in the middle of the room. This indicates that there is an air current crossing the room on a floor level and most likely it is moving upwards next to Row 1 and close to the wall, next moving across the room below the ceiling and falling down on the opposite wall, close to Row 5.

Results of Test 1d are presented here, as it seems that the airflow pattern is changed comparing to Case 1b, see figure 5.8(b). It can be noticed, that also here an air current is observed on the floor level, however high velocities occur also on two corners on the left side of the room, which probably indicates that in these areas air is moving down. At the same time velocities in Column D are higher than in Test 1b, which may suggest that in this test air is raising up in the right part of the room.

Finally, results of Test 1c can be seen on figure 5.8(c), which appear to show airflow distribution different from two previous tests. Highest velocities occur also in the middle of the room, however, it is difficult to see any air current crossing the whole room. What is more, close to the right wall increase in velocity values can be observed, which may indicate stronger air current along this wall and which can not be seen in two other tests patterns. When looking at results of Cases 5, 8, 9 or 10, all the tests with different q and ΔT within the same case seems to show quite similar airflow distributions. For Case 1, however, discrepancies can be found between various tests. What is more, results for Case 1 showed unusual performance of the airflow in this set-up already on the design chart, see section 5.2. Possible reason for this situation might be some kind of instability of the airflow in the room for cases with equal heat gains distribution within the room and this problem will be investigated further in the next parts of this section. It should be noted that the tests for Case 1 that show airflow pattern similar to Test 1b can be found in appendix on figure A3.8.

Cases with different supply areas

Finally, various cases with different supply area and equally distributed heat sources are going to be described. Results for tests with three chambers working are presented on figure 5.8. Figure 5.9(a) shows results of a test, where air is supplied through whole ceiling, which is also a symmetric situation, like supplying air through three chambers. However results indicates different airflow pattern in the room with highest velocities in two diagonal corners in the room. An explanation for this situation might be that supplied air is dividing into two strong air currents and falling down along opposite corners. In the rest of the room air is probably moving upwards. This case seems to be more similar to Test 1d, in which air as well seems to be falling down in two corners, however located next to one wall.

Additionally, velocity results for test with supply of air only through Chambers 1 and 2 can be seen on figure 5.9(b) and as expected there is a strong downward flow in the part of the room located below the supply area. This situation has similarities with case with heat sources on only one side of the room, where as well strong air current is formed in one part of the room, see figure 5.6(a).

		Velocity [m/s]				
		A	B	C	D	E
1	1.7 m	0.07	x	x	0.11	0.11
	1.1 m	0.07	0.07	0.06	0.09	0.09
	0.1 m	0.09	0.10	0.13	0.13	0.12
2	1.7 m	0.08	x	x	0.09	0.09
	1.1 m	0.08	0.10	0.06	0.09	0.06
	0.1 m	0.06	0.08	0.10	0.12	0.11
3	1.7 m	0.08	x	x	0.09	0.07
	1.1 m	0.06	0.08	0.07	0.10	0.06
	0.1 m	0.05	0.05	0.07	0.10	0.09
4	1.7 m	0.06	x	x	0.08	0.06
	1.1 m	0.07	0.07	0.06	0.09	0.06
	0.1 m	0.12	0.11	0.11	0.06	0.04
5	1.7 m	0.11	x	x	0.05	0.07
	1.1 m	0.11	0.09	0.06	0.05	0.06
	0.1 m	0.11	0.10	0.11	0.06	0.05

(a)

		Velocity [m/s]				
		A	B	C	D	E
1	1.7 m	0.11	x	x	0.12	0.22
	1.1 m	0.14	0.17	0.19	0.15	0.21
	0.1 m	0.19	0.18	0.19	0.20	0.15
2	1.7 m	0.08	x	x	0.10	0.08
	1.1 m	0.12	0.12	0.07	0.14	0.09
	0.1 m	0.17	0.26	0.25	0.21	0.23
3	1.7 m	0.08	x	x	0.09	0.10
	1.1 m	0.11	0.11	0.05	0.13	0.11
	0.1 m	0.17	0.24	0.22	0.20	0.22
4	1.7 m	0.08	x	x	0.08	0.13
	1.1 m	0.09	0.10	0.07	0.11	0.13
	0.1 m	0.12	0.18	0.18	0.16	0.17
5	1.7 m	0.11	x	x	0.08	0.16
	1.1 m	0.12	0.12	0.12	0.11	0.15
	0.1 m	0.05	0.11	0.09	0.12	0.06

(b)

Figure 5.9: Velocity distribution in the room for a) Test 2b, b) Test 3.

5.3.2 Smoke investigations

Smoke experiments are performed for two different cases, Case 1 with mannequins equally distributed in the room and Case 4 with mannequins and radiators on one side of the room. More specific, Test 4b is chosen for the test experiment and for Case 1 smoke investigations are carried out for two tests with different q and ΔT conditions, Test 1b and Test 1d. For both cases schemes of airflow pattern are given on a cross-section, location of section cut on a plan of the room can be seen on figure 5.10.

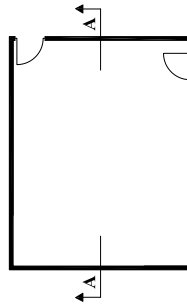


Figure 5.10: Plan view of the room with location of the cross-section cut.

Case 4

At first Case 4 is analysed, as this is the case with heat sources distributed unequally, which generates strong air current in the room, see section 5.3.1, and that is why it is expected that this set-up will result in a stable airflow. On figure 5.11(a) can be seen scheme of airflow pattern in the room and on figure 5.11(b) is presented picture showing the airflow direction in a part of the room highlighted on the scheme with blue dashed lines. It can be seen that in part of the room, where the heat sources

are located the airflow is strongly directed upwards and then it is falling down on the opposite side of the room. What is more air is moving downwards not only close to the wall, but also in the area next to it. Close to the floor, where the air falls down, the highest velocities in the occupied zone are measured. According to the velocity measurements, see figure 5.6(a), maximum measured velocity occurs in a distance 1.8 m from the wall and close to the floor, at 0.1 m height and it can be stated that smoke results are consistent with the velocity results. In addition, observed airflow pattern is steady during whole period of smoke experiment, which indicates that airflow distribution in this case can be considered as a stable one.

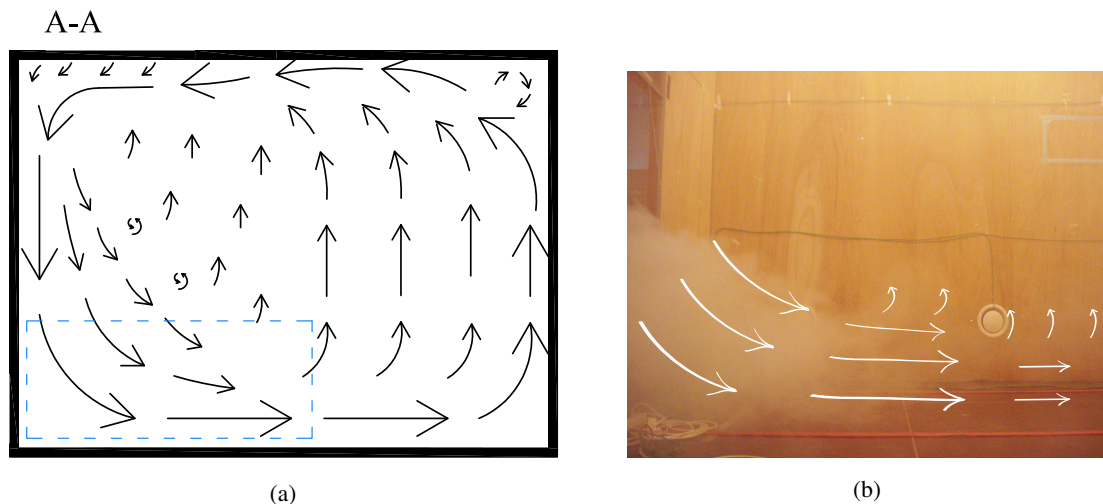


Figure 5.11: Figure showing a) scheme of the airflow pattern in the room for Test 4b b) picture of part of the room highlighted on the scheme with blue dashed lines.

Case 1

For tests with heat sources equally distributed in the room there is the highest risk of unstable airflow pattern and velocity results described in section 5.3.1 imply that the risk of unsteady flow resulting in varying airflow distribution might be possible. Firstly smoke experiment is made for Test 1d. On figure 5.12(a) can be seen scheme of airflow pattern in the room and on figure 5.12(b) picture showing the air flow direction in a part of the room highlighted on the scheme with blue dashed lines is presented. It can be observed that air is going up on one wall and falling down on the opposite one, which is a situation similar to Case 4, however here the strong air current appear close to the room's surfaces, while in Case 4 especially the downward flow is spread within some distance from the wall. What is more, airflow pattern in the room is more mixed, than in Case 4, which might be connected with weaker airflow currents in the room.

When smoke results are compared with velocity results for the same test, see figure 5.8(b), it can be seen that there are some discrepancies between them. As discussed in section 5.3.1 velocity results might indicate that air is moving downwards in areas close to left wall and rather moving up in the right part of the room. Although it is difficult to state that this airflow is certain, it is possible that airflow distribution in the room while performing the velocity measurements was different than while carrying out the smoke experiment. What should be also stated is that while performing smoke test two persons were present in the room, which may change to some extent conditions in

the room. Even though if a significant change in airflow pattern might be caused by small additional heat source, it also indicates that system is very sensitive and likely unstable.

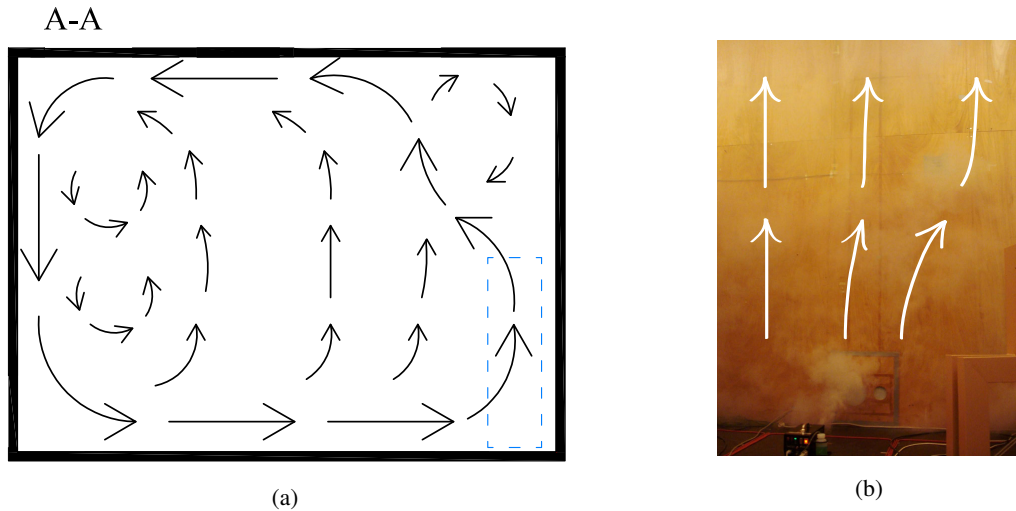


Figure 5.12: Figure showing a) scheme of the air flow pattern in the room for Test 1d, b) picture of part of the room highlighted on the scheme with blue dashed lines.

Second test, for which smoke experiment is performed is Test 1b. Scheme of airflow pattern is not presented here, as the airflow direction was changing during performing the smoke test, which made preparation of the scheme impossible. Instead of that two pictures are presented, see figure 5.13 on which smoke visualizations of the airflow are done next to the glass wall. It can be seen, that the airflow direction changes from upward to downward, which indicates that the main air current in the room is fluctuating. The time difference between taking these two pictures is few minutes.

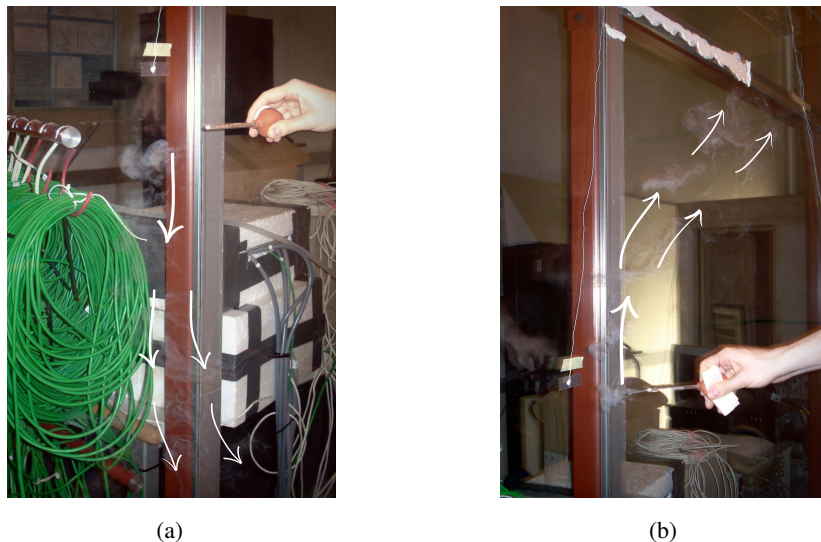


Figure 5.13: Pictures showing a) downward airflow close to the glass wall b) upward airflow close to the glass wall.

5.3.3 Stability problem

In this part stability problem is investigated by checking how velocities in the room change in time. Until now only mean values of velocity were used and here results of velocities are presented for whole measuring time with 0.1 s interval. If significant changes in velocity can be observed during the time of measurements, which is around 17.5 minutes, it may indicate that the airflow distribution is unstable. For each test velocity graphs are made for only one measuring point where the maximum mean velocity in the room is measured. In the main report only results for the most representative tests are presented and additional graphs for more tests can be found in appendix A3.1.2.

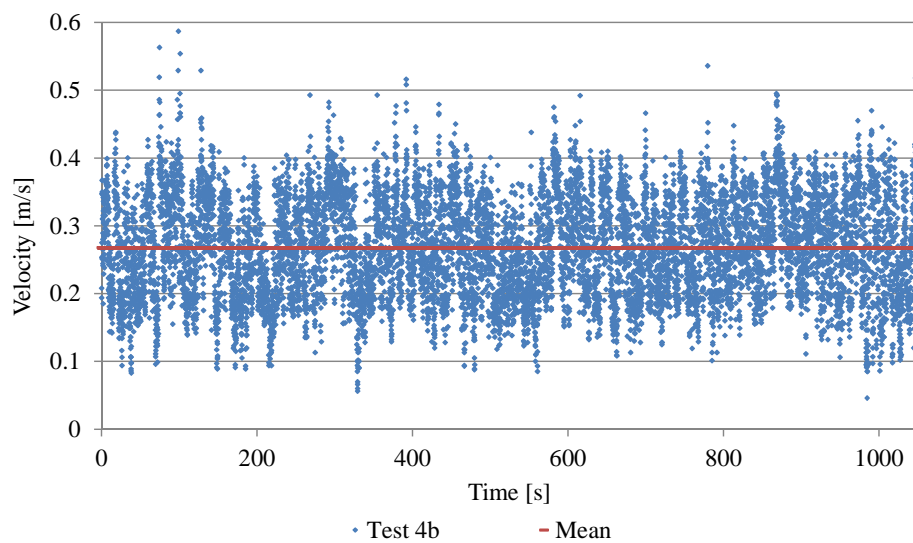


Figure 5.14: Velocity results for Test 4b with 0.1 s interval.

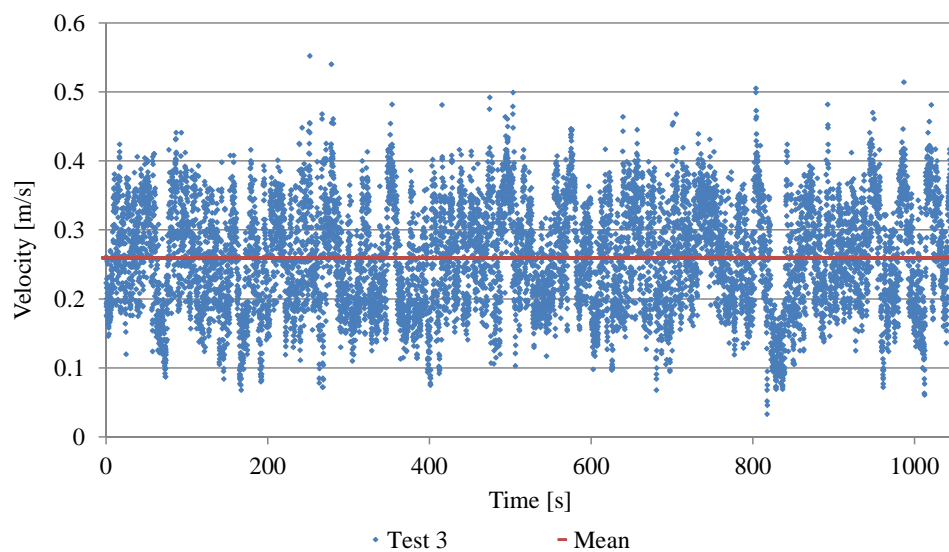


Figure 5.15: Velocity results for Test 3 with 0.1 s interval.

At first, two graphs are presented for tests with strong air current in the room, Test 4b and Test 3, as these tests are expected to show very stable airflow pattern. Results can be seen on figures 5.14 and 5.15 and it can be noticed that for both of them velocities are equally spread around the mean value, which for both of the test is around 0.26 m/s .

Next results are presented for two tests of Case 1, for which smoke experiments are performed, Test 1d and Test 1b, see figures 5.16 and 5.17. It can be noticed that velocities are dispersed around the mean value in much more disordered way than it is observed for Test 4b and Test 3 described above. Because velocities in the room for tests with symmetric supply area and heat sources location are in general lower than for tests with strong air current formed by the unequal conditions, lower mean velocity values are observed for these tests. The accuracy of the equipment is down to $\pm 0.05 \text{ m/s}$, so the lowest values scattered around 0.05 m/s , which can be expected when anemometers are used. Nevertheless, general pattern of the velocity distribution is much more chaotic and differ from Test 4b and Test 3. It should be noted, that results for the rest of tests of Case 1 are presented in appendix A3.1.2 and show similar velocity pattern to Tests 1b and 1d. Although based on this investigation it is difficult to confirm problems with stability for tests with equally distributed heat gains, it indicates that this problem may be possible. This could also explain unsteady conditions observed in the room while performing smoke experiment for Test 1b and finally unusual locations of points for Case 1 on a design chart.

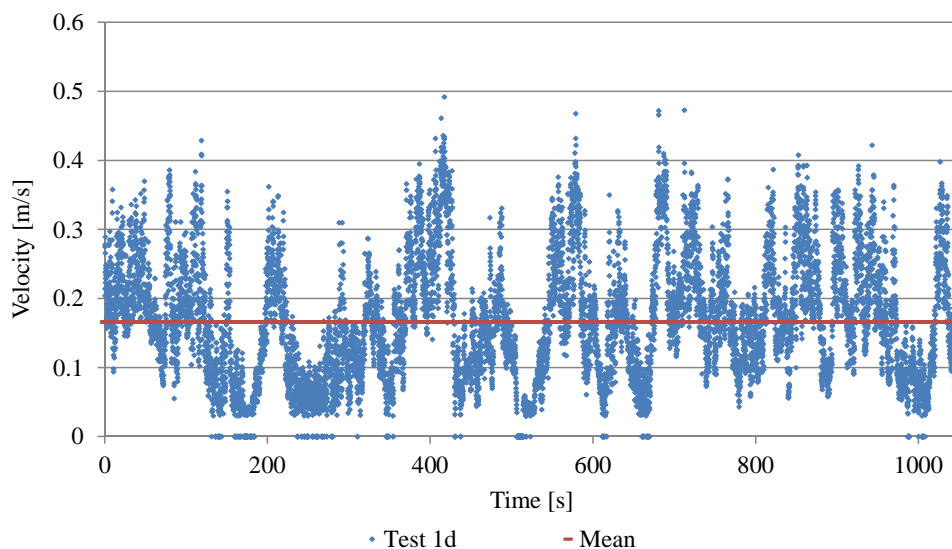


Figure 5.16: Velocity results for Test 1d with 0.1 s interval.

It should be noted, that results for Case 6, with radiator in the corner, Case 7, with radiator in the middle and Case 11 with only heating wires are presented in appendix A3.1.2 and their velocity distribution is more balanced than for Case 1, however not as equal as for Test 4b or Test 3.

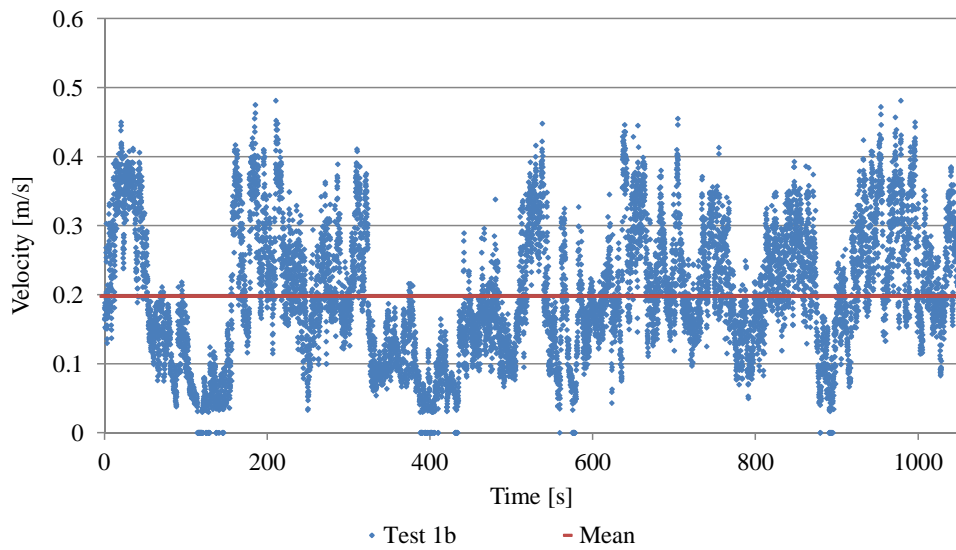


Figure 5.17: Velocity results for Test 1b with 0.1 s interval.

5.4 Dimensionless analysis

Design chart described in section 5.2 is based on measurements performed in a particular test room and should be applied only to design of spaces of similar dimensions. Naturally it can be expected that the general performance of DCV in a room with different dimensions will be comparable to this design chart, but it is important to check how big can be possible variations between them. This knowledge is necessary for the designers to be able to freely design diffuse inlet systems. Here only simple investigation is carried out to be able to better understand nature and scale of this problem.

The approach is to compare design charts for two test rooms with different sizes. All the experiments for this report are performed in room with inner dimensions of 6.00 by 4.65 by 4.40 m height, which is going to be called in this section as a large room. Results for the large room are compared with measurements described in Jakubowska [2009] and performed in a test room with dimensions

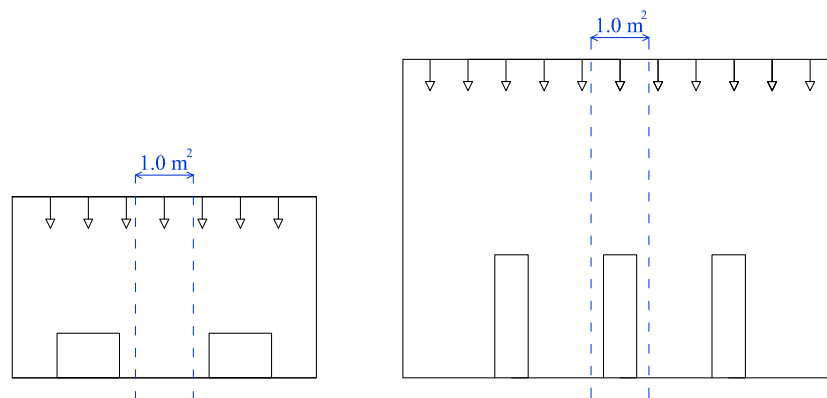


Figure 5.18: Graph presentig idea of the investigation.

of 4.2 by 3.6 by 2.5 m height, which gives room volume around three times smaller compared to the large room and that is why this room is going to be further called as a small room. Small room's set-up is introduced in section 2.3 and presented on figure 2.6(a). To be able to compare these two rooms it is necessary to recalculate values from the design charts with reference to the size of the room. Idea of the approach is presented on figure 5.18. It is wanted to obtain results independent of area of the room and this approach can be shown as an analyse for a space with area of 1.0 m^2 and height equal to height of the room cut from the room. To obtain area independent design chart, airflow rates are divided by the floor area for particular room and ΔT is not changed, as it is assumed that this value is constant within the area of the room.

Results are presented on figure 5.19 and calculations made to obtain the graph can be found in appendix B.2 - *Dimensionless_calculations.xlsx*. It should be noted, that all results presented on the graph are in the same range of Archimedes number, between around 30000 up to 110000 for both rooms, to minimize the influence of different conditions of the measurements. Three tests are chosen for the large room to be able to minimize the differences in set-up between two rooms. Set-up of the small room with two mannequins and two tables with computers and lamps located next to each other in the middle of the room is different from the set-up of tests performed for the large room. Most similar cases for the large room are Case 1 with mannequins equally distributed in the room and cases with heat sources distributed on one side of the room and it is expected, that set-up of the small room can be approximated by a combination of aforementioned cases.

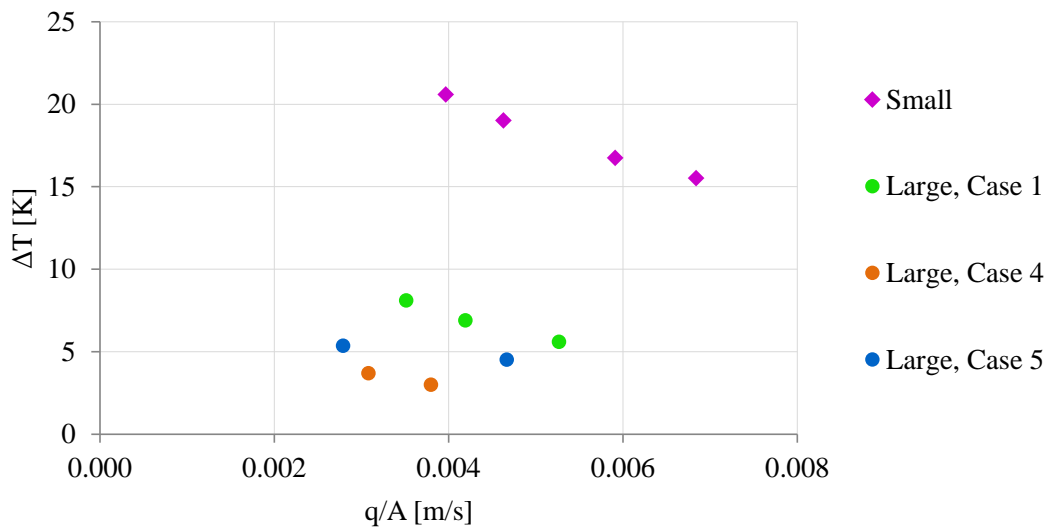


Figure 5.19: Graph presenting q , ΔT graph in a form independent of the area of the rooms.

Based on the assumption that case with set-up like in the small room, for the large room would be located between presented curves for Cases 1, 4 and 5, it seems that there is big influence of height of the room on the results. Change of room's height may influence the buoyancy forces in the space and it is known that these forces are the main ones, which generate air movement in this kind of ventilation systems. In the small room heat sources are located closer to the air inlet comparing to the large room and it is possible, that raising up of the plume is limited because of that. As a result higher q and ΔT can be used in the small room without causing a draught. This situation is similar

to change which appears, when the light bulbs are turned on in addition to heating wire, which is described in section 5.2.2. The buoyancy forces are decreased, because the plume from the heating wire is disturbed by the light bulbs, which results in lower velocities in the occupied zone.

Because of the fact that this investigation may be inaccurate due to all the assumptions that are made, and the problem seems to be very important for the performance of DCV, this issue will be investigated further in chapter 6 by means of CFD modelling.

5.5 Indoor environment

In this section additional indoor environment parameters regarding both thermal comfort and indoor air quality are investigated, based on measurements in the test room. These include calculations of vertical temperature gradients and resulting local discomfort for the occupants, determination of temperature effectiveness for the ventilation system and radiant asymmetry connected with the cool ceiling in the room. Finally the ventilation effectiveness is calculated, based on tracer gas concentration measurements. What is more some variations are made on the design chart, by changing the criteria for the draught rate in the room and by including indoor air quality requirements.

5.5.1 Parameters connected with temperature distribution

In the first place vertical temperature gradients in the room are discussed. Measured vertical temperature gradients are considered regarding the total height of the room and presented in a dimensionless form, as a dimensionless temperature profile, in accordance with equation 5.1. It should be noted that all the temperatures used for these calculations are measured on the middle column in the room.

$$t^* = \frac{t_l - t_s}{t_e - t_s} \quad (5.1)$$

t^*	Dimensionless temperature [—]
t_l	Local temperature depending on the height [°C]
t_s	Supply air temperature [°C]
t_e	Extract air temperature [°C]

Results for three exemplary tests can be seen on figure 5.20. Results of tests 1a and 4a are representative for most of the tests and that is why temperature profiles for other tests are not presented here and can be found in appendix B.1 - *Vertical_temperature_gradients.xlsx*. It can be observed that up to height of around 3.5 m the dimensionless temperatures are almost equal for all of the tests and close to 1.0, which means that temperatures within the space are very uniform and air in the room is well mixed. In the distance from 3.5 m up to 4.3 m some differences can be observed between tests. Especially for Test 6, with radiator in the corner of the room, the temperature is outstanding, what may be caused by condensed plume of the radiator, which rises in corner of the room and then while crossing the ceiling might influence temperature measurements in the middle of the room. Differences might be also observed between Tests 1a and 4a. It can be seen that temperatures for Test 1a are lowered already at height 4.1 m, while for Test 4a, they start decreasing at the height of

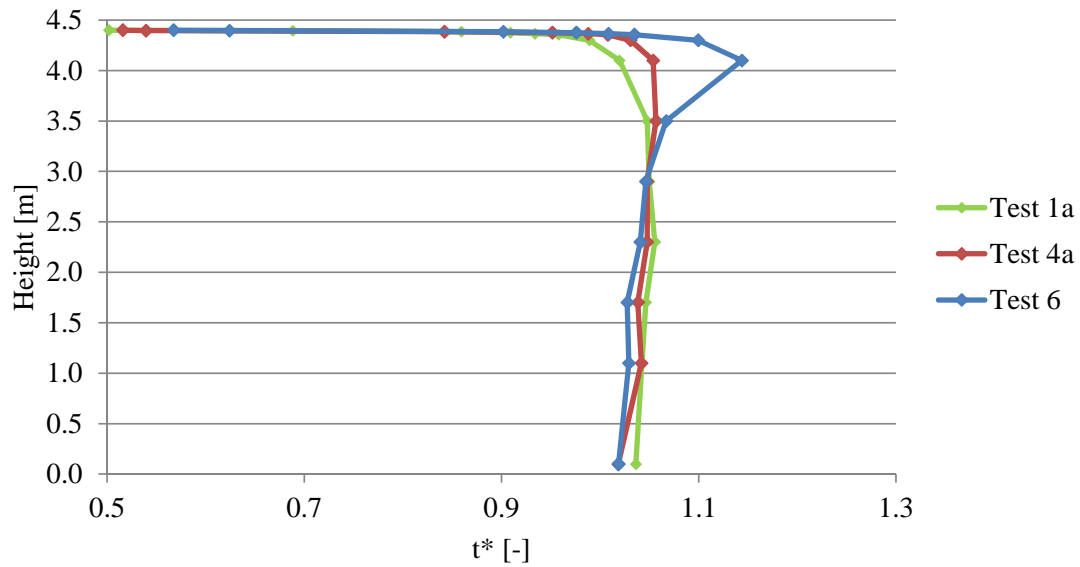


Figure 5.20: Dimensionless temperature profiles for a room with diffuse ceiling ventilation.

4.3 m. This might be connected with the fact, that buoyancy forces in Case 1 are more balanced and generated airflow is weaker, compared to Case 4. That is why this weaker current might mix more with the supply air and lower temperatures are observed already at the height of 4.1 m, while for Case 4 strong airflow is not that affected by mixing with supply air and lower temperatures are observed only very close to the ceiling.

Finally, the distance from 4.3 m height, up to the ceiling should be analysed. To be able to easier compare the results, figure with temperature profiles only in the distance up to 0.1 m from the ceiling is presented below, see figure 5.21.

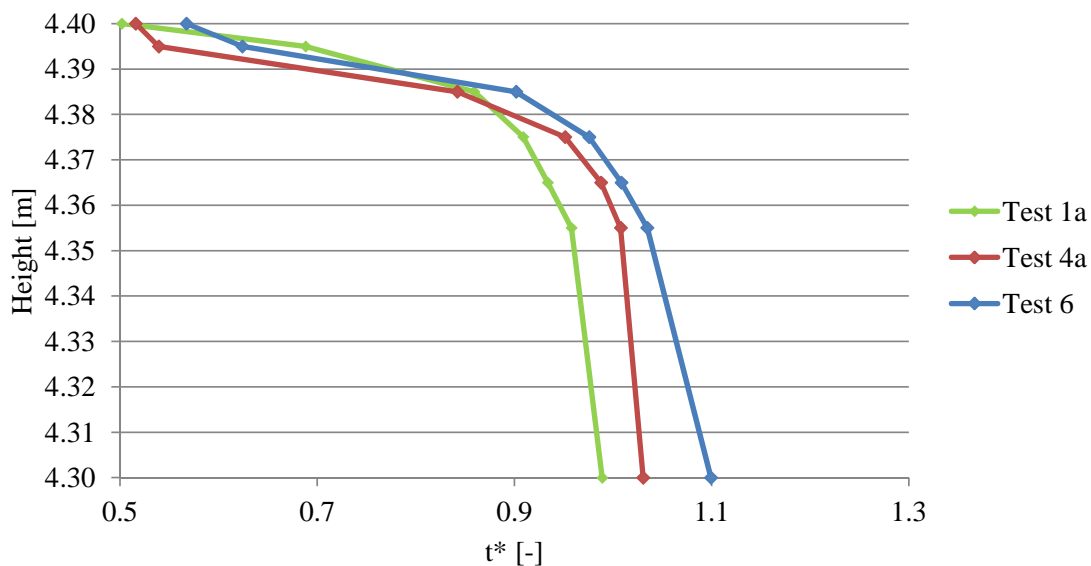


Figure 5.21: Dimensionless temperature profiles in distance up to 0.1 m from the ceiling.

It can be noticed that the layer of cool supply air is formed very close to the ceiling in the distance of around 0.05 m from the ceiling, while the highest temperature gradients are observed in the distance up to 0.02 m from the ceiling's surface. What is more profiles for all the tests in this distance are very similar to each other, which indicates that location of heat sources in the room does not influence this layer. What is more even if the supply area is changed from three chambers to the whole ceiling, the thickness of the cool layer is not changed.

Next in this section, PD_{VTG} indices and temperature effectiveness of ventilation system are described. It should be noted that for these calculations values measured at the movable columns are taken into consideration, however some of the sensors are affected by plumes of the heat sources and these values are excluded from the calculations. Temperature results for all the tests can be found in appendix B.1 - *Results_t_u_DR.xlsm*.

As described in section 3.2.2, vertical temperature gradient in the room between person's head and ankle level, 1.1 m and 0.1 m, is one of the main local discomfort parameters. In this approach results can be presented as Percentage Dissatisfied, PD_{VTG} , which is a function of the vertical temperature gradient. Equation, which is used to calculate PD_{VTG} , can be found in appendix A1.1. As observed already, when analysing dimensionless temperature profiles in the room, the temperatures in the occupied zone are very well mixed and it can be expected that PD_{VTG} values are very low. Indeed, maximum temperature gradient between head and ankle level for all of the test is lower than 1 K, which corresponds to PD_{VTG} value of around 0.75%, which is significantly below the requirement for category B buildings, 5%.

Next issue connected with temperatures in the room is temperature effectiveness of the ventilation system, ϵ_t , introduced in section 3.2. Due to the fact that equation used to calculate this effectiveness is very similar to equation used for dimensionless temperature profiles calculation, it can be expected that also here results are close to 1.0. Indeed, the ventilation effectiveness for all of the tests are in range from 0.91, for Test 8c with heating wire and light bulbs, up to 0.99, for Test 4c with mannequins located on one side of the room, and mean temperature effectiveness for all of the tests is equal to 0.97. Results of ϵ_t for all of the tests can be found in appendix B.1 - *Vertical_temperature_gradients.xlsx*. According to theory about DCV, presented in chapter 2, this type of system can be considered as kind of mixing ventilation system, as the ϵ_t is close to 1.0 and results for diffuse ceiling tested in this report confirm this thesis.

To conclude investigations in this section, it can be stated that for diffuse ceiling ventilation there is no problem with vertical temperature gradients, as the airflow pattern is well mixed, what is confirmed by the temperature effectiveness close to 1.0, which is a typical value for mixing ventilation type.

5.5.2 Radiant asymmetry

In this section another local thermal discomfort parameter is discussed, namely radiant asymmetry between floor and ceiling temperature. This parameter is introduced in section 3.2.2 and the criterion for category B buildings is defined, PD_{RA} must be lower than 5%, which corresponds to 14 K difference between floor and ceiling temperature. Ceiling surface temperatures and calculated temperature differences for all the cases can be found in appendix B.1 - *Results_t_u_DR.xlsm*. It should be noted that temperatures of the ceiling are not uniform for the experiment cases, as for most of the tests inlet area consist of three chambers and the rest of the ceiling has higher temperature than

area of the inlet and even in the case with whole ceiling supplying air, the ceiling's temperature is not homogeneous. That is why in calculations of radiant asymmetry it is decided to use mean temperature of inlet area of the ceiling for each case as the temperature of the whole ceiling. In this way the calculations are significantly simplified and even though the results are not consistent with real situation in the room, by taking into account more critical values it is ensured that if calculated asymmetry fulfills the requirements, for authentic situation the criteria will be also satisfied.

Results of radiant asymmetry for all the tests are in range from 1.5 K, for Test 12b with only light bulbs working, up to 8.4 K, for Test 3 with only two chambers supplying air to the room. Mean radiant asymmetry for all of the tests is equal to 4.5 K, which is significantly lower than the requirements. The lowest temperature difference for case, with only light bulbs, might be explained by the fact, that in this experiment airflow supplied to the room can be characterised by the lowest product of q and ΔT and the temperature of the ceiling is not cooled significantly. On the other hand, for Test 3, in real situation area of inlet consists only of two chambers and the assumption of using mean temperature of the inlet as the whole ceiling temperature for this case overestimates results more than for cases with three chambers working.

5.5.3 Ventilation effectiveness based on Case 13 measurements

As described in section 3.3, ventilation effectiveness, ϵ_v , is an important parameter connected with indoor air quality. That is why experiment for Case 13 is performed and ventilation effectiveness is calculated based on measurement results presented in appendix A3.2. Description of set-up for Case 13 can be found in section 4.3. Tracer gas concentration in the extract air is equal to around 278 ppm and in the breathing zone, sampling point at 1.7 m height, is equal to around 280 ppm. To be able to calculate ϵ_v it is also necessary to know pollution concentration in the supply air, which is calculated based on reading of flowmeter measuring dinitrogen oxide flow into Chamber 2 and the airflow supplied by the chamber, which gives the tracer gas concentration of around 47 ppm. Based on this results, the ventilation effectiveness can be calculated and is equal to around 0.99. Ventilation efficiency close to 1.0 indicates again, that DCV can be considered as mixing type of ventilation. What is more, results can be compared with measurements described in Yang [2011] and introduced in section 2.3, which show similar values of ventilation effectiveness. In addition, author tested if increasing the ACH in the room will increase the ventilation effectiveness and the results did not show significant improvement of ϵ_v .

5.5.4 Variations of the design chart

In this section basic design chart, presented in section 5.2, is modified in two ways. Firstly limiting velocity values are changed and it is showed how the cooling capacity of the system changes if other category of indoor environment quality is chosen. Next, additional limiting values are added on the design chart, connected with minimum airflow due to indoor air quality requirements.

Limiting criterion for the design chart is draught risk, however this criterion is described by maximum velocity in the occupied zone. When draught rate is considered, see section 3.2.1 and table 3.2, it can be seen that for category B of buildings it should be lower than 20%. For other categories, A and C, it is respectively 10% and 30%. In section 3.2.1 is shown as well that draught rate, DR, is dependent on three local parameters, which are velocity, temperature and turbulence. These three parameters can variate in the occupied zone and in some range can create discomfort

connected with draught. However, it is sometimes convenient to analyse draught risk only with respect to velocity, because other two parameters in expected range do not change and affect the results significantly.

It is important to know how the design chart presented in section 5.2 looks for other categories of buildings. When range of temperatures from standard DS/EN ISO 7730 [2006] is considered and turbulence is expected not to exceed 60%, the maximum velocities that can occur in occupied zone not to create discomfort from draught can be found from equation 3.2. The table with results for three building categories can be found in table 5.3.

Building category	DR [%]	Temperature range [°C]	Maximum velocity [m/s]
A	10	24.5 ± 1.0	0.10
B	20	24.5 ± 1.5	0.15
C	30	24.5 ± 2.5	0.20

Table 5.3: Calculated maximum velocities for three categories of buildings based on DS/EN ISO 7730 [2006]

When these three velocities are taken into consideration design chart can be recalculated to present new possible spans of q and ΔT , which are not causing discomfort connected with draught risk. To present the results Case 4, with heat load located on one side of the room, is chosen and three curves for different categories of buildings can be seen on figure 5.22. For instance, when design airflow is equal to $0.08 \text{ m}^3/\text{s}$, ΔT is equal to 1, 4 and 9 K for category A, B and C, respectively. It can be seen that for higher maximum limiting velocity, the possible range of q and ΔT increases, but as higher is the maximum velocity, the change between categories is slightly larger. When designing a specific building a design chart for the specific requirements should be chosen.

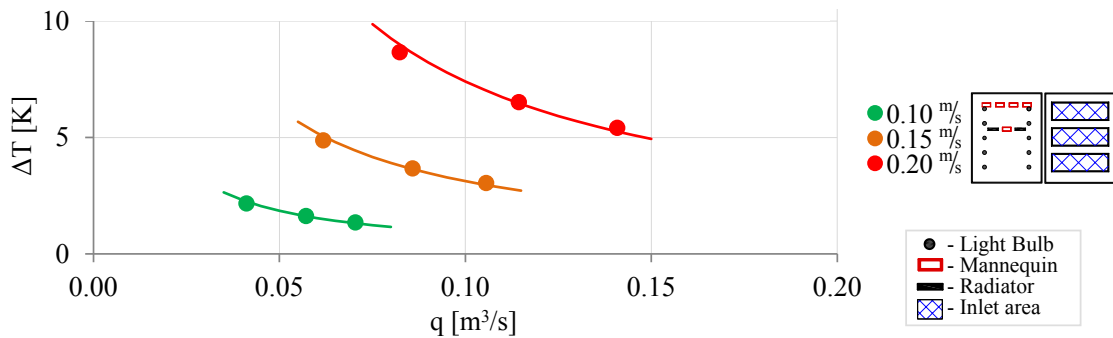


Figure 5.22: Design chart for Case 4. Lines for different velocities correspond to various categories of buildings.

Another possible modification of the design chart is to include additional limiting parameters on the graph. One of the possible limitations for the ventilation system might be minimum ventilation rate required in the space to maintain good indoor air quality. In section 3.3 required ventilation rates for B category of buildings and various types of the rooms are specified. Based on given values, two

representative airflows are chosen, $0.04 \text{ m}^3/\text{s}$ for office and $0.12 \text{ m}^3/\text{s}$ for classroom, and these values are presented on design chart on figure 5.23. It can be noticed that indoor air quality requirements for a typical office can be easily fulfilled when using DCV. For typical classroom, which is a type of space with dense occupation and high ventilation demands, curves on the edesign chart are limited and not only draught rate has to be taken into consideration, when designing such a system, but also limits regarding indoor air quality.

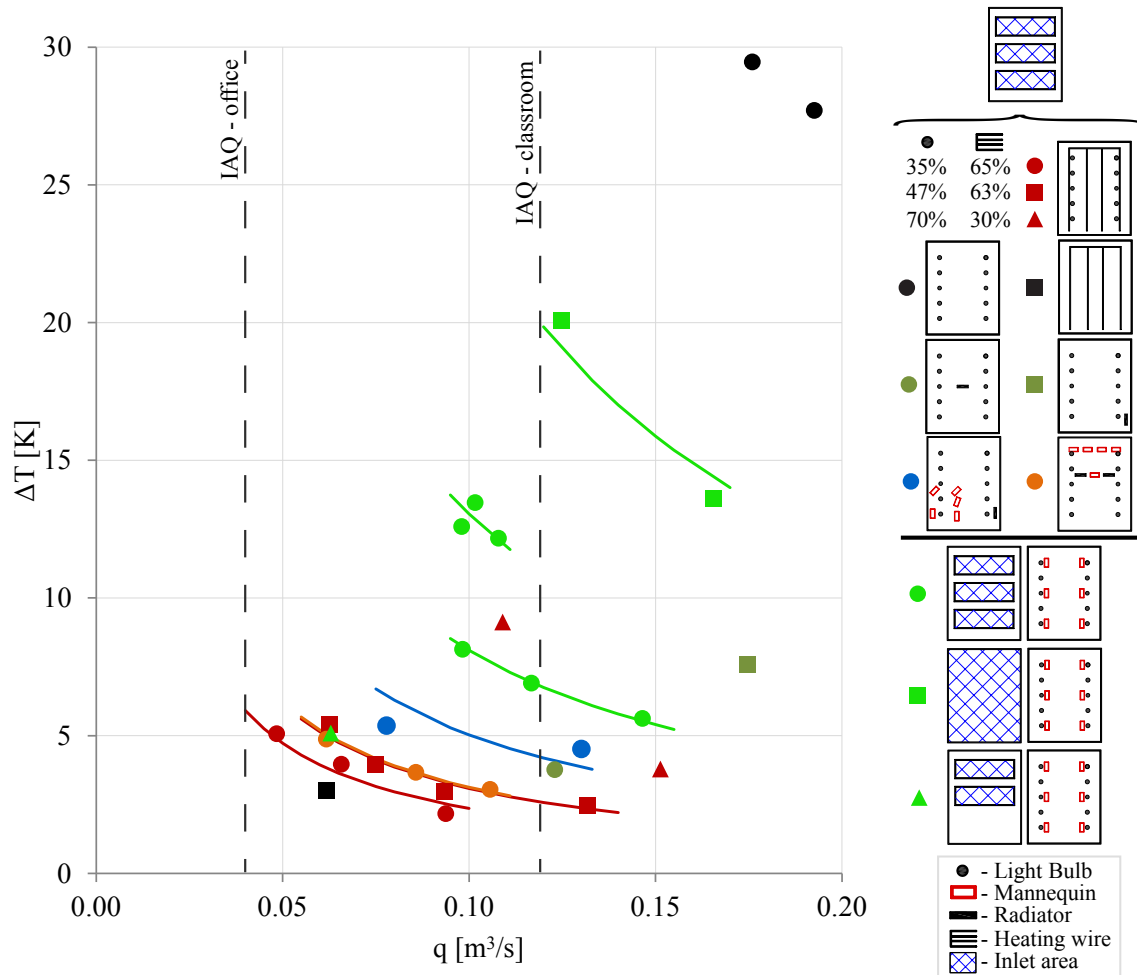


Figure 5.23: Design chart with additional lines regarding the minimum requirements for indoor air quality.

5.6 Radiation in DCV

Mixing of the air in DCV system is driven by buoyancy forces in the room, which are generated by heat loads, however, heat exchange is not only limited to convection. Radiative heat transfer should be investigated to fully understand heat flow in the room. When cool air is supplied through the diffuse ceiling, its temperature is decreasing. This lower temperature increase radiative heat transfer between the ceiling and other, warmer surfaces in the room. In addition, when heat loads in the room are applied, the sources' surfaces are warmer than the room's surfaces. Heat exchange due

to radiation is proportional to the difference of the temperatures raised to the fourth power, so even small changes can affect strongly the heat flow.

The calculation are based on radiation balance presented by Incropera et al. [2006]. Equation 5.2 is used to calculate heat flow by calculating radiosity of each surface in the room. In the calculation reflection is taken into consideration, however, the calculation are simplified only to the surfaces of the walls, floor and ceiling. Therefore, it can be expected that heat exchange between cool surfaces is underestimated.

$$\frac{\sigma T_i^4 - J_i}{(1 - E_i)/E_i A_i} = \sum_{j=1}^N \frac{J_i - J_j}{(A_i F_{ij})^{-1}} \quad (5.2)$$

σ	Stefan-Boltzmann constant [$\text{W}/\text{m}^2 \text{K}^4$]
T	Temperature [K]
J	Radiosity [W/m^2]
E	Emissivity [$-$]
A	Area [m^2]
N	Number of surfaces [$-$]
F_{ij}	View factor from surface i to j [$-$]

Emissivity of the surfaces is chosen based on Infrared Services [2013] and chosen values and materials are presented in table 5.4.

Surface	Material	Emissivity [$-$]
Floor	Plywood: commercial, smooth finish, dry	0.82
Walls 1, 2 and 4	Plywood: untreated	0.83
Wall 3	Glass	0.92
Ceiling	Paint: TiO ₂ , white	0.94

Table 5.4: Emissivity values used in calculation for the surfaces in the room

The calculation are made in MATLAB program in script. The script is located and can be found in appendix B.1 - *Radiation_script.m*. View factors are calculated based on equations presented by John R. Howell [2010]. Final results for heat flow for each of the surface can be found in appendix B.1 - *Radiation_results.xlsx*.

Results show that for measured cases the only surface that is warmed up due to radiation is ceiling. Moreover, even when only three chambers are used, temperature of the rest of the ceiling is cooled enough by the air to be heated by radiation in the room, but heat flow is much smaller than for the chambers. In the majority of tests it can be seen that heat flow to the working chambers is equal to 80% of total radiative heat flow to the ceiling. The radiant heat flow not only warms the surface of the ceiling and the supply air, but the ceiling also works as radiant cooling surface, which is one of the most effective ways to cool the room, because it does not require air movement and

does not cause draught. Warmer ceiling surface due to radiation means also that problem with cold ceiling for radiant asymmetry should be smaller.

What is more, in example, for Case 4 calculated total heat transfer by radiation to the ceiling is equal around 510 W, when the heat load in the room is 2000 W. This means that 25% of heat load is transferred to the ceiling by radiation. Radiant heat flow to the ceiling is affecting the surface temperature, but also the ceiling inside due to conduction. This energy is transferred to the air, which means that when air enters the room it is warmer than measured by thermocouples in the ducts. This increase of air enthalpy will be used later in CFD to calculate the temperature of air, which enters the test room. It is assumed that the whole energy that is transferred to the chambers by radiation warms up the supply air.

Another example might be Test 12b, which is characterised by the lowest radiant heat flow in respect to heat load in the room, but this can be connected with the lowest cooling capacity of supply airflow for this case, which is also mentioned in section 5.5.2. Additionally it may be also explained by specific character of the heat load generated by light bulbs.

5.7 Pressure test

This section is based on pressure drop measurements described in Jensen and Jensen [2012] and additional own measurements. Results of pressure tests performed on ten samples and the real ceiling are presented and compared with pressure drop measurements for other diffuse ceiling constructions.

For ventilation system it is preferable to decrease the pressure drop on the diffuser, because of noise problems and needed higher pressure generated by fan in the system. Higher pressure drop and higher velocities in the diffuser result in higher noise level. From design of ventilation system in the room it is expected to avoid generating higher A-weighted sound power level than specified in criteria, see CR 1752 [1998]. For the diffuse ceiling, because of high inlet area and low inlet velocities, the noise level is expected to be low, however no investigation of noise level for the room is made in this report. Another effect of pressure drop is how it affects the power of the fan that supply air to the room. Higher pressure drop from the diffuser means that the static pressure generated by inlet fan needs to be increased, which effect in higher power consumption. It can be a problem, when an energy efficient building is considered to be designed.

Diffuse ceiling that is mounted in the room is described in section 4.1.1, but the construction can vary. The ceiling that is chosen is very clean and white, but at the same time a few layers of white paint are used to cover the diffusive part, see sample on figure 4.5. Ten samples were tested in Jensen and Jensen [2012] to investigate differences in pressure drop for different construction of samples. Later measurements on real ceiling are conducted. To check correctness of the results few more tests are carried out. Results for pressure test conducted on diffuse ceiling in the room and 10 additional samples can be seen on figure 5.24. It should be noted that measurement for sample 9 was repeated with different set-up, because none of the samples showed the same pressure drop as measurement for real ceiling mounted in the room. Corrected measurements showed that real pressure drop for sample 9 should be higher and the same change should be considered for the rest of the samples.

On the figure it can be seen that pressure drop for different samples of the ceiling can vary in span from 5 Pa to 50 Pa for ventilation flow rate equal to $50 \text{ m}^3/\text{h m}^2$, while results for the real ceiling

are showing 70 Pa. However when correction for the error of measurements for samples is taken into consideration it can be stated that the pressure drop on the ceiling is similar to Sample 4 that shows the highest pressure drop and which construction is similar to the real ceiling, see Jensen and Jensen [2012]. Summing up pressure drop for samples shows that there is a large span of possible variations, but the real ceiling, due to its construction, can be characterised by one of the highest pressure drop.

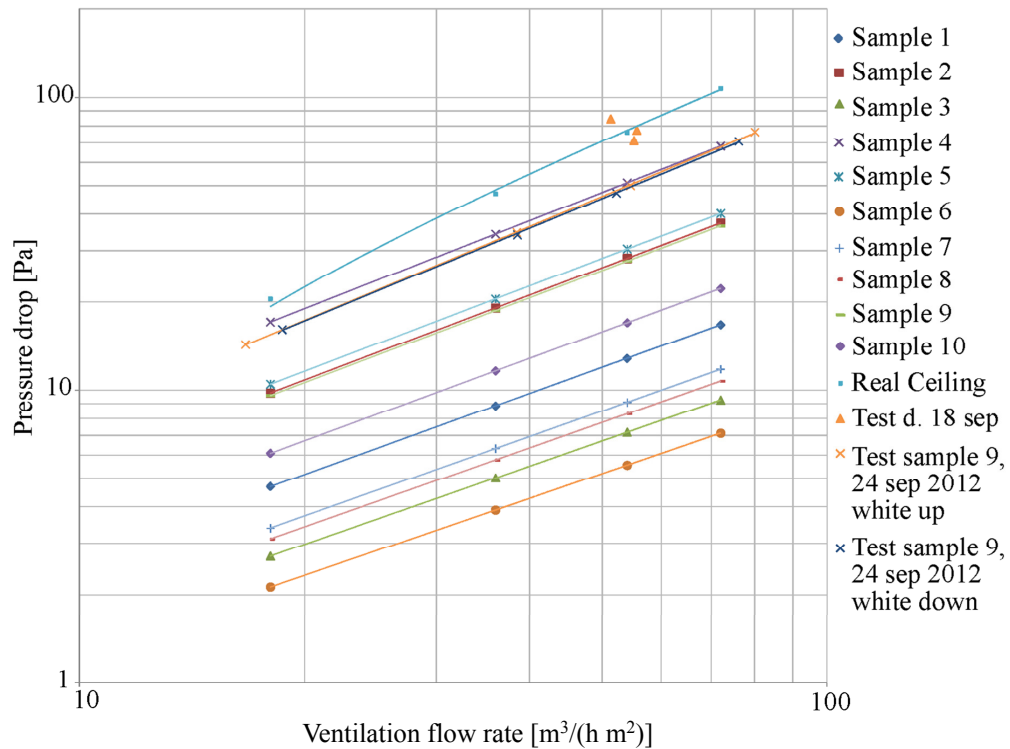


Figure 5.24: Pressure drop as a function of a volume flow rate. Average values of two tests for each sample and of measurements on real ceiling with additional three measurement points from 18th September and additional tests for sample 9. Edited from Jensen and Jensen [2012]

5.7.1 Other diffuse ceiling constructions

Application of diffuse ceiling ventilation give a large span of possible solution for construction of the diffuser, see chapter 2. In case, when a suspended ceiling with 7 mm holes is used to supply air to a room, described in Yang [2011], it is shown that the pressure drop for DCV can be lower comparing to other standard solutions for diffusers available on the market. When noise requirements are also considered the pressure drop for standard diffuser and diffuser ceiling can be respectively 12 Pa and 3 Pa, see section A3.3 in appendix. Lifetime cost of the system should be taken into consideration in the comparison to make final conclusion. For example for diffuse ceiling ventilation it is possible to lower the costs, when panels with small holes are used as a diffuser, because costs of production are lower then standard diffusers as well as pressure drop, as it is shown.

Similar construction is presented in Jacobs and Knoll [2009], where different solutions are analysed with air supplied through 25 mm holes in suspended ceiling to the classrooms. In comparison

of different ventilation systems it is shown that decentralised solution with low pressure drop diffuser like diffuse ceiling inlet can decrease significantly specific fan power of the system even by around 98 %, see table A3.2 in appendix, but only with limmited air flow, see table A3.3 in appendix. Deteiled description of the results can be found in appendix in section A3.3.

In Jakubowska [2009] there is used a suspended ceiling with mineral wool panels and it is shown that pressure drop for the whole ceiling is low and variates between 1 and 5 Pa for airflows lower than $40 \text{ m}^3/\text{h m}^2$. Detailed investigation shows that low pressure drop is connected with air leakage through gaps between panels instead of airflow through the panels. The reason of that is that the pressure drop for panels is more then ten times higher than for the gaps, see figure 5.25, which effects in almost no airflow through panels.

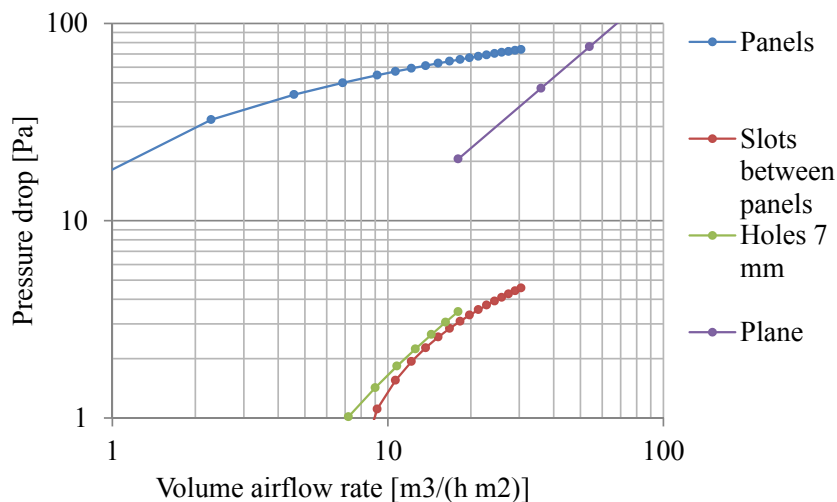


Figure 5.25: Pressure drop as a function of a volume flow rate. Average values of two tests for each sample and of measurements on real ceiling with additional three measurement points from 18th September and additional tests for sample 9. Edited from Yang [2011] and Jakubowska [2009]

All in all, it can be concluded that there are a few possible solutions of the construction for diffuse ceiling inlets, based on analyse presented above, which show a large span of pressure drop, what is presented in figure 5.25.

It can be seen that the ceiling used in the tested room results in similar pressure drop as mineral wool panels. On the other hand solution with holes or slots in the ceiling can result in low resistance for airflow. Advantage of white and plane ceiling can be not enough when confronted with higher pressure drop. Another solutions can be discussed and their effect on airflow in the room can be investigated to find compromise.

5.7.2 Leakage in the ceiling

Besides pressure drop measurements, two tracer gas measurements are conducted for the test room, which are presented in sections A3.2 and A3.3. Analysing their results can help to understand airflow in the ceiling.

It can be seen on figures A3.19 and A3.19 that the concentration in chambers is rather constant after a period of time. Small decrease of concentration for Chamber 2 is connected with a decrease in supplied flow of tracer gas, because the controlling valve did not keep the constant pressure. However, the results indicate that there is a possibility of flow of fresh air to the chambers. It is possible that even when the valves are closed on the ducts there is still a small airflow that is not observed on pressure drop measured on the orifice due to its accuracy.

Additionally, on figure A3.19 a difference between concentration in Chambers 2 and 3 can be observed. It can be seen that the concentration in Chamber 2 increases in a fast manner, while concentration in Chamber 3 builds up much slower. This can be explained by the fact that there is an airflow between the chambers, even when they are tight. When the construction of the ceiling is considered, it is shown in section 4.1.1 that there are two main layers in this diffuse ceiling. The former is a diffusive layer and the latter is a paint layer. It is possible that there is a difference of pressure drop for both layers, and because the paint layer is more dense, part of the airflow can pass by the connection between Chamber 1 and the ceiling and flow to plenum space and later to Chamber 2. Chamber 3 is not affected significantly because the distance is longer. Therefore, when Chamber 2 is used as an inlet both Chamber 1 and Chamber 3 can be affected, due to the same distance from the inlet.

As a result, the pressure drop is not only measured for the chambers, because a small part of the supply air can always flow through the whole ceiling. Because of this, pressure drop results can be underestimated. Moreover if the air is supplied through the whole ceiling, even when it is decided to use only three chambers, the ceiling temperature can be affected. The chambers temperature is warmer and the rest of the ceiling is cooler.

What is more, this problem can have influence on design chart results as well. In section 5.2.3 the difference between using different area of the ceiling is presented. If it is possible that for tests with only three chambers working, the air may flow as well through the whole ceiling, it can indicate that real cooling capacity for the curves should be lower. Additionally, temperature of inlet air can increase due to possible heat losses in the plenum space, see section 5.2.3, which can additionally affect the results.

CFD investigations

In this chapter results from numerical investigation of diffuse ceiling ventilation for the test room is presented. Computational fluid dynamics is used to compare two models with different height.

Computational Fluid Dynamics, CFD, is based on fluid mechanics and Navier-Stokes equations for conservation of mass, momentum, energy. The equations are used to describe fluid behavior in specified conditions on base of physics laws are discussed by Versteeg and Malalasekera [2007]. To derive the equations three physics law are used, namely the first law of thermodynamics, the mass conservation and that the sum of forces is equal to the change of momentum. The final four equations for momentum and continuity, because of their similar form, can be presented in one main general equation, when additional parameters for different terms are used. The governing equation 6.1 can be seen below. Dependent variables for the equation are described in table 6.1.

$$\underbrace{\frac{\partial(\rho\phi)}{\partial\tau}}_{\text{Transient}} + \underbrace{\nabla(\rho\phi u)}_{\text{Convective}} = \underbrace{\nabla(\Gamma\nabla\phi)}_{\text{Diffusion}} + \underbrace{S_\phi}_{\text{Source}} \quad (6.1)$$

ϕ	Dependent variable, see table 6.1
Γ	Diffusion coefficient [$\text{kg}/\text{m s}$], see table 6.1
τ	Time [s]
S_ϕ	Source term, see table 6.1

	ϕ	Γ	S_ϕ
Continuity	1	0	0
Momentum, x direction	u	μ	$-\frac{\partial p}{\partial x} + \rho_x g$
Momentum, y direction	v	μ	$-\frac{\partial p}{\partial y} + \rho_y g$
Momentum, z direction	w	μ	$-\frac{\partial p}{\partial z} + \rho_z g$

Table 6.1: *Dependent variables for five Navier-Stokes equations used in the general equation.*

Computational Fluid Dynamic is used to predict fluid behavior. Instead of writing own numerical description of the equations it is more convenient to use one of the programs available on the market.

STAR-CCM+ 7.02 is used to develop model, generate mesh, set conditions and run calculation for CFD.

6.1 Test room model

The model used in CFD calculation is based on the test room described in section 4.1. However, a few main changes should be mentioned. Firstly, the model is limited to the surface of the ceiling, so the chambers are not simulated. The heat load is added to the room from mannequins, radiators and light bulbs, but their shapes are simplified. Outlet is simplified as well to round opening in the wall.

It is chosen to analyse Case 4a with heat load located on one side of the room, because this case gives stable airflow in the room. Five mannequins, two radiators and ten light bulbs are placed in the model of the room. Precise location of heat sources can be seen on figure A2.5. The model of the room can be seen on figure 6.1.

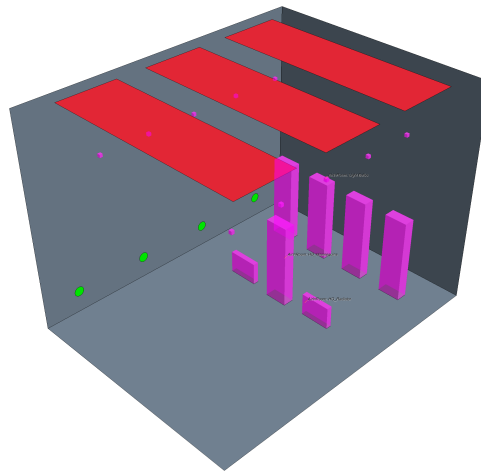


Figure 6.1: Picture presenting model of the room with selected parts in colours: inlet in red, outlet in green, heat sources in pink and walls in grey.

To be able to test effect of height of the room on airflow a second model with only three meter height ceiling is build. Using this model it is tried to simulate conditions close to the room presented in Jakubowska [2009]. Therefore 3 m is chosen, because in the study distance between mannequins and ceiling is equal to 1.3 m, so the same distance is set in the second room to give the same conditions for plume to develop.

6.1.1 Mesh

When the model is finalised the next step is to discretise the geometry of the model to cells and surfaces. This is one of the most important step in Computational Fluid Dynamics, however, in this report due to limitations only one mesh, which is using tetrahedra, is presented. Variety of discretisations are tested, but the results are not valid. One of the encountered problems that is found, can be worth mentioning. The model is based on elements, which are parallel to each other, in other words, no curvatures are used. It can be expected that mesh based on cubes will fit the geometry in a

good way, cell skewness will be minimal and it is the simplest representation. However, even when all the cell size are smaller then for tetrahedral mesh the results do not represent correct conditions. Heat load that is set in the room is not transferred to the air and it is not warmer.

The main difference that is observed between used tetrahedral mesh and cubes is growth rate. When cubes are used in the model and the cell size should be increased for the next cell, the edge length is doubled. It was not possible to change this growth for the cells, so more cells were used before the size change, but this was not enough. Finally tetrahedral mesh with surface growth rate equal to 1.2 is used.

The main cell size that is set for the model is 0.10 m, however, some surfaces are refined to increase the precision of the calculation. Cell size for outlet is set to 0.05 m. Heat source are discretised with cells equal to 0.010, 0.015 and 0.020 m for light bulbs, radiators and mannequins, respectively. The smallest cells are chosen on the sources' surfaces, because the largest problems create heat exchange. Larger edges are chosen for surfaces with lower heat fluxes. Final mesh can be seen on figure 6.2(a) and figure 6.2(b) in close-up. Total number of cells that are generated is equal to 4 133 834. Maximum skewness of the mesh cells is 72 degrees. It needs to be noted that final mesh validation is not conducted, which means that the results can be questionable.

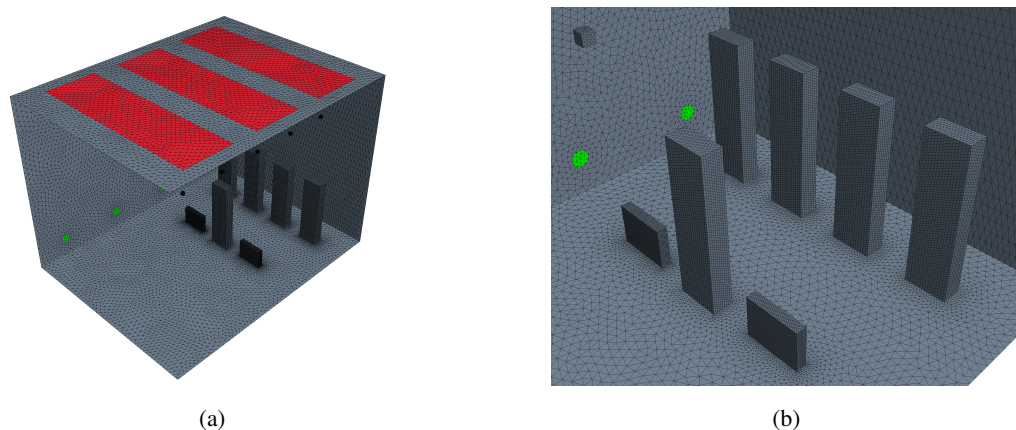


Figure 6.2: Pictures showing a) generated mesh, b) generated mesh in close-up for heat sources.

6.1.2 Physics

When the mesh is generated the physics for the model can be chosen. Description of the physics is based on STAR-CCM+ Manual [2013]. Calculation are conducted for air and a constant parameters are this fluid are chosen. The model is three dimensional and is symulated in steady state, so transient part of equation 6.1 can be cancel out. As a one of the momentum equation source gravity is added, however, density is set to zero, because it is decided to apply Boussinesq Model. Boussinesq model is only applicable in conditions, where density do not change much as a function of temperature, which mean that temperature variation in the calculation is not large. Thermal expansion coefficient and reference temperature needs to be added to the model.

Next step is to choose a turbulent model. It is decided to use realizable $k - \epsilon$ model based on Reynolds-Averaged Navier-Stokes equation for turbulence. This model is relatively precise and quite fast, due to only two additional equations. To solve the equations in the model coupled calcu-

lation for energy and flow are used, because it is described in STAR-CCM+ Manual [2013] that this solver should be robust for solving fluid dynamics with strong source terms like buoyancy.

Finally, wall treatment is set to two-layer treatment, for which calculation are divided into two layers, as it is more flexible then other methods and it is correct with either low Y^+ values or higher Y^+ . Xu et al. model for buoyancy driven flows is chosen, due to specific boundary conditions.

It should be noted that chosen methods are not strictly correct and all of the chosen models are characterised by some restrictions. This models try to predict correct solution for specify conditions but they do not guarantee it.

6.1.3 Results

The final models can be found in appendix B.2 - *OneSide_Thetra_3m.sim* for high room's model and in appendix B.2 - *OneSide_Thetra_3m.sim* for the low room's model.

Before the results are shown the post-process is shortly described. To post-process and present the results two cross-sections and three plane cuts are used. Cross-section parallel to the largest walls, Walls 2 and 4, and placed in the middle of the model is named as Long cross-section, see figure 6.3(a), and cross-section parallel to the Walls 1 and 3, and placed in the middle of the model is named as Short cross-section, see figure 6.3(b). Three plane cuts are done through the whole room at 0.1, 1.1 and 1.7 heights, see figure 6.3(c).

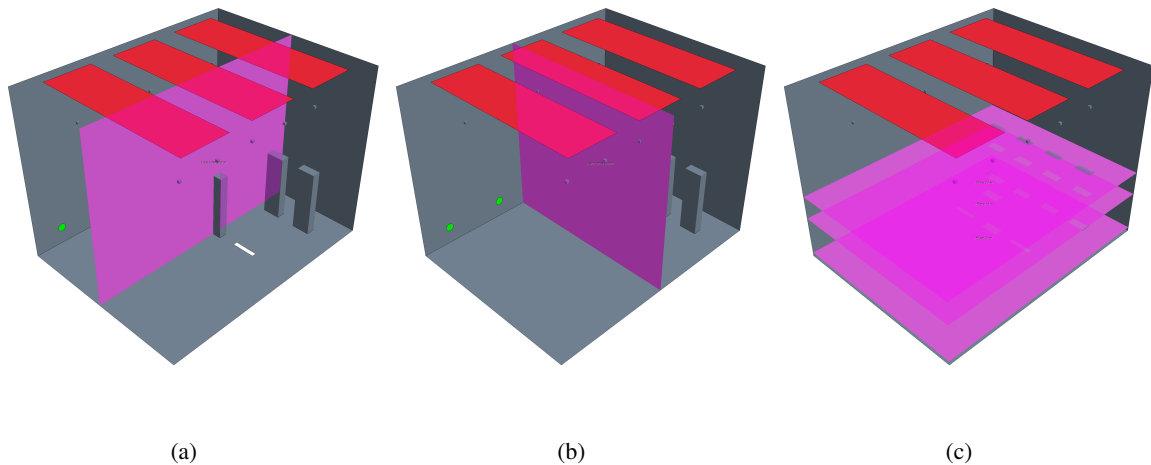


Figure 6.3: Pictures showing a) test room from inside, b) test room from outside, c) insulation above the room.

The results are presented in pairs, one for velocity and one for temperature, for each of five cuts. Firstly results for 4.4-meter high room are presented and this results are followed by 3-meter high room. In the main report only results for Long plane cut are presented. Results can be seen on figure 6.4 for the high room and figure 6.5 for the low room. The rest of the results can be found in appendix in section A4.

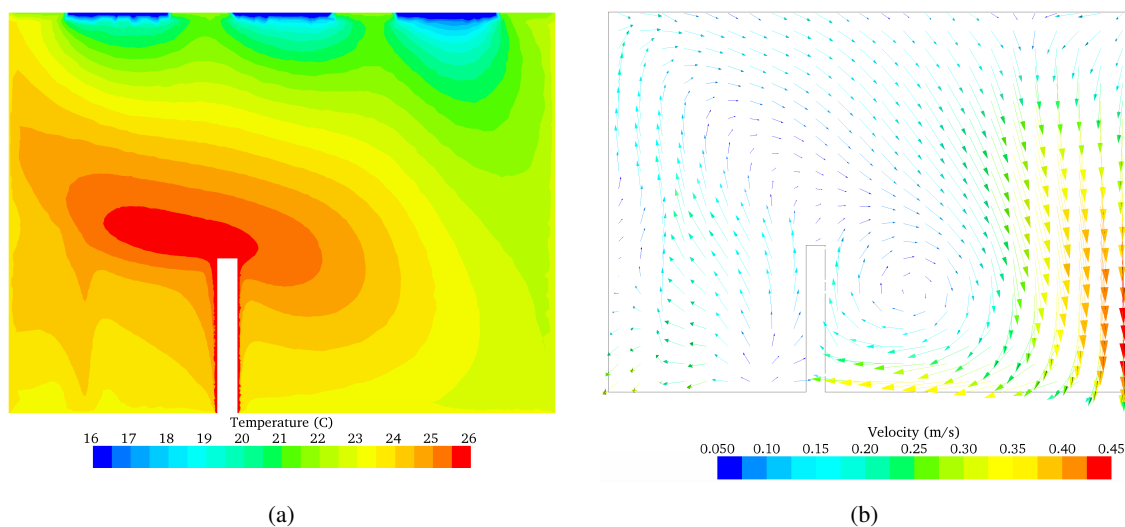


Figure 6.4: High room's model results on a Long cross-section for a) temperature, b) velocity

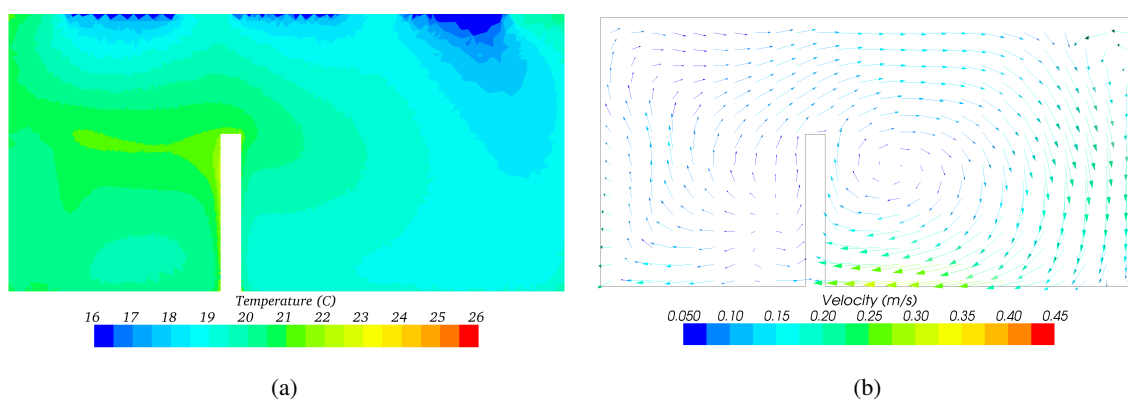


Figure 6.5: Low room's model results on a Long cross-section for a) temperature, b) velocity

On the figures it can be seen that the results are consistent with calculation presented in section 5.4. Higher velocities are observed for the high room's model, where it can be seen that in the middle of the room at 0.1 m height it is around 0.35 m/s . In the low room's model the velocity is equal to 0.25 m/s .

Conclusions and perspectives

In this chapter conclusions based on the experimental and numerical analysis of the diffuse ceiling ventilation are made. What is more problems experienced while performing investigations are discussed and possible suggestions for future work are given.

Investigations made in this report can be divided into two main parts, full-scale measurements on the diffuse ceiling ventilation and the CFD modeling. At first conclusions will be made based on results of the experiment part. The main purpose of performing the experiments was to obtain data, which is needed to construct the design chart for DCV. This chart, based on the similarity principles, enables to find maximum acceptable q and ΔT values, which ensure that selected critical parameters will be in acceptable range. In this report chosen critical parameter was draught rate in the occupied zone, and more detailed maximum acceptable velocity, however, it was presented that another parameters, like minimum airflow needed due to indoor air quality requirements, or noise level can be used as the limiting values, and that limiting parameters taken into account while designing should be chosen depending on specifics of the system.

Constructing design chart for diffuse ceiling ventilation itself would not have significant impact on the knowledge about this system, because in available literature these type of charts can be already found for few types of diffuse ceiling inlets. That is why to extend the understanding of the DCV performance, various types of measurements were performed in order to find relationships between different parameters and the system's operation. Due to the fact that in spaces with diffuse ceiling type of ventilation, main force generating flow is the buoyancy force, experiments with different location of the heat loads in the room were performed. It was tried to check their influence on the airflow pattern in the room and in result on the indoor environment in the space. Both horizontal and vertical changes of the heat sources within the space were investigated. It was showed that influence of the heat loads distribution on the performance of the system is significant and what is more the most advantageous localizations were found. Design chart results indicated that the highest cooling capacity of the system can be obtained for rather equally distributed heat sources, or at least heat loads which are dispersed within the space. What is more it was found that heat loads placed at the floor level gives the highest risk of draught and in opposite, it is very beneficial to locate heat sources higher in the room. Highly located heat gains, like lighting in the room not only do not cause draught, but when other heat loads are placed in the lower part of the room, lighting can even decrease the risk of draught, compared to situation without the lighting. Even though it was proved that system's performance depends a lot on the distribution of heat loads, in reality it may be often

difficult to predict their localization. Common situation in buildings is that main part of heat loads is generated by people, in types of spaces like offices they have own working spaces, so the problem is not that significant, however for example in museums people change their location within the space and the layout of heat loads is not constant. That is why in practical design it might be advised to consider the most critical results of the cooling capacity for the system as the reference values.

What is more, when performing measurements for the case with equally distributed heat sources, a problem with the stability of airflow pattern appeared. It was expected that airflow pattern in the room is similar for all test with the same heat loads distribution, however for case with mannequins located uniformly in the room, different airflow distributions were observed for tests with various q and ΔT conditions. It was tried to investigate this problem further, by means of smoke visualizations of the airflow pattern and by checking detailed data for the velocity measurements. All of these studies indicated, that the system's performance with uniform set-up of heat loads is different compared to other tests, however nature of this problem is still unknown. What can be stated, is that equally distributed heat loads in the room creates airflow pattern, which is very sensitive to any changes in the room and it is possible, that airflow pattern in the room may change in time, which is unwanted situation in the ventilated spaces.

In available literature about DCV systems it was always assumed that whole ceiling's area is used as an inlet, supplying air. However in many designs it might be necessary to use part of the ceiling by other systems. That is why set of experiments was conducted with different inlet area of the ceiling and it was checked how significant will be the change in the system's performance and in addition, how the system will react on asymmetrical layout of the inlet. Results showed that inlet area is a crucial parameter and the highest cooling capacity of the system can be obtained, when whole ceiling's surface is used to supply air. In opposite, in case with asymmetric inlet area risk of draught can occur, when significantly lower q and ΔT parameters are used, compared to cases with uniform distribution of the inlet area.

Moreover, additional results of measurements were used to determine various parameters of the ventilation system. It was showed that vertical temperature gradients within the space are very low and that the system can be considered as mixed ventilation type, with temperature effectiveness of the system equal to around 0.97. Results of tracer gas concentration measurements confirmed this theory, calculated ventilation effectiveness was equal to around 0.99. It was showed as well that the radiant asymmetry caused by the cool ceiling is not high and for all of the cases results are significantly lower than requirements to ensure comfort of the occupants. Cold ceiling can be very efficient in supplying cool into the room, because radiant cooling generate comparable lower airflow in the room.

Finally, pressure tests were performed to determine the pressure loss across the ceiling. For the tested ceiling, pressure drop appeared to be rather high, compared to other tested samples, which is a result of its specific construction, the ceiling is very smooth and white, and the aesthetic aspects have disadvantageous influence on the performance of the diffusive part of the ceiling. Still, it was showed that the span of possible ceiling's construction is very large and the pressure drop on the ceiling may vary a lot for different solutions. What is more, while performing tracer gas concentration measurements, an unusual performance of the ceiling's construction was observed. It is possible that due to different pressure drop on a diffusive and paint layers of the ceiling, some part of the airflow, which is supposed to be supplied to the room through the chambers, passes through the diffusive part of the ceiling back to the plenum space. It is observed that there is a large span

of possible solutions for construction of the ceiling that can be used for DCV. This solution can be investigated to find optimal one that will give the best comfort in the room and will not generate high pressure drop.

What is more, CFD calculation gave another view on the problem with different heights of the room. Some kind of investigation, like measurements for different room, in reality are too expensive, but CFD give an opportunity to study this problems without high additional costs. For two models that were tested it is observed that height of the room can significantly affect velocities in occupied zone and change airflow. This result is consistent with dimensionless analysis conducted for the test room and an other small room. One of the main advantages of CFD is that, once the model for the system is done, it can be used multiple times and generate large span of different results, which are sometime even unavailable for the measurements. On the other hand it should be noted that CFD models should be validated and the best way to do this is to compare with measurements. However, unambiguity conditions for CFD model should be as close to measuring conditions as it is possible.

Part I

Appendix

Appendix report

This appendix is an enclosed report where detailed description of the experiment set-up, experiment results not presented in the main report and additional calculation methods can be found. There are regularly references from the main report to the appendix report.

A1 Design criteria	1
A1.1 Local thermal discomfort indices	1
A2 Experiment set-up	3
A2.1 Equipment	3
A2.2 Test cases	5
A3 Experiment results	11
A3.1 Airflow distribution	11
A3.2 Tracer gas concentration measurements for Case 13	21
A3.3 Pressure drop	22
A4 CFD Results	27
 I Drawings	 33
Bibliography	37

CD appendix

The following appendix contains a list of files included on the attached CD.

B.1 Experiment results

The present appendix contains a folder with files used for post-processing of the experiment data. The folder contains the following files.

Results_t_u_DR.xlsm

File with results of temperatures, velocity and draught risk.

DCV_design_chart.xls

File used to create a design chart.

Dimensionless_calculations.xlsx

File used for the dimensionless calculations.

Vertical_temperature_gradients.xlsx

File with vertical temperature gradients and ventilation temperature effectiveness results.

Radiation_script.m

File with MATLAB script for radiation balance calculation.

Radiation_results.xlsx

File with results for radiation balance calculation.

B.2 CFD results

The present appendix contains a folder with files for CFD models. The folder contains the following files.

OneSide_Thetra_3m.sim

File with low room's model.

OneSide_Thetra_3m.sim

File with high room's model.

Bibliography

- BR10, 2010.** BR10. *Danish building regulations 2010*. Danish Energy Agency, 2010. URL <http://www.bygningsreglementet.dk>. Date of download: 2013.02.19.
- CR 1752, 1998.** CR 1752. *Ventilation for buildings - Design criteria for the indoor environment*, 1998.
- DS/EN ISO 7726, 2001.** DS/EN ISO 7726. *Ergonomics of the thermal environment - Instruments for measuring physical quantities*, 2001.
- DS/EN ISO 7730, 2006.** DS/EN ISO 7730. *Ergonomics of the thermal environment-Analytical determination and interpretation of thermal comfort using calculation of the PMV and PPD indices and local thermal comfort criteria*, 2006.
- EN 12792, 2003.** EN 12792. *Ventilation for buildings - Symbols, terminology and graphical symbols*, 2003.
- EN 13779, 2007.** EN 13779. *Ventilation for non-residential buildings - Performance requirements for ventilation and room-conditioning systems*, 2007.
- Incropera, Dewitt, Bergman, and Lavine, 2006.** Frank P. Incropera, David P. Dewitt, Theodore L. Bergman, and Adrienne S. Lavine. *Fundamentals of heat and mass transfer*. Sixth edition. Wiley, 2006.
- Infrared Services, 2013.** Infrared Services. *Emissivity Values for Common Materials*. URL: www.infrared-thermography.com, 2013. Download date: 2013.03.11.
- Jacobs and Knoll, 2009.** Piet Jacobs and Bas Knoll. *Diffuse Ceiling ventilation for fresh classrooms*. 4th Intern. Symposium on Building and Ductwork Air tightness and 30th AIVC Conference "Trends in High Performance Buildings...", October 1-2, Berlin, Germany, 2009.
- Jacobs, Oeffelen, and Knoll, 2008.** Piet Jacobs, Elisabeth C.M. van Oeffelen, and Bas Knoll. *Diffuse Ceiling ventilation, a new concept for healthy and productive classrooms*. Indoor Air 2008, Copenhagen, Denmark, 2008.
- Jacobsen, 2008.** Lis Jacobsen. *Air Motion and Thermal Environment in Pig Housing Facilities with Diffuse Ceiling*. PhD Thesis Defended in public at the Danish Institute of Agricultural Sciences Research Centre Bygholm, 2008.
- Jakubowska, 2009.** Ewa Jakubowska. *Air Distribution in Rooms with Diffuse Ceiling Inlet*. COLD CLIMATE HVAC 2009 : Sisimiut Greenland, 16-19 March 2009, 2009.
- Jensen and Jensen, 2012.** R. L. Jensen and L. M. Jensen. *Airflow Test of Acoustic Board Samples*. DCE Contract Report No. 123. Contract Report from Aalborg University, 2012.

- John R. Howell, 2010.** John R. Howell. *A catalog of Radiation Heat Transfer Configuration Factors*. URL: www.engr.uky.edu/rtl/Catalog/index.html, 2010. Download date: 2013.03.11.
- Nielsen, 2007.** Peter V. Nielsen. *Analysis and Design of Room Air Distribution Systems*, volume 13:6. 2007.
- Nielsen, 2011.** Peter Vilhelm Nielsen. *The "Family Tree" of Air Distribution Systems*. Roomvent 2011, 2011.
- Nielsen and Jakubowska, 2009.** Peter Vilhelm Nielsen and Ewa Jakubowska. *The Performance of Diffuse Ceiling Inlet and other Room Air Distribution Systems*. COLD CLIMATE HVAC 2009: Sisimiut Greenland, 16-19 March 2009, 2009.
- Nielsen, Jensen, and Rong, 2010.** Peter Vilhelm Nielsen, Rasmus Lund Jensen, and Li Rong. *Diffuse Ceiling Inlet Systems and the Room Air Distribution*. Clima 2010: 10th Rehva World Congress, 2010.
- Skistad, Mundt, Nielsen, Hagström, and Railio, 2002.** Hakon Skistad, Elisabeth Mundt, Peter V. Nielsen, Kim Hagström, and Jorma Railio. *Displacement Ventilation in Non-industrial Premises*. ISBN: 82-594-2369-3, Guidebook. Rehva, 2002.
- STAR-CCM+ Manual, 2013.** *STAR-CCM+ Manual*. 2013.
- Versteeg and Malalasekera, 2007.** H.K. Versteeg and W. Malalasekera. *An Introduction to Computational Fluid Dynamics - Finite Volume Method*. ISBN: 978-0-13-127498-3, 2nd edition. Person Education Limited, 2007.
- Yang, 2011.** Honglu Yang. *Experimental and Numerical Analysis of Diffuse Ceiling Ventilation*. Master Thesis, Technical University of Denmark, 2011.